

N 80 6000
NASA CR 66896

GENERATION OF UNCERTAINTY BOUNDARY

FOR ARCASONDE 1A TEMPERATURE SENSOR SYSTEM

Progress Report under
NASA Grant NGR 45-003-025

August 1969

DEPARTMENT OF ELECTRICAL ENGINEERING
UNIVERSITY OF UTAH
SALT LAKE CITY, UTAH



GENERATION OF UNCERTAINTY BOUNDARY
FOR ARCASTONDE 1A TEMPERATURE SENSOR SYSTEM

Progress Report under
NASA Grant NGR 45-003-025

August 1969

University of Utah
Electrical Engineering Department

Shigetaka Kikkawa
Forrest L. Staffanson

Forrest L. Staffanson
Forrest L. Staffanson
Principal Investigator

ABSTRACT

A method of computing error bars, i.e., a running estimate of the overall uncertainty, for the temperature profile from a thermistor-type meteorological rocketsonde is presented. The resultant uncertainty is derived from estimated uncertainties in the parameter values assumed in the mathematical data correction relations. The "uncertainty boundary" is defined and the method of combining uncertainties is discussed.

A computer program in FORTRAN V is developed which computes corrections and uncertainties for real flight data. Simulated flight data is generated and used for illustration. Nominal values and uncertainty estimates for the parameters are those associated with the ARCAISONDE 1A film-mounted thermistor sensor system.

Quantitative results reveal the relative sensitivity of the corrected temperature to the various parameters. Sensor improvement with the use of a radiation shield is illustrated in terms of reduced uncertainty boundary.

TABLE OF CONTENTS

ABSTRACT	ii
LIST OF ILLUSTRATIONS AND TABLES	v
GLOSSARY	vii
I. INTRODUCTION	1
II. DESCRIPTION OF THE ARCASTONDE 1A TEMPERATURE MEASUREMENT SYSTEM	4
2.1 Mathematical Model of ARCASTONDE 1A Sensor System	5
2.2 Data Correction System	10
III. PROPAGATION OF UNCERTAINTIES	13
3.1 Uncertainty Definition	13
3.2 Uncertainty Distribution	15
3.3 Propagation of Uncertainties	17
IV. UNCERTAINTY BOUNDARY OF ARCASTONDE 1A SYSTEM	19
4.1 Expression of Uncertainty Boundary	19
4.2 Sensitivity Analysis	20
4.3 Estimated Nominal Values and Uncertainties of Parameters	26
4.4 Simulation Study of ARCASTONDE 1A System	35
A. Simulation	35
B. Results	36
C. With Shield	42
D. Cold Shield	43
V. CONCLUSIONS	51
APPENDIX A. APPROXIMATION OF THE RESULTANT STANDARD DEVIATION . .	53

APPENDIX B. EXPRESSIONS FOR SENSITIVITY COEFFICIENTS	58
APPENDIX C. SENSITIVITY OF TIME INVARIANT PARAMETERS	80
APPENDIX D. RADIATION HEAT TRANSFER	83
APPENDIX E. SIMULATION PROGRAM	91
REFERENCES .	103

LIST OF ILLUSTRATIONS AND TABLES

<u>Figure</u>		<u>Page</u>
1	Temperature measurement system	1
2	ARCASONDE 1A thermistor sensor	4
3	Complete system description of ARCASONDE 1A measurement system	12
4	Pseudo distribution curve	16
5	Pseudo density function	17
6	Graphical description $\frac{\partial T_{\text{air}}^i}{\partial p_j}$	20
7	Percent uncertainty of recovery factor	30
8	Block diagram of simulation study	37
9	Uncertainty boundary	38
10	Uncertainty boundary with a shield	44
11	Uncertainty boundary with cold shield	45
D.1	Geometric factor for the three sensor shapes of a circular region located 90 degrees from the sensor axis subtending half angle θ_0	86
E.1	Block diagram	92

<u>Table</u>		
1	Uncertainties and nominal value of parameters	27
2	Uncertainty of convective coefficient	31
3	Nominal values and uncertainties of the geometric factor	32
4	Nominal values and uncertainties of radiant emittance .	32
5	Uncertainty components	39
6	Nominal values and uncertainties of the geometric factor (with shield)	42

<u>Table</u>		<u>Page</u>
7	Nominal values and uncertainties of radiant emittance (with shield)	43
8	Uncertainty components (with shield)	46
9	Uncertainty components (cold shield)	48
10	Comparison of uncertainty boundary	50
A.1	Comparison of approximated and simulated $\sigma_{T_{air}}$	57

GLOSSARY

a	= albedo
A	= total body surface
c	= specific heat of bead, wire, or film
c_p	= specific heat of air
D	= diameter of bead, wire, or thickness of film
D_{es}	= distance between the earth and the sun
$E_{b\lambda}(T)$	= plank radiant energy spectral distribution function for the source in $d\Omega$ at temperature T
$f_{i,j}$	= geometric factor for ith body with respect to jth source
g	= gravitational acceleration
h	= convective heat transfer coefficient
I_j	= radiant emittance of jth source
k	= thermal conductivity of the body
ℓ	= length of the wire
m	= mass of the parachute and the rocketsonde
q	= radiation heat input
r	= recovery factor
R	= radius of the earth
R_s	= radius of the sun
S	= solar constant
T	= temperature of bead, wire, or film
T_{air}	= temperature of the air
T_m	= measured value of T_b

T_s = sensor temperature
 T'_{wb} = temperature gradient at the bead wire junction
 T_r = recovery temperature
 v = volume of bead, wire, or film
 V = air speed
 W = electric power dissipation
 α = long-wave absorptivity
 α_s = solar absorptivity
 $\alpha_{i,j}$ = absorptivity of ith body with respect to jth source
 α_λ = spectral absorptivity
 $\bar{\alpha}_j$ = mean absorptivity relative to the jth source
 β_j = radiation input perturbation factor
 ϵ = emissivity
 ϵ_λ = spectral emissivity
 Ω = solid angle subtended by the environment at the source
 θ = angle between sensor surface element dA and the direction
 toward $d\Omega$
 λ = radiation wavelength
 σ = Boltzmann constant
 σ_{p_ℓ} = standard deviation of parameter p_ℓ
 η_{p_ℓ} = mean value of parameter p_ℓ
 ρ = mass density of the sensor
 $\mu_{\ell,m}$ = correlation coefficient between p_ℓ and p_m

Subscript

i = 1 bead
i = 2 wire
i = 3 film
j = 1 sun
j = 2 albedo
j = 3 long-wave radiation from the earth
j = 4 sonde parts in view of the sensor as a long-wave source
b bead
w wire
f film
fm Mylar part of the film
fs silver part of the film

I. INTRODUCTION

In order to increase the altitude capability of rocketsonde atmospheric temperature sensors, many different sensor configurations have been considered and developed.

Evaluation of sensor performance is necessary in order to compare sensors and improve the sensor system. This study employs the mathematical modeling approach to the theoretical study of immersion-type thermometer sensors used in current meteorological rocketsonde systems.

Figure 1 represents the system block diagram of a temperature measurement system. Input to the system is air temperature, T_{air} , which is transformed to the temperature of the sensor, T_s . The value of T_s is different from T_{air} due to heat flux associated with the following error sources:

1. Radiation
2. Aerodynamic heating
3. Heat conduction
4. Self heating
5. Thermal time lag

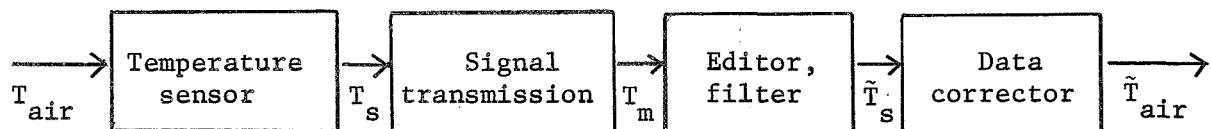


Fig. 1. Temperature measurement system.

T_s is then converted to the frequency of a blocking oscillator and relayed to a ground station where the signal is detected and recorded. This temperature, T_m , in general, contains measurement noise. Commonly, the data is filtered and edited to reject noise and spurious values and to obtain an improved representation, \tilde{T}_s , of the sensor temperature. Finally, computed corrections based on physical knowledge of the sensor and environment leads to the corrected air temperature, \tilde{T}_{air} .

Physical knowledge of the sensor system is embodied in a mathematical model of the form

$$T_s = f(T_{air}, \underline{p}) \quad (1)$$

where \underline{p} is a vector notation representing the set of parameters used in the thermistor heat equation. From Eq. 1, an inverse function is derived and is used for data reduction using parameter estimates $\tilde{\underline{p}}$.

$$\tilde{T}_{air} = f^{-1}(\tilde{T}_s, \tilde{\underline{p}}) \quad (2)$$

The better system is generally considered as the system which has the smaller difference between T_s and T_{air} . However, if accurate information is known about each parameter, \tilde{T}_{air} can be computed with small uncertainty by Eq. 2, regardless of the difference between T_s and T_{air} . The better system is actually the one which has the smaller

uncertainty in \tilde{T}_{air} .

In the following, a method is developed for computing the uncertainty in \tilde{T}_{air} due to parameter uncertainties, and is applied to the ARCASTONDE 1A meteorological rocketsonde temperature sensor.

II. DESCRIPTION OF THE ARCASTONDE 1A TEMPERATURE MEASUREMENT SYSTEM

In the following two sections, a mathematical model of ARCASTONDE 1A temperature sensor and data correction system will be derived. The configuration of the ARCASTONDE 1A sensor is shown in Fig. 2. Detail dimensions are listed in Table 1, page 27.

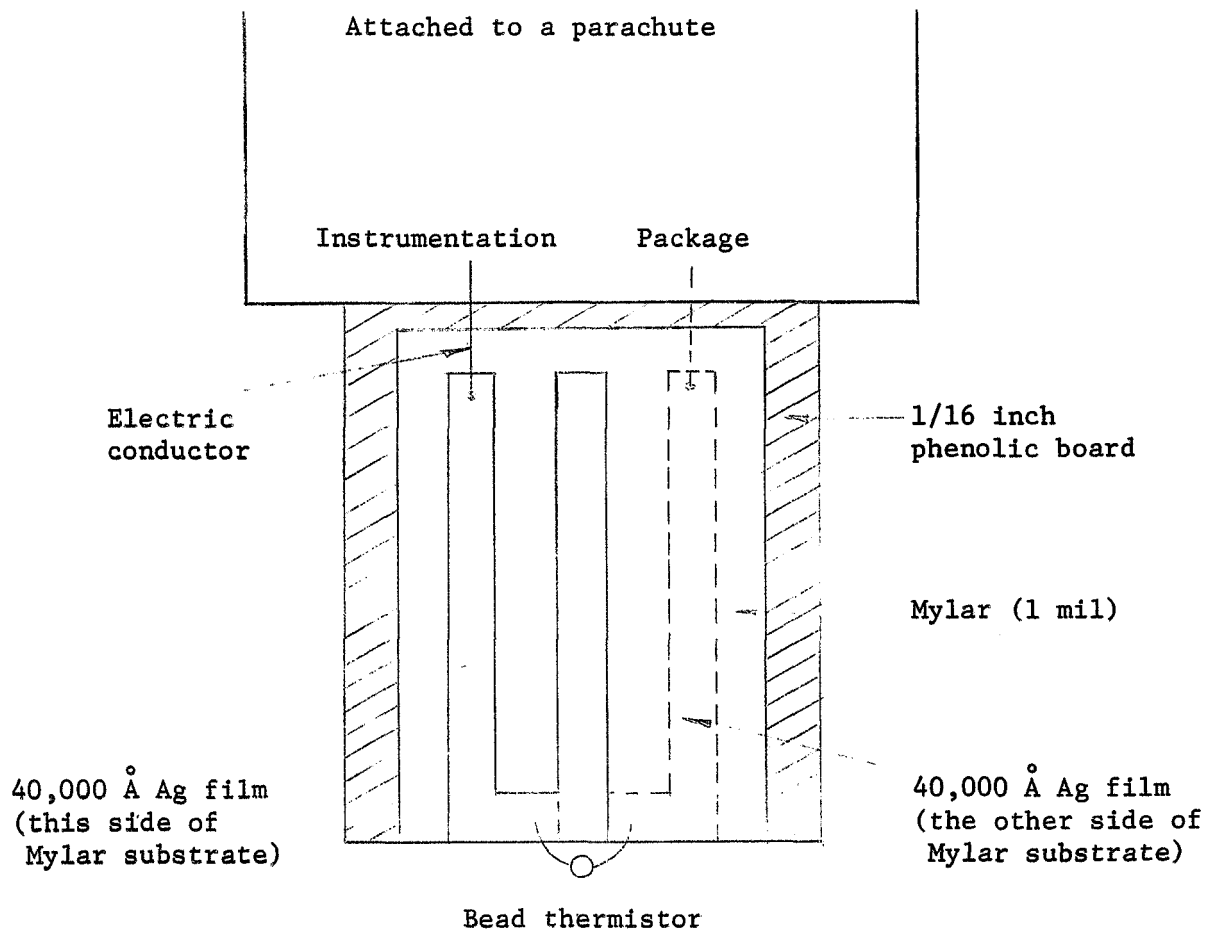


Fig. 2. ARCASTONDE 1A thermistor sensor.

2.1 Mathematical Model of ARCASTONDE 1A Sensor System

The temperature which is read by the electronic circuit in the sonde is that of the thermistor bead, i.e., T_s of Fig. 1 is T_b in the present discussion. The bead temperature is influenced by heat conduction from the wire, which is proportional to the temperature gradient in the wire at the point of contact with the bead. Using the bead and film temperatures as boundary conditions, the temperature gradient in the wire can be obtained.

The heat balance equations for the bead, wire, and film are:

(Bead)

$$(\rho c v)_b \frac{\partial T_b}{\partial t} = h_b A_b \left(T_{air} + r_b \frac{V^2}{2c_p} - T_b \right) + q_b A_b - A_b \sigma \epsilon_b T_b^4 + W_b \\ + 2k_w \frac{\pi}{4} D_w^2 T'_{wb}$$
(3.a)

(Wire)

$$(\rho c v)_w \frac{\partial T_w}{\partial t} = h_w A_w \left(T_{air} + r_w \frac{V^2}{2c_p} - T_w \right) + q_w A_w - A_w \sigma \epsilon_w T_w^4 + W_w \\ + k_w \frac{\partial^2 T_w}{\partial x^2}$$
(3.b)

(Film)

$$(\rho cv)_f \frac{\partial T_f}{\partial t} = h_f A_f \left(T_{air} + r_f \frac{V^2}{2c_p} - T_f \right) + q_f A_f - A_f \sigma \epsilon_f T_f^4 + w_f$$

(3.c)

$$+ k_f v_f \left(\frac{\partial^2 T_f}{\partial x^2} + \frac{\partial^2 T_f}{\partial y^2} \right)$$

where subscript b, w, f indicate bead, wire, and film, respectively,
where

ρ = mass density of an element

c = specific heat of an element

v = volume of an element

h = convective heat transfer coefficient

T'_{wb} = temperature gradient at the bead and the wire junction

r = recovery factor

V = relative speed of air

c_p = specific heat of air

q = radiation heat input

A = surface of an element

w = self heating

k = thermal conductivity

σ = Stefan-Boltzmann constant

D_b, D_w, D_f = diameter of bead, diameter of wire, thickness of film,
respectively

ϵ = emissivity

These equations are coupled by conductive boundary conditions at surfaces of contact.

The radiation environment is considered in four parts, designated by the subscript $j = 1, \dots, 4$, according to radiant heat sources as follows:

- $j = 1$ direct solar illumination
- $j = 2$ indirect solar illumination
- $j = 3$ earth radiation
- $j = 4$ sonde radiation

The radiation input to a surface element of the sensor system is represented by

$$q_i = \sum_{j=1}^4 \alpha_{i,j} f_{i,j} I_j$$

where

α = radiation absorptivity

f = geometric factor

I = radiant emittance

and subscript $i = 1, 2, 3$ indicates the sensor part (body) b, w, f, respectively. More complete discussion concerning radiation terms is given in Appendix D.

It is not practical to solve the nonlinear simultaneous partial differential equation. The following assumptions have been made

in order to simplify the computation:

1. Time constant of the wire is very small compared with that of the film and the bead. Therefore, we can assume

$$\frac{\partial T_w}{\partial t} = 0$$

2. Temperature of the film is not influenced by heat exchange with the wire.
3. Temperature distribution of the film is assumed to be uniform near the film-wire junction.

By the above assumptions, Eqs. 3.a, 3.b, and 3.c are simplified as follows:

(Bead and wire)

$$\frac{(\rho c D)_b}{6} \frac{dT_b}{dt} = h_b \left(T_{air} + r_b \frac{v^2}{2c_p} - T_b \right) + q_b + \frac{W_b}{A_b} - \sigma \epsilon_b T_b^4 + X \quad (4.a)$$

(Film)

$$\frac{(\rho c D)_f}{2} \frac{dT_f}{dt} = h_f \left(T_{air} + r_f \frac{v^2}{2c_p} - T_f \right) + q_f - \sigma \epsilon_f T_f^4 \quad (4.b)$$

where

$$X = H_k \left(K_1 T_{air} + P + Q T_f - T_b \right)$$

$$H_k = c_2 \lambda_w \coth \lambda_w \ell$$

$$K_1 = \frac{h_w \left(1 - \operatorname{sech} \lambda_w \ell \right)}{h_w + 4\sigma \epsilon_w^3 T_{aw}}$$

$$P = \frac{\left(1 - \operatorname{sech} \lambda_w \ell \right) \left(h_w r_w \frac{v^2}{2c_p} + 3\sigma \epsilon_w^4 T_{aw}^4 \right)}{h_w + 4\sigma \epsilon_w^3 T_{aw}}$$

$$Q = \operatorname{sech} \lambda_w \ell$$

$$\lambda_w = \left(\frac{4(h_w + 4\sigma \epsilon_w^3 T_{aw}^3)}{(kD)_w} \right)^{1/2}$$

$$c_2 = \frac{(kD)_w D}{2D_b^2}$$

These constitute a set of two simultaneous differential equations representing the sensor system.

2.2 Data Correction System

From Fig. 1, the desired air temperature, T_{air} , is obtained by correcting the data, \tilde{T}_b , representing the sensor temperature, T_b . The required mathematical expressions are obtained from Eq. 4.a and 4.b, which expressed in one-step finite difference form are:

$$\tilde{T}_{air}^i = \frac{1}{\tilde{h}_b^i + \tilde{H}_k^i \tilde{K}_l} \left[\frac{(\tilde{\rho} \tilde{c} \tilde{D})_b}{6} \dot{\tilde{T}}_b^i + \left(\tilde{h}_b^i + 4\sigma \tilde{\varepsilon}_b (\tilde{T}_b^i)^3 + \tilde{H}_k^i \right) \tilde{T}_b^i \right. \\ \left. - \left(\tilde{h}_b^i \tilde{r}_b^i \frac{(\tilde{V}_b^i)^2}{2c_p} + 3\sigma \tilde{\varepsilon}_b (\tilde{T}_b^i)^4 + \frac{\tilde{W}_b^i}{A_b} + \tilde{q}_b^i + \tilde{H}_k^i \tilde{p}^i \right) - \tilde{H}_k^i \tilde{Q}^i \tilde{T}_f^i \right] \quad (5.a)$$

$$T_f^i = \left[1 - \frac{2\Delta t}{(\tilde{\rho} \tilde{c} \tilde{D})_f} \left(\tilde{h}_f^i - 1 + \sigma \tilde{\varepsilon}_f (\tilde{T}_f^i - 1)^3 \right) \right] T_f^{i-1} \\ \left. + \frac{2\Delta t}{(\tilde{\rho} \tilde{c} \tilde{D})_f} \left(\tilde{q}_f^i - 1 + \tilde{h}_f^i - 1 \tilde{r}_f^i - 1 \frac{(\tilde{V}_f^i - 1)^2}{2c_p} \right) + \tilde{h}_f^i - 1 \frac{2\Delta t}{(\tilde{\rho} \tilde{c} \tilde{D})_f} \tilde{T}_{air}^i \right] \quad (5.b)$$

where superscript i indicates the time, and

$$\tilde{H}_k^i = \tilde{c}_2 \tilde{\lambda}_w^i \coth \tilde{\lambda}_w^i \tilde{\lambda}$$

$$\tilde{K}_1^i = \frac{\tilde{h}_w^i \left(1 - \operatorname{sech} \tilde{\lambda}_w^i \right)}{\tilde{h}_w^i + 4\sigma \tilde{\epsilon}_w \left(\tilde{T}_{air}^i\right)^3}$$

$$\tilde{P}^i = \frac{\left(1 - \operatorname{sech} \tilde{\lambda}_w^i\right) \left(\tilde{h}_w^i \tilde{r}_w^i \frac{\left(\tilde{v}^i\right)^2}{2c_p} + 3\sigma \tilde{\epsilon}_w \left(\tilde{T}_{air}^i\right)^4 \right)}{\tilde{h}_w^i + 4\sigma \tilde{\epsilon}_w \left(\tilde{T}_{air}^i\right)^3}$$

$$\tilde{Q}^i = \operatorname{sech} \tilde{\lambda}_w^i$$

$$\tilde{\lambda}_w^i = \left\{ \frac{4 \left(\tilde{h}_w^i + 4\sigma \tilde{\epsilon}_w \left(\tilde{T}_{air}^i\right)^3 \right)}{(\tilde{k}\tilde{D})_w} \right\}^{1/2}$$

$$\tilde{c}_2 = \frac{(\tilde{k}\tilde{D})_w \tilde{D}_w}{2\tilde{D}_b^2}$$

Δt = sampling interval of \tilde{T}_s (uniform)

Assume the entire sensor system is initially uniform, i.e., $\tilde{T}_f^0 = \tilde{T}_b^0$.

Solution proceeds in time steps by computing alternately, T_f^i , then T_{air}^i . A schematic representation of the data correction process, together with the simulated sensors as it was programmed for use in this study, is shown in Fig. 3.

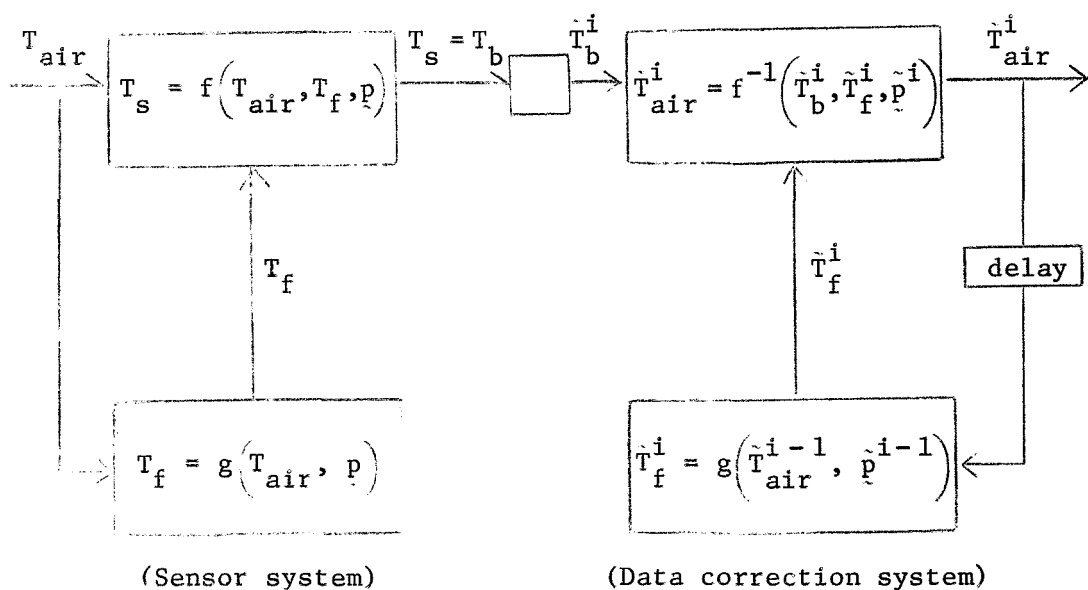


Fig. 3. Complete system description of ARCASONDE 1A measurement system.

III. PROPAGATION OF UNCERTAINTIES

A method of generating the uncertainty boundaries for the corrected air temperature function, \tilde{T}_{air} , discussed in the previous section is developed as follows. Successful assessment of variance in \tilde{T}_{air} will require error examination in four categories:

1. Dimensions and properties (manufacturing variability).
2. Data handling (measurement errors).
3. Environmental parameters.
4. Approximations in the thermal analysis (model errors).

Uncertainty associated with error in the basic mathematical model of the sensor is assumed negligible.

3.1 Uncertainty Definition

The corrected air temperature is a function of a set of parameters, \tilde{p} .

$$\tilde{T}_{air} = f(\tilde{p}_1, \tilde{p}_2, \tilde{p}_3, \dots, \tilde{p}_n) \quad (6)$$

Estimated value for the parameters are obtained from:

1. Specific laboratory measurements (such as for sensor emissivity, wire length).
2. In-flight measurement (such as for air speed).
3. Past experimental data (such as for earth albedo).

4. Theoretical calculations (such as for geometric factors, convective coefficients).

Suppose the error in a parameter estimate is defined as the difference between the estimated value and the true value of the parameter. Suppose further, that estimated values for a given flight are derived independently by many sufficiently qualified investigators. The estimated value, and therefore the error, would exhibit some statistical distribution, analogous to the results from a multiple sample experiment. The standard deviation and the mean of the estimated value may be defined as they are for a multiple sample experiment. If \tilde{p}_i is the estimated value of a parameter from many different investigators, then the mean and standard deviation is defined as

$$\bar{n}_{p_i} = \int_{-\infty}^{+\infty} p_i f(p_i) dp_i = \tilde{p} \quad (7)$$

$$\sigma_{p_i}^2 = \int_{-\infty}^{+\infty} (p_i - \bar{n}_{p_i})^2 f(p_i) dp_i \quad (8)$$

where $f(p_i)$ is a density function of p_i .

If \bar{n}_{p_i} and σ_{p_i} are given for each parameter in Eq. 6, $n_{T_{air}}$ and $\sigma_{T_{air}}$ can be computed. If T_{air} is distributed normally, one can expect to find, or can be confident of finding, true T_{air} lying

in the interval, $T_{air} \pm 2\sigma_{T_{air}}$, 95.45 percent of the time. It is expected that, in fact, T_{air} tends to be distributed normally because of the central limit theorem. The uncertainty boundary (or simply "uncertainty") is defined as $\pm 2\sigma$ of the nominal value.

3.2 Uncertainty Distribution

Though the distribution of the estimated value of a parameter may be conceptually defined, it is really known quantitatively for the parameters in the present discussion. For some parameters the uncertainty is given in the form of $p_i \pm \Delta p_i$. If only limiting values are known, the worst case method is sometimes used. The worst case method is a nonstatistical approach that employs the possible extremes of the parameters.

$$\Delta T_{air} = \sum_{i=1}^n \left| \left(\frac{\partial f}{\partial p_i} \right)_{p_i} \right| \Delta p_i \quad (9)$$

This usually gives an unrealistically pessimistic result. Even if they are strongly correlated, the assumption that the algebraic signs of all terms are the same is not statistically justified.

In order to obtain a more realistic uncertainty boundary, the concept of "uncertainty distribution" will be introduced. Kline and McClintock [9, 1953] applied this concept to describe uncertainties in single-sample experiments.

Suppose the variable p_i is expressed by $p_i \pm \Delta p_i$, where the value Δp_i is an estimation. An equivalent expression is the following:

$$P(p_i \leq p_i + \Delta p_i) \approx 1$$

(10)

$$P(p_i \leq p_i - \Delta p_i) \approx 0$$

If we define $F(X) = P\{p_i \leq X\}$, the above expression can be shown graphically as in Fig. 4.

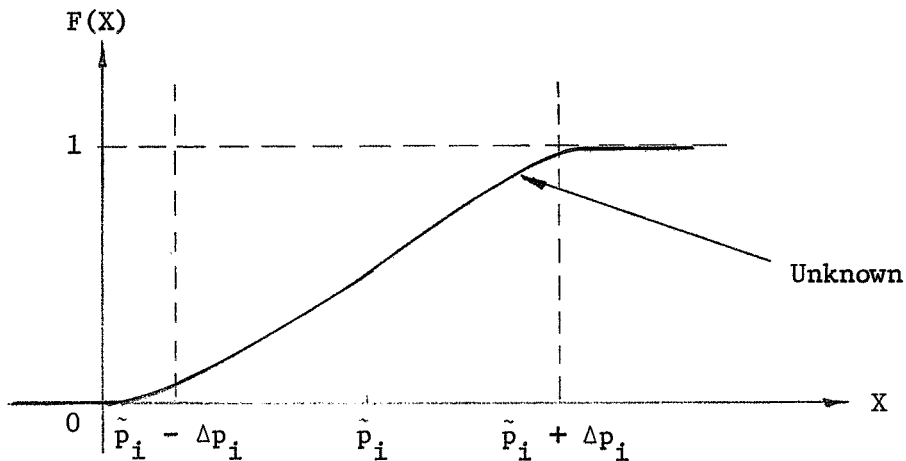


Fig. 4. Pseudo distribution curve.

Even if, between $p_i - \Delta p_i$ and $p_i + \Delta p_i$, there is no information, a

pseudo distribution may be imagined.

The corresponding pseudo density function may then be defined as $f(X) = dF(X)/dX$. One might feel that the pseudo distribution is

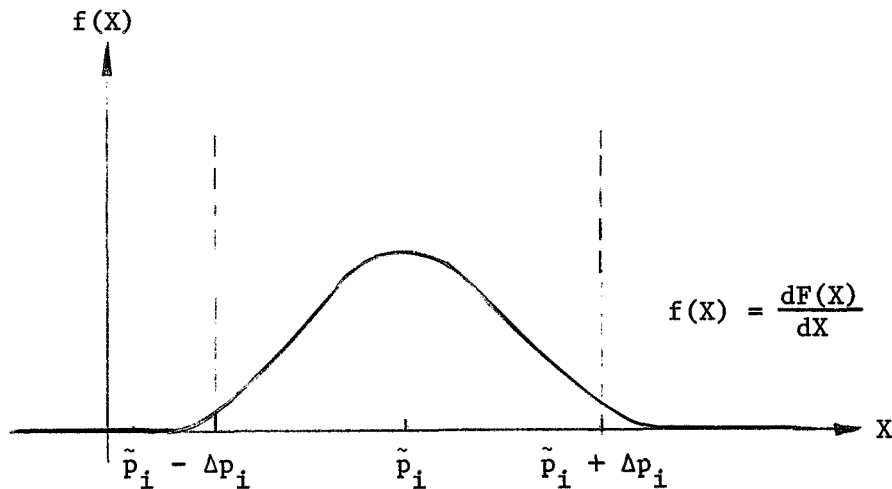


Fig. 5. Pseudo density function.

uniform for some parameters. For other parameters, however, intuition may suggest the errors are more likely near the center than near the ends of their respective ranges. Therefore, one might attempt to simulate this feeling by assuming the density function to be approximately normal, and Δp_i to be $2\sigma_{p_i}$ [7, Eisenhart 1963].

3.3 Propagation of Uncertainties

Now that we have estimated (or imagined) σ_{p_i} , the next step is to relate to the σ_{p_i} in accordance with $\sigma_{T_{air}}$, Eq. 6. Papoulis [10, 1965] discussed an approximation for this relation for the case of two

parameters. The idea is easily extended to n parameters (Appendix A).

$$\sigma_{T_{air}}^2 = \sum_{i=1}^n \left(\frac{\partial f}{\partial p_i} \right)_{p_i} \sigma_{p_i}^2 + \sum_{i=1} \sum_{j=1, i \neq j} \left(\frac{\partial f}{\partial p_i} \right) \left(\frac{\partial f}{\partial p_j} \right) \frac{\text{cov}(p_i, p_j)}{\sigma_{p_i} \sigma_{p_j}} \quad (11)$$

where

$$\begin{aligned} \text{cov}(p_i, p_j) &= \int_{-\infty}^{\infty} \int_{-\infty}^{\infty} (p_i - \bar{p}_i)(p_j - \bar{p}_j) f(p_i, p_j) dp_i dp_j \\ &= \mu_{ij} \sigma_{p_i} \sigma_{p_j} \end{aligned}$$

The validity of the above equation depends on the nonlinearity of $f(p_1, p_2, \dots, p_n)$ and the distribution of the parameters, but the approximation error within a sufficiently small range of the parameters is assumed to be small compared with the estimation error in the σ_{p_i} .

Thorough mathematical study of the approximation error is beyond the scope of the present discussion, but Monte-Carlo simulation studies indicate the error is small in the ARCA SONDE 1A system for a considerably large range of the parameters.

IV. UNCERTAINTY BOUNDARY OF ARCASONDE 1A SYSTEM

The method of generating the uncertainty boundary in \hat{T}_{air} , which was discussed in Chapter III, will be applied to the ARCASONDE 1A system which was introduced in Chapter II.

4.1 Expression of Uncertainty Boundary

Equations 5.a and 5.b can be expressed in the following form:

$$T_{\text{air}}^i = f^i \left(p_j^k \right) \quad \begin{matrix} j = 1, \dots, n \\ k = 1, \dots, i \end{matrix} \quad (12)$$

where the input parameters include the sensor temperature \hat{T}_b^k . The subscript j denotes the particular parameter, and k denotes the time.

Applying Eq. 11 to Eq. 12 gives

$$\sigma_{T_{\text{air}}}^2 = \sum_{j=0}^i \sum_{m=1}^n \left(\frac{\partial f^i}{\partial p_m^j} \right)^2 \sigma_{p_m^j}^2 + \sum_{j=0}^i \sum_{k=0}^i \sum_{m=1}^n \sum_{l=1}^n \left(\frac{\partial f^i}{\partial p_m^j} \right) \left(\frac{\partial f^i}{\partial p_l^k} \right) \frac{\text{cov}(p_m^j, p_l^k)}{\sigma_{p_m^j} \sigma_{p_l^k}} \quad (13)$$

$l \neq m, j \neq k$

The term $\left(\frac{\partial f^i}{\partial p_j^m} \right)$ is called the sensitivity coefficient [16, Tomovic 1962] and contains information about the system. $\sigma_{p_m^j}$ and $\text{cov}(p_m^j, p_l^k)$ are

independent of the sensor system and the values are estimated according to conditions at each point in time.

4.2 Sensitivity Analysis

In order to obtain the value of $\sigma_{T_{air}^i}$, the sensitivity coefficients have to be computed for each parameter at each preceding time point. Therefore, at each time i , we have to compute $i \times n$ sensitivity coefficients. One might consider this a very time consuming process for a system of many parameters and over many points in time, but actually $\frac{\partial f^i}{\partial p_l^j} \rightarrow 0$ when $(i - j) \rightarrow \infty$, therefore, older terms become negligible.

The sensitivity coefficient $\frac{\partial T_{air}^i}{\partial p_l^j}$ indicates the effect on T_{air}^i at time i of variation in p_l at time j . As shown in Fig. 6, an error

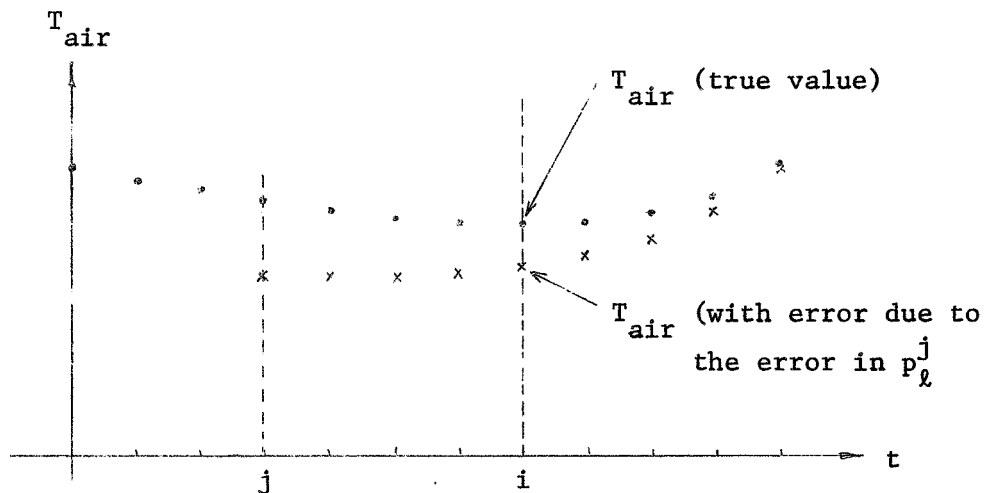


Fig. 6. Graphical description of $\frac{\partial T_{air}^i}{\partial p_l^j}$.

in p_ℓ at time j will have a diminishing effect on succeeding values of T_{air} .

Sensitivity coefficients are computed as follows. Equations 5.a and 5.b may be written in the form

$$T_{air}^i = f(p_z^i, T_f^i) \quad (14.a)$$

$$T_f^i = g(p_z^{i-1}, T_f^{i-1}, T_{air}^{i-1}) \quad (14.b)$$

where

$$\underline{p}_z^i = \begin{bmatrix} p_1^i \\ p_2^i \\ \vdots \\ \vdots \\ p_n^i \end{bmatrix}$$

Assume the sensitivity coefficients have been computed up to the time $(i - 1)$. Let already computed quantities be enclosed in parentheses. Only the bracketed quantities need be computed at the i th point in time. For the parameter, p_ℓ :

j = i

$$\frac{\partial T_{air}^i}{\partial p_\lambda^j} = \frac{\partial T_{air}^i}{\partial p_\lambda^j} = \left[\frac{\partial f^i}{\partial p_i} \right]$$

Expression for the $\frac{\partial f^i}{\partial p_i}$ for the ARCA SONDE 1A are listed in Appendix B.

j = i - 1

$$\frac{\partial T_{air}^i}{\partial p_\lambda^j} = \frac{\partial T_{air}^i}{\partial p_\lambda^{i-1}} = \left[\frac{\partial f^i}{\partial T_f^i} \right] \left[\frac{\partial T_f^i}{\partial p_\lambda^{i-1}} \right]$$

where

$$\frac{\partial f^i}{\partial T_f^i} = \left[\frac{\partial f^i}{\partial G^i} \right] \left[\frac{\partial G^i}{\partial T_f^i} \right] + \left[\frac{\partial f^i}{\partial T_f^i} \right]$$

$$\frac{\partial T_f^i}{\partial p_\lambda^{i-1}} = \left[\frac{\partial g^i}{\partial p_\lambda^{i-1}} \right] + \left[\frac{\partial g^i}{\partial T_{air}^{i-1}} \right] \left(\frac{\partial T_{air}^{i-1}}{\partial p_\lambda^{i-1}} \right)$$

Computation of $\frac{\partial f^i}{\partial G^i}$ and $\frac{\partial G^i}{\partial T_f^i}$ are shown in Appendix B.

j = i - 2

$$\frac{\partial T_{air}^i}{\partial p_\lambda^j} = \frac{\partial T_{air}^i}{\partial p_\lambda^{i-2}} = \left(\frac{\partial f^i}{\partial T_f^i} \right) \left[\frac{\partial T_f^i}{\partial p_\lambda^{i-2}} \right]$$

$$\frac{\partial T_f^i}{\partial p_\lambda^{i-2}} = \left(\frac{\partial g^i}{\partial T_{air}^{i-1}} \right) \left(\frac{\partial T_{air}^{i-1}}{\partial p_\lambda^{i-2}} \right) + \left[\frac{\partial g^i}{\partial T_f^{i-1}} \right] \left(\frac{\partial T_f^{i-1}}{\partial p_\lambda^{i-2}} \right)$$

Computation of $\frac{\partial g^i}{\partial T_f^{i-1}}$ is shown in Appendix B.

j = i - 3

$$\frac{\partial T_{air}^i}{\partial p_\lambda^j} = \frac{\partial T_{air}^i}{\partial p_\lambda^{i-3}} = \left(\frac{\partial f^i}{\partial T_f^i} \right) \left[\frac{\partial T_f^i}{\partial p_\lambda^{i-3}} \right]$$

$$\frac{\partial T_f^i}{\partial p_\lambda^{i-3}} = \left(\frac{\partial g^i}{\partial T_{air}^{i-1}} \right) \left(\frac{\partial T_{air}^{i-1}}{\partial p_\lambda^{i-3}} \right) + \left(\frac{\partial g^i}{\partial T_f^{i-1}} \right) \left(\frac{\partial T_f^{i-1}}{\partial p_\lambda^{i-3}} \right)$$

j = 0

$$\frac{\partial T_f^i}{\partial p_\ell^0} = \left(\frac{\partial f^i}{\partial T_f^i} \right) \left(\frac{\partial T_f^i}{\partial p_\ell^0} \right)$$

$$\frac{\partial T_f^i}{\partial p_\ell^0} = \left(\frac{\partial g^i}{\partial T_{air}^{i-1}} \right) \left(\frac{\partial T_{air}^{i-1}}{\partial p_\ell^0} \right) + \left(\frac{\partial g^i}{\partial T_f^{i-1}} \right) \left(\frac{\partial T_f^{i-1}}{\partial p_\ell^0} \right)$$

Notice that only simple multiplication is needed for derivatives with respect to parameter values older than $i - 3$.

The correlation coefficient in time for a truly constant parameter p_ℓ is $\mu_\ell = 1$. The contribution of p_ℓ to $\sigma_{T_{air}^i}$, $\sigma_{T_{air}^i(p_\ell)}$ is

$$\sigma_{T_{air}^i(p_\ell)} = \frac{\partial T_{air}^i}{\partial p_\ell} \sigma_{p_\ell}$$

For constant parameters, the above procedure for computing the sensitivity coefficients is simplified by solving a set of difference equations.

From Eqs. 14.a and 14.b

$$\frac{\partial T_{air}^i}{\partial p_\ell} = \frac{\partial f^i}{\partial p_\ell} + \frac{\partial f^i}{\partial T_f^i} \frac{\partial T_f^i}{\partial p_\ell}$$

$$\frac{\partial T_f^i}{\partial p_\ell} = \frac{\partial g}{\partial p_\ell} + \frac{\partial g}{\partial T_f^{i-1}} \frac{\partial T_f^{i-1}}{\partial p_\ell} + \frac{\partial g}{\partial T_{air}^{i-1}} \frac{\partial T_{air}^{i-1}}{\partial p_\ell}$$

Substituting $U^i = \frac{\partial T_{air}^i}{\partial p_\ell}$ and $V^i = \frac{\partial T_f^i}{\partial p_\ell}$,

$$U^i = \frac{\partial f^i}{\partial p_\ell} + \frac{\partial f^i}{\partial T_f^i} V^i \quad (15.a)$$

$$V^i = \frac{\partial g^i}{\partial p_\ell} + \frac{\partial g^i}{\partial T_f^{i-1}} V^{i-1} + \frac{\partial g^i}{\partial T_{air}^{i-1}} U^{i-1} \quad (15.b)$$

which is a special case of the more general procedure given above

(Appendix C). The required computation is obviously much less for constant parameters.

4.3 Estimated Nominal Values and Uncertainties of Parameters

Sensor Properties

A list of input parameters for the ARCAISONDE 1A temperature sensor is presented in Table 1. Since the film is a composition of silver and Mylar, properties of both must be used. Subscript fm, fs indicate the Mylar and silver parts of the film, respectively. Subscript f indicates the effective value.

A. D_b , D_w , D_{fm} , D_{fs} (diameter of bead, wire, and the thickness of the film). Uncertainty in these quantities is due to manufacturing variability and imperfections in shape.

The uncertainty is estimated to be 10 percent.

B. $(\rho c)_b$, $(\rho c)_w$, $(\rho c)_{fm}$, $(\rho c)_{fs}$, $(\rho c)_f$ (density times heat capacity). The effective value of ρc for the film is given by

$$(\rho c)_f = \frac{D_s (\rho c)_s + D_m (\rho c)_m}{D_s + D_m}$$

The uncertainties for $(\rho c)_b$, $(\rho c)_w$ are estimated to be 5 percent due to lack of knowledge of composition, and 10 percent for $(\rho c)_f$ due to an estimated variability in Mylar thickness.

TABLE 1

Uncertainties and Nominal Value of Parameters

	Nominal Value	Uncertainty	Reference
D_b	$.28 \times 10^{-3}$ m (11 mil)	10%	Drews [4]
D_w	$.25 \times 10^{-4}$ m	10%	Drews
D_{fm}	$.25 \times 10^{-4}$ m		Drews
D_{fs}	$.4 \times 10^{-5}$ m		Drews
D_f	$.31 \times 10^{-4}$ m	7%	
$(\rho c)_b$	1.95×10^6 J/m ³ - °K	5%	Wright [19]
$(\rho c)_w$	2.79×10^6 J/m ³ - °K	5%	Wright
$(\rho c)_{fs}$	2.45×10^6 J/m ³ - °K		Weast [18]
$(\rho c)_{fm}$	1.84×10^6 J/m ³ - °K		Dupont [5]
$(\rho c)_f$	1.96×10^6 J/m ³ - °K	10%	
k_w	30.98 watt/m - °K	5%	Weast
k_{fm}	.152 watt/m - °K	5%	Dupont
k_{fs}	408 watt/m - °K	5%	Weast
α_b	.11	25%	Thompson [15]
α_w	.10	10%	Thompson
α_{fs}	.02		Weast
α_{fm}	.80		Drews
α_f	.65	50%	
α_{sb}	.16	40%	Thompson
α_{sw}	.19	50%	Thompson
α_{sfs}	.07		Weast
α_{sfm}	.06		Drews
α_{sf}	.22	50%	
λ	3.2×10^{-3} m	50%	Drews

C. k_w , k_{fm} , k_{fs} , k_f (thermal conductivity). The uncertainty for k is estimated to be 5 percent because of the impurity of materials and experimental error in published data [11, Powell, Ho, Liley]. Effective value of k is k_{fs} because $(kD)_s \gg (kD)_m$.

D. α_b , α_w , α_{fs} , α_{fm} (absorptivity of long wave radiation). The effective absorptivity of the Mylar-exposed side of a silver-plated region is taken as

$$\alpha = \alpha_m + \left[\alpha_s + \alpha_m (1 - \alpha_s) \right] (1 - \alpha_m)$$

which assumes the reflectivity of the Mylar to be small.

Similarly, the emissivity is assumed to be

$$\varepsilon = \varepsilon_m + (1 - \alpha_m) \left[(1 - \alpha_s) \varepsilon_m + \varepsilon_s \right]$$

which includes approximately the emission of the Mylar forward that emitted backward and reflected by the silver, and the emission of silver through the Mylar and, which incidentally, is the same value as the above absorptivity.

The effective emissivity of the film is computed by averaging that of the inner and outer film strips, and using their lengths as weighting factors.

Uncertainty in α_b is estimated to be about 25 percent

because of the condition of coating the sphere surface [15, Thompson 1966]. Uncertainty of ϵ_f is estimated to be 50 percent due to a nonuniform plastic coating of unknown composition over the silver.

E. α_{sb} , α_{sw} , α_{sfs} , α_{sfm} , α_{sf} (absorptivity of short wave radiation). Uncertainty of α_{sb} and α_{sw} are assumed to be 40 percent due to the manufacturing variation in the surface [15, Thompson 1966]. The uncertainty in α_{sf} is estimated to be 50 percent due to the plastic coating.

F. l (length of the wire). Uncertainty in the length of the wire is estimated to be about 50 percent due to manufacturing variation.

Convective Environment

Convective coefficient h and recovery factor r are computed using the interpolation formula [13, Staffanson and Alsaj 1968].

$$h = \frac{1}{\frac{1}{h_1} + \frac{1}{h_2}}, \quad r = r_1 + K_n \frac{r_2 - r_1}{Kn + Kn_0}$$

Subscript 1, 2 denote continuum and free molecular values, respectively. The uncertainty increases in the transition flow region where knowledge is least reliable. The uncertainty in recovery factor is estimated as shown in Fig. 7.

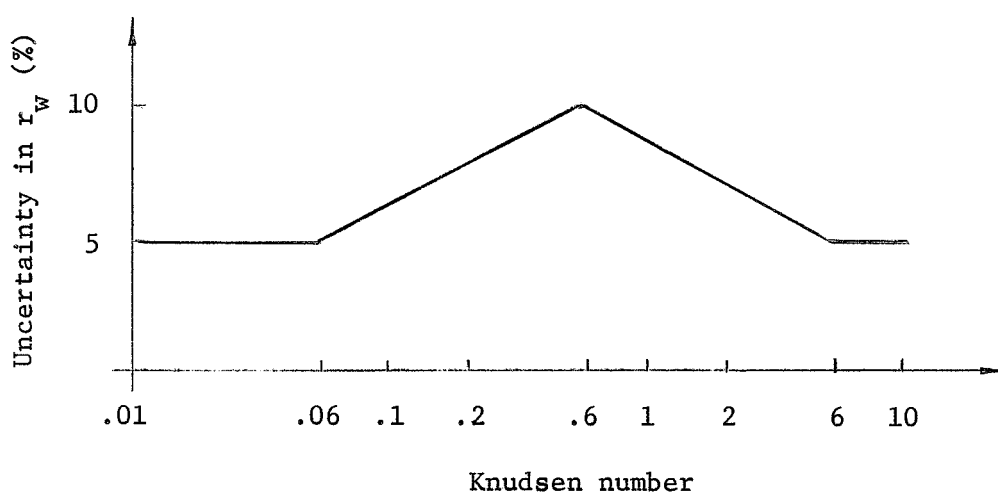
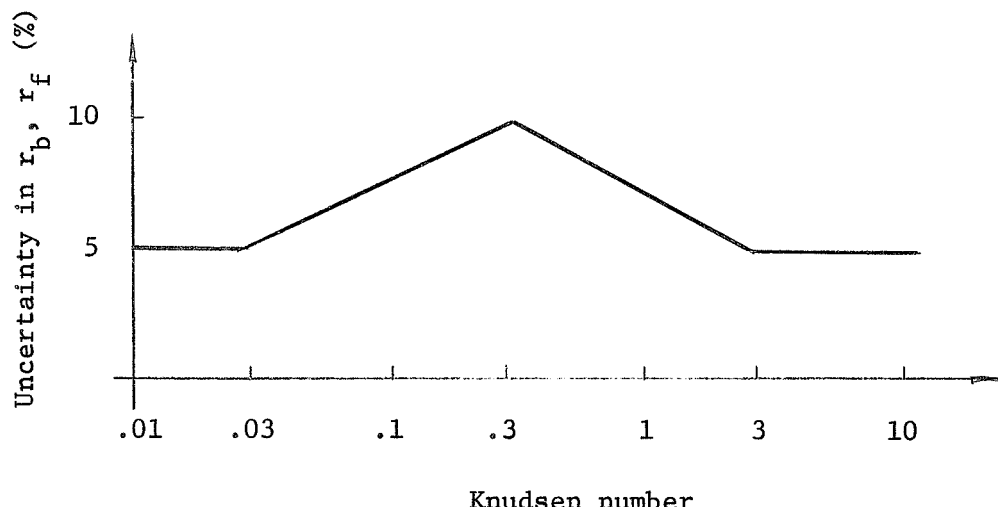


Fig. 7. Percent uncertainty of recovery factor.

Table 2 indicates the assumed uncertainty in h with respect to Reynolds number. Linear interpolation gives the uncertainty at any Reynolds number.

TABLE 2
Uncertainty of Convective Coefficient

Reynolds Number	Uncertainty (%)
$\leq 10^{-2}$	5%
10^{-1}	7.5%
1	10%
10	15%
10^2	18%
10^3	15%
10^4	10%
10^5	7.5%
$\geq 10^6$	5%

Radiation Environment

The geometric factor, $f_{i,j}$, is a quantity which depends on the shape of the sensor surfaces, the solid angle subtended by the source, and the orientation of the sensor relative to the source. The method of obtaining the values of $f_{i,j}$ is presented in Appendix D and the nominal values are presented in Table 3.

TABLE 3
Nominal Values and Uncertainties of the Geometric Factor

	Sphere	Cylinder	Plate
Sun	$.272 \times 10^{-5} \pm 100\%$	$.347 \times 10^{-5} \pm 100\%$	$.535 \times 10^{-5} \pm 100\%$
Albedo	$0.40 \pm 15\%$	$0.40 \pm 15\%$	$0.40 \pm 15\%$
Earth	$0.42 \pm 5\%$	$0.43 \pm 10\%$	$0.41 \pm 10\%$
Sonde	$0.087 \pm 3\%$	$0.108 \pm 3\%$	$0.044 \pm 3\%$

The radiant emittance, I_j (total radiant power emitted per unit area), of a solid surface depends on its emissivity, ϵ_λ , and its absolute temperature, T. I_j is computed in Appendix D. The nominal values of I_j are presented in Table 4.

TABLE 4
Nominal Values and Uncertainties of Radiant Emittance

Sun	$6.4558 \times 10^7 \text{ watt/m}^2 \pm 1\%$
Albedo	$460.7 \text{ watt/m}^2 \pm 36\%$
Earth	$233.8 \text{ watt/m}^2 \pm 20\%$
Sonde	$458 \text{ watt/m}^2 \pm 15\%$

- A. $f_{1,1}$, $f_{2,1}$, $f_{3,1}$ (geometric factors with respect to the sun). Uncertainties of $f_{2,1}$ are 100 percent because there is, in general, no knowledge as to sensor aspect to the sun. The sensor might be completely in the shade or exposed "broadside" to the sun.
- B. $f_{1,3}$, $f_{2,3}$, $f_{3,3}$ (geometric factors with respect to the earth long-wave radiation). As indicated in Appendix D, $f_{3,3}$ varies as the sensor rotates relative to the earth.
If we assume the parachute has less than 45° coning motion, the variation of $f_{2,3}$ and $f_{3,3}$ due to the motion is about 10 percent.
- C. $f_{1,2}$, $f_{2,2}$, $f_{3,2}$ (geometric factor with respect to the earth albedo). The albedo geometric factor is dependent on the position of the sun and cloud distribution, as well as to sensor attitude. The uncertainties in $f_{1,2}$ are estimated to be 15 percent.
- D. $f_{1,4}$, $f_{2,4}$, $f_{3,4}$ (geometric factor with respect to the sonde surfaces or shield). The errors in estimated nominal values, $f_{1,4}$, are estimated to be 3 percent.
- E. I_1 , I_2 , I_3 , I_4 (radianc emittance). The uncertainty of

I_1 is due to the seasonal variation of the distance between the sun and the earth and is estimated to be 1 percent [8, Johnson 1954].

The uncertainty of I_2 is due to the cloud cover variability and is estimated to be 36 percent (see Appendix D).

The uncertainty of I_3 is due to variability of earth surface matter and temperature. The analysis of Tiros II (1960) data by Bandeen [2, 1961] gives about ± 20 percent variation in earth temperature at a given time over the North American continent. Assuming the uncertainty in the effective black body, temperature of the local region of the earth is 5 percent, uncertainty in I_3 is 20 percent.

The uncertainty of I_4 is due to the variability in the sonde temperature and emissivity. Uncertainty in I_4 is arbitrarily estimated to be 15 percent.

Self Heating

An estimation of the power dissipated by the thermistor is about 20×10^{-6} watts [4, Drews 1966]. The uncertainty is due to the temperature dependency of the power dissipation and is estimated to be 15 percent.

Data

Measurement error of T_b is estimated to be 2°K , and the uncertainty in T_b is assumed to be 10 percent. The uncertainty of the rela-

tive velocity, V , is about 5 percent based on the assumed angular motion about the center of mass trajectory recorded by the tracking radar.

Correlation Coefficient $\nu_{m, l}$

For the present study, all parameters are assumed that independent so $\text{cov} \left(p_m^j, p_l^k \right)$ and, therefore, $\nu_{m, l}$ are set equal to zero if $m \neq l$.

4.4 Simulation Study of ARCASONDE 1A System

A. Simulation

Sensor air flow is simulated by computing parachute motion based on the ballistic coefficient and drag [6, Eddy 1965] properties of the ARCASONDE system.

Total parachute-sonde mass $m = 2.33 \text{ kg}$

Parachute reference area $A = 16.4 \text{ m}^2$

The U.S. Standard Atmosphere (1962) will be used for density of the air, ρ .

Initial conditions of the parachute motion are arbitrarily chosen as

Initial altitude 70 km

Horizontal velocity 30 m/s

Vertical velocity -180 m/s

At every second, the altitude and the relative speed with respect to the air are computed. At each altitude, the properties of the air are obtained from the atmosphere table, which already has been read in, including T_{air} . Values of h and r are obtained, based on the given altitude and the air speed. Those values are used in Eq. 4.a and 4.b in order to obtain T_b .

The simulated T_b is used as input \hat{T}_b to the data corrector. Parameter values, p_j , used in the simulator are also used as input \hat{p}_j in the data corrector. Therefore, \hat{T}_{air} is equal to T_{air} . Now the objective of the study is to produce the uncertainty boundary of T_{air} .

The uncertainties in the parameters which were discussed in Section 4.3 are combined with Eq. 13, where sensitivity coefficients are computed by the method discussed in Section 4.2. The computational procedure is shown in Fig. 8.

Notice in Fig. 8 that part A corresponds to the "sensor system" in Fig. 2, and part B corresponds to "data reduction system" in Fig. 2.

B. Results

As shown in Fig. 9, the uncertainty boundary increases rapidly with altitude. This is due to the decrease of convective coupling with the air, while the radiation input remains constant.

As h_b and h_w decrease with altitude, there is more conductive heat flow from the film. The sensor is, therefore, more sensitive to the film temperature as altitude increases. This is clear if you compare the effect of h_b and h_f at 70 and 50 km in Table 5. The uncer-

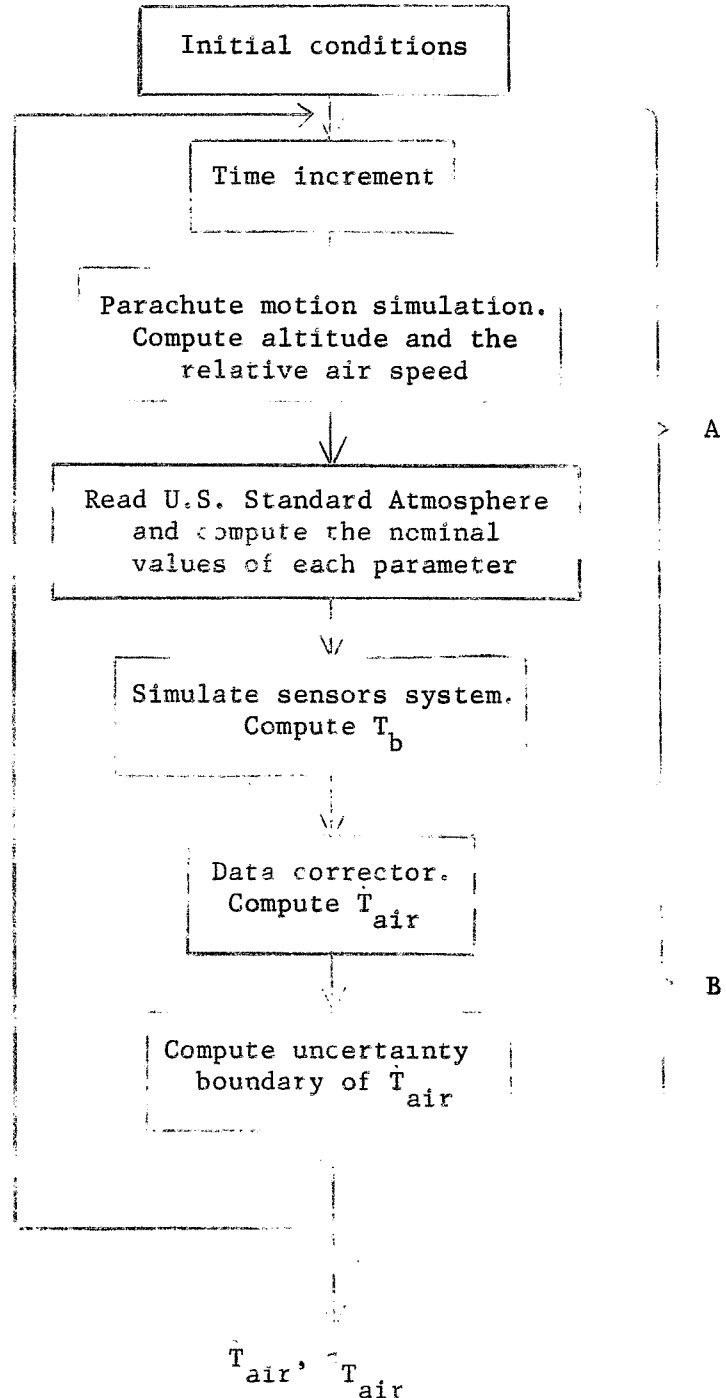


Fig. 8. Block diagram of simulation study.

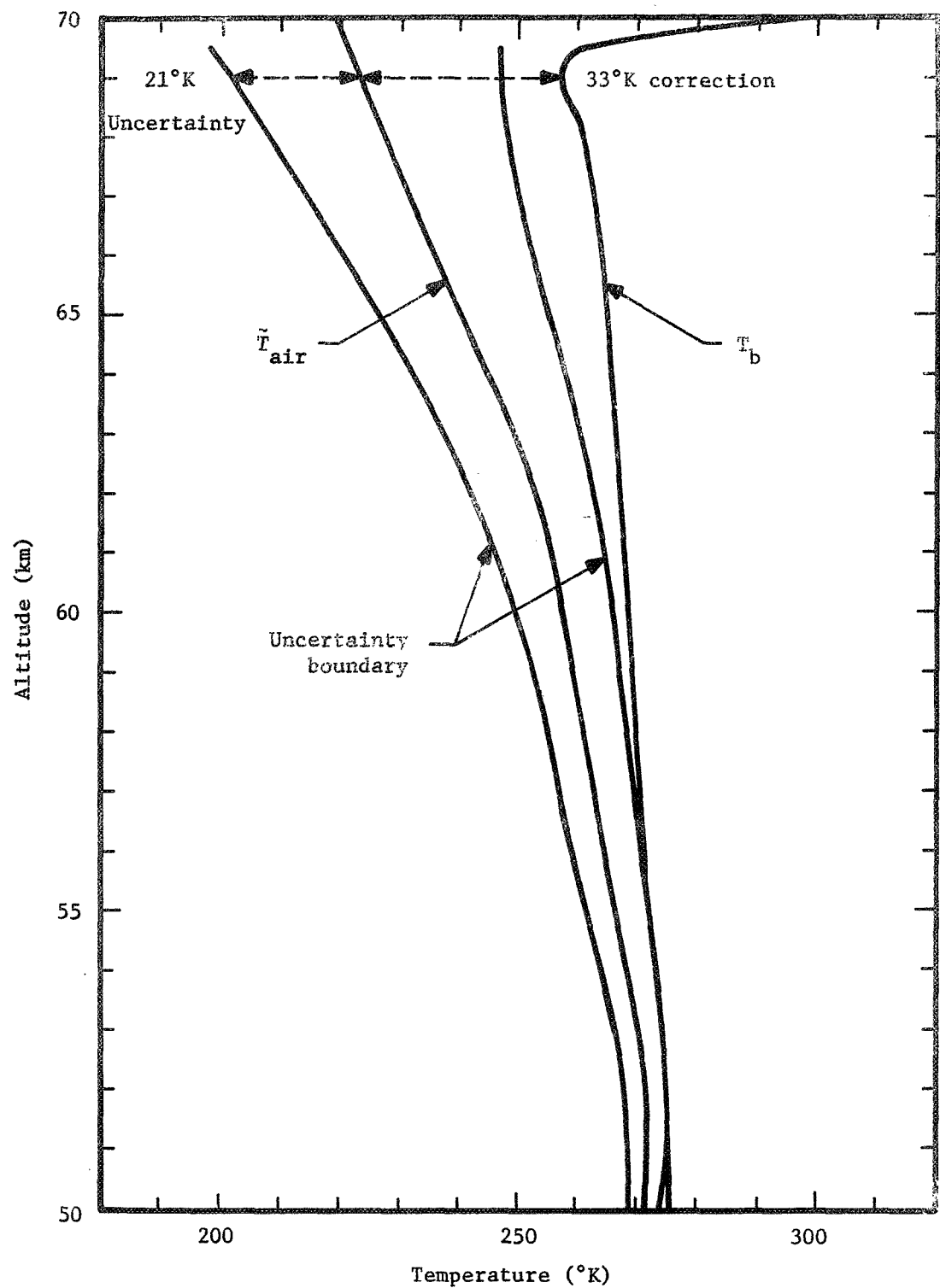


Fig. 9. Uncertainty boundary.

TABLE 5
Uncertainty Components

Altitude (km)	70	65	60	55	50
h_b	.27	.86-1	.63-1	.43-1	.30-1
r_b	.32	.33	.19	.11	.57-1
h_w	.14	.78-2	.37-2	.41-2	.25-2
r_w	.38	.32	.16	.76-1	.48-1
h_f	.35	.11	.29-1	.46-3	.50-2
r_f	.76-1	.51-1	.17-1	.53-2	.16-2
V	1.38	1.16	.56	.27	.13
T_b	3.47	2.34	1.71	1.37	1.19
\dot{T}_b	.23	.59-2	.12-2	.29-3	.18-2
$f_{1,1}$.92	.53	.31	.19	.12
$f_{1,2}$.15	.83-1	.48-1	.29-1	.19-1
$f_{1,3}$.18-1	.10-1	.60-2	.36-2	.23-2
$f_{2,1}$	1.38	.77	.43	.24	.14
$f_{2,2}$.17	.95-1	.53-1	.30-1	.17-1
$f_{2,3}$.33-1	.18-1	.10-1	.57-2	.33-2
$f_{3,1}$	4.17	2.26	1.24	.65	.32
$f_{3,2}$.33	.18	.99-1	.52-1	.26-1
$f_{3,3}$.34	.18	.10	.53-1	.26-1
w_b	.40	.23	.13	.80-1	.51-1
α_b	.48-1	.43-1	.34-1	.26-1	.19-1
α_w	.41-1	.30-1	.21-1	.14-1	.93-2

TABLE 5

(continued)

Uncertainty Components

Altitude (km)	70	65	60	55	50
D_b	.19-1	.16	.94-1	.60-1	.31-1
$(\rho c)_b$.40-1	.15-2	.42-2	.26-3	.93-3
D_w	.11	.24	.14	.93-1	.54-1
k_w	.41-1	.79-1	.49-1	.32-1	.19-1
λ	.66	1.18	.74	.48	.29
$(\rho c)_f$.30	.35-2	.10-2	.97-3	.58-4
D_f	.21	.25-2	.70-3	.68-3	.40-4
$f_{1,4}$.23-2	.15-2	.10-2	.71-3	.50-3
$f_{2,4}$.25-2	.16-2	.11-2	.70-3	.44-3
$f_{3,4}$.51-1	.29-1	.16-1	.85-2	.42-2
α_{sb}	.40	.27	.18	.13	.87-1
α_{sw}	.53	.34	.23	.15	.91-1
α_{sf}	7.59	4.37	2.42	1.26	.62
I_1	.11	.65-1	.37-1	.20-1	.10-1
I_2	2.30	1.35	.78	.43	.23
I_3	1.70	.98	.55	.29	.15
I_4	.28	.96	.92-1	.50-1	.25-1
resultant	23.98	14.06	8.36	4.98	3.20

tainty components listed in Table 5 are the terms

$$\left\{ \sum_{j=0}^i \left(\frac{\partial T_{air}^i}{\partial p_\ell^j} \right)^2 \sigma_{p_\ell^j}^2 \right\}^{1/2}$$

Quantities listed in Tables 5, 8, 9, and 10, pages 39, 46, 48, and 50, respectively, at 70 km are actually those computed at 69.5 km. Those computed at the initial altitude, 70 km, are those at ejection from the rocket and are not of interest here. Values tabulated, nevertheless, exhibit some effect of the initial transient, e.g., the small values at 70 km of ℓ , k_w , D_w .

The sensitivity to error in T_b (measurement error) approaches unity at low altitudes and increases rapidly at high altitudes. As the convective coefficients, h_i , decrease, sensitivity to air temperature decreases; i.e., a given variation in T_b corresponds to increasingly larger variations in T_{air} .

Notice that the uncertainty contribution associated with direct solar heating, $\alpha_s f_{i,1} I_1$, is large compared with other parameters. This suggests that a solar shield would significantly decrease the overall uncertainty. In the following, the ARCASTONDE 1A sensor is assumed to be placed one radius deep into a cylindrical tube. The tube is oriented with its axis parallel to the flow, and with radius sufficiently large so that the boundary layer is away from the sensor.

C. With Shield

The purpose of the shield is to replace a sufficient part of the highly variable natural radiation environment with an environment whose influence on sensor temperature is both small enough and well enough known to enable precise correction of the sensor data.

A shield with a downward view half angle of $\theta = 45^\circ$ is used, and the inside of the shield is painted black. The black painted wall will minimize the effect of radiation arising from reflections within the shield, which would cause large uncertainties. The emissivity of the black paint is assumed to be 1, and the geometric factors are computed by the method discussed in Appendix D. The temperature of the shield is assumed to be $300 \pm 2^\circ\text{K}$. Input values are listed in Tables 6 and 7.

TABLE 6

Nominal Values and Uncertainties of the Geometric Factor (with Shield)

	Sphere	Cylinder	Plate
Sun	0	0	0
Albedo	.147 \pm 15%	.16 \pm 15%	.09 \pm 15%
Earth	.147 \pm 5%	.16 \pm 10%	.09 \pm 10%
Sonde	.853 \pm 3%	.84 \pm 3%	.91 \pm 3%

TABLE 7
Nominal Values and Uncertainties of Radiant Emittance (with Shield)

Sun	0	
Albedo	460.7 watt/m ² ± 36%	
Earth	233.8 watt/m ² ± 20%	
Sonde	458.0 watt/m ² ± 2%	$T_{\text{shield}} = 300^{\circ}\text{K} \pm 2^{\circ}\text{K}$
	221.0 watt/m ² ± 4%	$T_{\text{shield}} = 250^{\circ}\text{K} \pm 2^{\circ}\text{K}$

Figure 10 shows the distinct improvement of performance at high altitude. Comparison of Tables 5 and 8 shows the increase of the effect of uncertainty in h . Increased heating due to the shield increases the sensitivity to h and to other parameters such as λ . This suggests that a colder shield would significantly improve the sensor.

D. Cold Shield

The benefit of a cool shield is investigated by letting the shield temperature be 250°K . The corresponding value of I_4 is included in Table 7.

The results are especially significant at higher altitude as shown in Fig. 11. Notice in Table 8 that uncertainties due to λ , h are much smaller for the cold shield case.

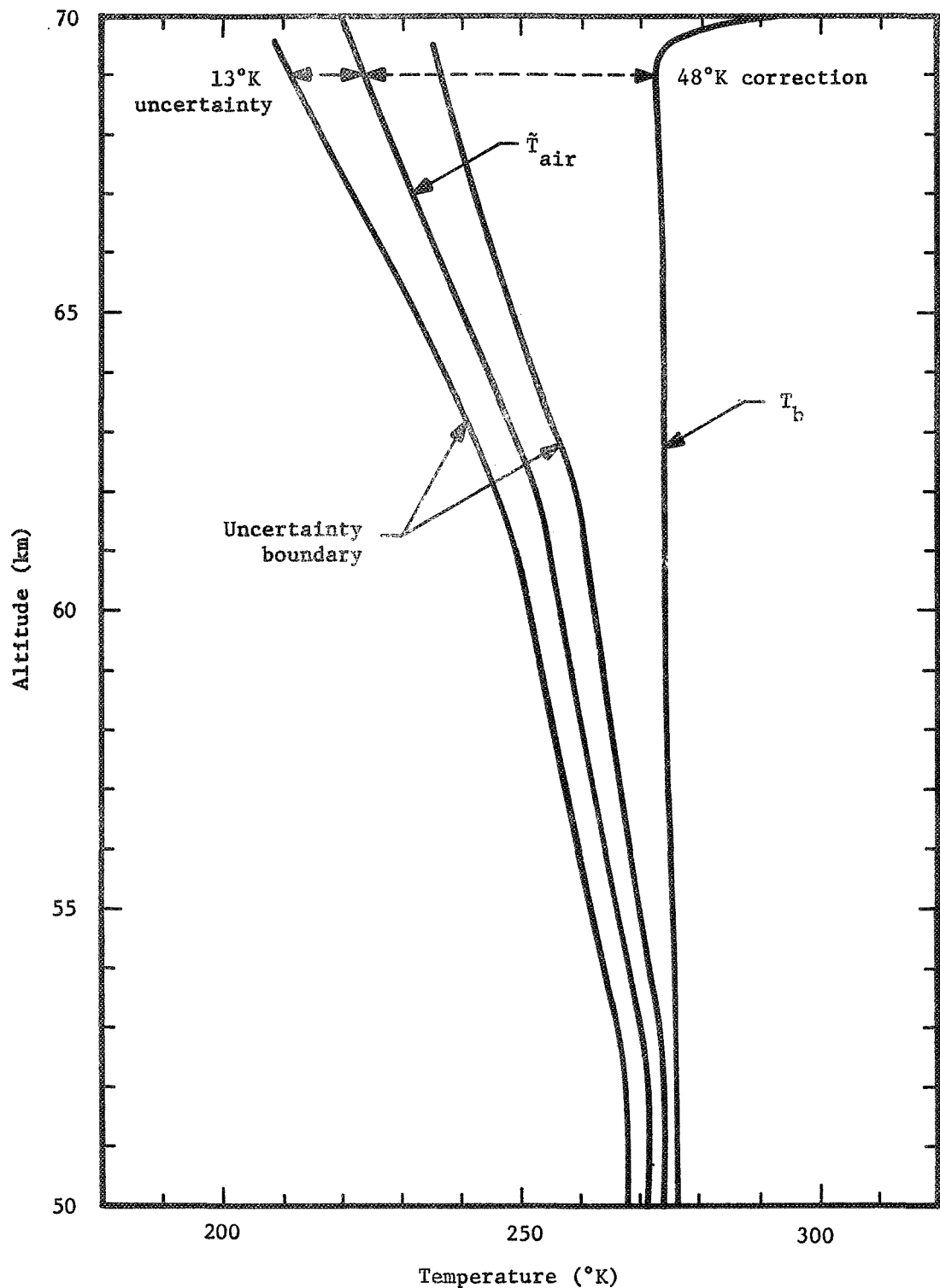


Fig. 10. Uncertainty boundary with a shield.

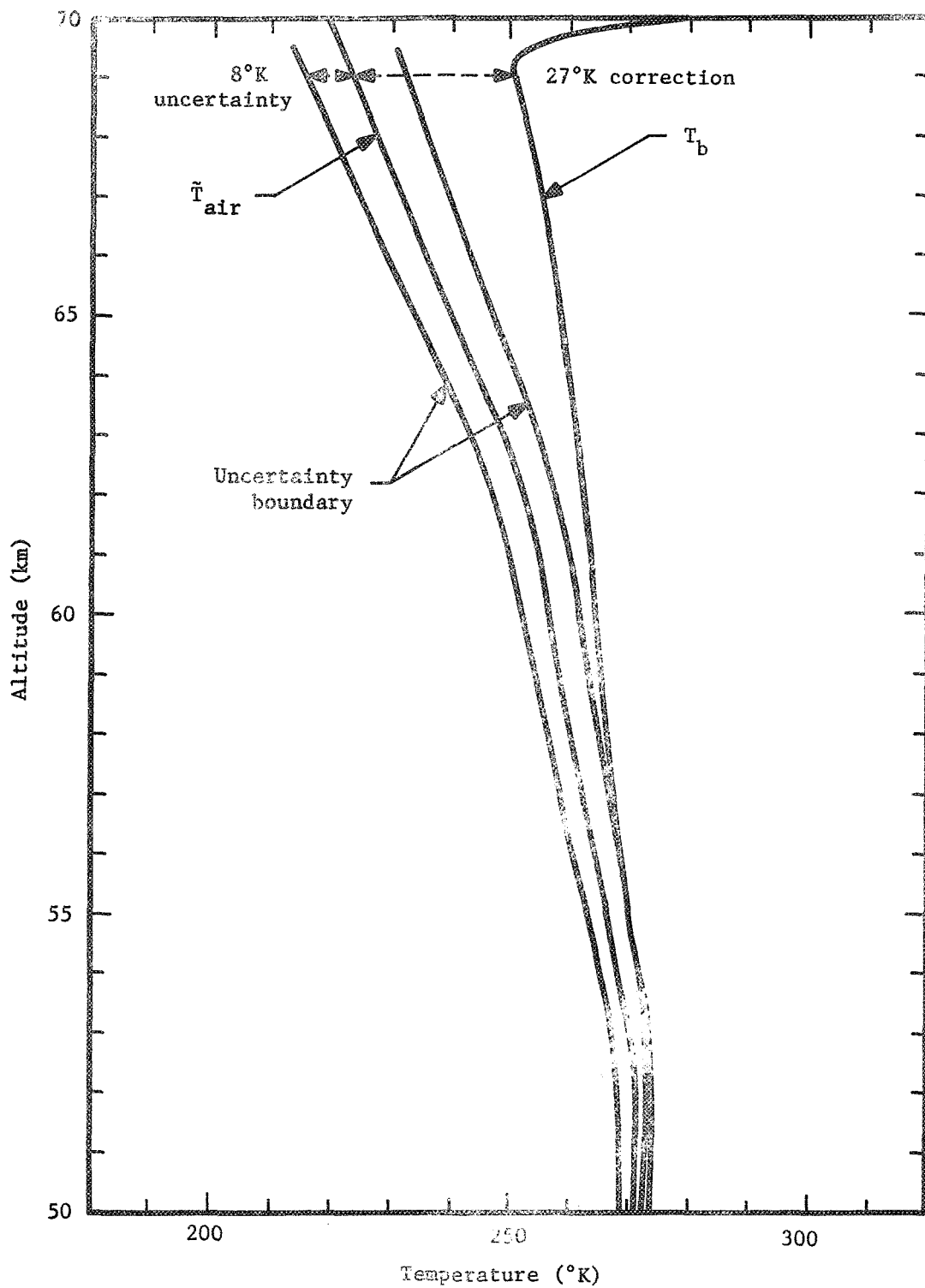


Fig. 11. Uncertainty boundary with cold shield.

TABLE 8
Uncertainty Components (with Shield)

Altitude (km)	70	65	60	55	50
h_b	.55	.31	.20	.12	.72-1
r_b	.32	.33	.19	.11	.57-1
h_w	.38	.19	.14	.91-1	.60-1
r_w	.38	.32	.16	.76-1	.48-1
h_f	.67	.35	.17	.84-1	.40-1
r_f	.74-1	.49-1	.16-1	.52-2	.16-2
V	1.38	1.16	.56	.27	.13
T_b	3.48	2.34	1.71	1.37	1.19
\dot{T}_b	.96-1	.94-3	.32-3	.18-3	.26-2
$f_{1,1}$.0	.0	.0	.0	.0
$f_{1,2}$.53-1	.30-1	.18-1	.11-1	.68-2
$f_{1,3}$.62-2	.35-2	.21-2	.12-2	.79-3
$f_{2,1}$.0	.0	.0	.0	.0
$f_{2,2}$.68-1	.34-1	.21-1	.12-1	.69-2
$f_{2,3}$.12-1	.67-2	.38-2	.21-2	.12-2
$f_{3,1}$.0	.0	.0	.0	.0
$f_{3,2}$.73-1	.40-1	.22-1	.11-1	.57-2
$f_{3,3}$.73-1	.40-1	.22-1	.11-1	.57-2
w_b	.40	.23	.13	.80-1	.51-1
α_b	.60-1	.35-1	.23-1	.15-1	.10-1
α_w	.56-1	.37-1	.25-1	.16-1	.98-2

TABLE 8
(continued)
Uncertainty Components (with Shield)

Altitude (km)	70	65	60	55	50
α_f	3.47	2.13	1.05	.49	.23
D_b	.41	.17	.15	.10	.59-1
$(\rho c)_b$.25-1	.51-3	.16-3	.12-3	.14-2
D_w	.62	.33	.28	.20	.12
k_w	.22	.12	.10	.73-1	.47-1
ℓ	3.56	1.97	1.70	1.21	.79
$(\rho c)_f$.13	.11-2	.17-3	.53-3	.17-3
D_f	.88-1	.76-3	.12-3	.37-3	.12-3
$f_{1,4}$.23-1	.15-1	.10-1	.71-2	.49-2
$f_{2,4}$.21-1	.13-1	.86-2	.55-2	.34-2
$f_{3,4}$	1.0	.57	.32	.17	.82-1
α_{sb}	.79-1	.51-1	.35-1	.24-1	.06-1
α_{sw}	.10	.64-1	.42-1	.27-1	.17-1
α_{sf}	.56	.32	.18	.93-1	.46-1
I_1	.0	.0	.0	.0	.0
I_2	.56	.33	.20	.11	.63-1
I_3	.36	.21	.12	.36-1	.33-1
I_4	.69	.40	.22	.12	.60-1
resultant	13.12	8.16	5.54	3.92	2.94

TABLE 9
Uncertainty Components (Cold Shield)

Altitude (km)	70	65	60	55	50
h_b	.12	.43-1	.26-1	.14-1	.42-2
r_b	.32	.33	.19	.11	.57-1
h_w	.17-1	.11	.80-1	.37-1	.38-1
r_w	.38	.32	.16	.76-1	.48-1
h_f	.22	.12-1	.32-1	.34-1	.23-1
r_f	.77-1	.51-1	.17-1	.53-2	.16-2
V	1.38	1.16	.56	.27	.13
T_b	3.47	2.33	1.71	1.37	1.19
\dot{T}_b	.29	.85-2	.19-2	.35-3	.12-2
$f_{1,1}$.0	.0	.0	.0	.0
$f_{1,2}$.53-1	.30-1	.18-1	.11-1	.70-2
$f_{1,3}$.62-2	.35-2	.21-2	.12-2	.79-3
$f_{2,1}$.0	.0	.0	.0	.0
$f_{2,2}$.68-1	.38-1	.21-1	.12-1	.69-2
$f_{2,3}$.12-1	.68-2	.38-2	.21-2	.12-2
$f_{3,1}$.0	.0	.0	.0	.0
$f_{3,2}$.76-1	.42-1	.23-1	.12-1	.58-2
$f_{3,3}$.76-1	.42-1	.23-1	.12-1	.58-2
w_b	.40	.23	.13	.80-1	.51-1
α_b	.75-2	.95-2	.12-1	.11-1	.94-2
α_w	.34-1	.27-1	.20-1	.14-1	.90-2

TABLE 9
(continued)
Uncertainty Components (Cold Shield)

Altitude (km)	70	65	60	55	50
α_f	.81	.23	.42	.34	.21
D_b	.37-1	.24	.17	.12	.66-1
$(\rho c)_b$.47-1	.19-2	.51-3	.36-3	.61-3
D_w	.21	.34	.26	.18	.11
k_w	.73-1	.12	.88-1	.63-1	.40-1
λ	1.14	1.75	1.33	.98	.64
$(\rho c)_f$.40	.48-2	.14-2	.12-2	.21-5
D_f	.28	.34-2	.99-3	.83-3	.15-5
$f_{1,4}$.11-1	.69-2	.49-2	.34-2	.23-2
$f_{2,4}$.93-2	.60-2	.40-2	.26-2	.16-2
$f_{3,4}$.52	.30	.17	.87-1	.42-1
α_{sb}	.73-1	.48-1	.34-1	.23-1	.16-1
α_{sw}	.94-1	.60-1	.41-1	.26-1	.16-1
α_{sf}	.61	.35	.19	.10	.49-1
I_1	.0	.0	.0	.0	.0
I_2	.59	.35	.21	.12	.65-1
I_3	.39	.23	.13	.68-1	.35-1
I_4	.72	.42	.23	.12	.62-1
resultant	8.60	6.64	4.72	3.56	2.78

TABLE 10
Comparison of Uncertainty Boundary

Altitude(km)	Without Shield(°K)	With Hot Shield(°K)	With Cold Shield(°K)
70	23.98	13.12	8.60
65	14.06	8.16	6.64
60	8.36	5.54	4.72
55	4.98	3.92	3.56
50	3.20	2.94	2.78

V. CONCLUSIONS

The automatic computation of the running error of a measurement system, according to time-varying estimates of error in assumed parameter values, provides a useful quantitative basis for system evaluation and improvement. A plot of the uncertainty boundary about the nominal output value from a simulated system provides a clear graphical model of operational capability. The uncertainty envelope computed along with the reduction of real data provides the user with a convenient indicator of the quality of measurement results.

Results obtained for the current ARCASTONDE 1A sensor indicate that the system uncertainty exceeds the magnitude of the correction for altitudes below about 53 km, so corrections tend to be meaningless for this sensor in the stratosphere and below. The uncertainty appears to remain greater than half the correction throughout the mesosphere (50-80 km). The chief contributing factors to the overall uncertainty are uncertainties in film absorptivity, emissivity, and aspect with respect to the sun. The contribution of an assumed 1°K error in acquiring the sensor temperature is the major contributor at low altitudes.

The hypothetical addition of a simple cylindrical shield to the ARCASTONDE 1A sensor, while increasing its error, considerably improves its performance in terms of greater accuracy after corrections. Corrections may be needed to lower altitude, however, when a shield is used. The increased radiant heat input from the relatively hot

shield at 300°K limits the benefit of a shield. Reducing the shield temperature to 250°K decreases error flux into the sensor sufficient to considerably decrease sensitivity to h_1 and other parameters, as well as to direct solar parameters.

APPENDIX A

APPROXIMATION OF THE RESULTANT STANDARD DEVIATION

The following is a brief examination of the assumptions underlying the relation (Eq. 13) used in this dissertation to compute the overall uncertainty in the corrected temperature.

Expansion of a function of n variables in Taylor's series

$$f(\underline{p}) = \sum_{k=0}^{\infty} \frac{1}{k!} \left[\sum_{j=1}^n \Delta p_j \frac{\partial}{\partial p_j} \right]^k f(\underline{p}) \quad (A.1)$$

Neglecting third-order terms and higher,

$$= f_o + \sum_{j=1}^n \frac{\partial f}{\partial p_j} \Big|_0 \Delta p_j + \frac{1}{2} \sum_{j=1}^n \frac{\partial^2 f}{\partial p_j^2} \Big|_0 \Delta p_j^2 \quad (A.2)$$

$$+ \sum_{i=1}^n \sum_{j=1}^n \frac{\partial^2 f}{\partial p_i \partial p_j} \Big|_0 \Delta p_i \Delta p_j \quad (i \neq j)$$

where Δp_j is the variation of the jth variable from its expected value.

$$\Delta p_j = p_j - \bar{p}_j, \quad \bar{p}_j = p_j \Big|_0 = E[p_j]$$

The coefficients

$$f_0 = a, \frac{\partial f}{\partial p_j} \Big|_0 = b_j, \frac{\partial^2 f}{\partial p_j^2} \Big|_0 = c_j, \frac{\partial^2 f}{\partial p_i \partial p_j} \Big|_0 = d_{ij}$$

are independent of the variation. The expected value of f is then

$$E[f] = a + \frac{1}{2} \sum_{j=1}^n c_j \sigma_j^2 + \sum_{i=1}^n \sum_{j=1}^n d_{ij} \text{cov}(p_i, p_j) \quad (\text{A.3})$$

The terms of the variance, $\sigma_f^2 = E[f^2] - E^2[f]$ of $f(p)$ in the two-variable case are found as follows:

$$f = a + b_1 \Delta p_1 + b_2 \Delta p_2 + \frac{1}{2} c_1 \Delta p_1^2 + \frac{1}{2} c_2 \Delta p_2^2 + d_{12} \Delta p_1 \Delta p_2$$

$$E[f] = a + \frac{1}{2} c_1 \sigma_1^2 + \frac{1}{2} c_2 \sigma_2^2 + d_{12} \text{cov}(p_1, p_2)$$

$E^2(f)$ contains 10 terms and $E(f^2)$ has 19 terms. Their difference after cancellation contains 21 terms.

$$\sigma^2 = E(f^2) - E^2(f) = b_1^2 \sigma_1^2 + b_2^2 \sigma_2^2 + 2b_1 b_2 \text{cov}(p_1, p_2)$$

$$+ b_1 c_1 E(\Delta p_1^3) + b_2 c_2 E(\Delta p_2^3)$$

$$+ (2b_1 d_{12} + b_2 c_1) E(\Delta p_1^2 \Delta p_2)$$

$$+ (2b_2 d_{12} + b_1 c_2) E(\Delta p_1 \Delta p_2^2)$$

$$+ \frac{1}{2} c_1^2 \left[E(\Delta p_1^4) - \sigma_1^4 \right] + \frac{1}{2} c_2^2 \left[E(\Delta p_2^4) - \sigma_2^4 \right]$$

$$+ 2d_{12}^2 \left[E(\Delta p_1 \Delta p_2^2) - \text{cov}^2(p_1, p_2) \right]$$

$$+ \frac{1}{2} c_1 c_2 \left[E(\Delta p_1^2 \Delta p_2^2) - \sigma_1^2 \sigma_2^2 \right]$$

$$+ c_1 d_{12} \left[E(\Delta p_1^3 \Delta p_2) - \sigma_1^2 \text{cov}(p_1, p_2) \right]$$

$$+ c_2 d_{12} \left[E(\Delta p_1 \Delta p_2^3) - \sigma_2^2 \text{cov}(p_1, p_2) \right]$$

If, in addition to the implied initial assumptions that higher order terms in the Taylor's expansion are negligible, it is assumed that the distribution of the p_j 's are symmetrical so that $E(\Delta p_1^3)$ and $E(\Delta p_2^3)$ are small, that $c, d \ll b$, and that third and fourth-order moments are small, then the above rather lengthy expression reduces to

$$\sigma^2 = b_1^2 \sigma_1^2 + b_2^2 \sigma_2^2 + 2b_1 b_2 \operatorname{cov}(p_1, p_2)$$

The corresponding relation for the n-variable case is

$$\sigma_f^2 = \sum_{j=1}^n b_j^2 \sigma_j^2 + 2 \sum_{i=1}^n \sum_{j=1}^n b_i b_j \operatorname{cov}(p_i, p_j) \quad (i \neq j)$$

as can be seen by introducing additional variables from the beginning and dropping small terms. An indication of the validity of Eq. 13 was found by a Monte Carlo computation in which the \tilde{p} 's were generated as random variables. The resulting standard deviation of T_{air} , using normal and uniform distributions for the parameters, with $\sigma_j = \Delta p_j / 2$ and $p_j - \Delta p_j < p_j < p_j + \Delta p_j$, respectively, is compared with $\sigma_{T_{\text{air}}}$ from Eq. 13 in Table A.1. Recall that uncertainty in T_{air} is comparable to twice the standard deviation. The tabulated results are those of the unshielded ARCASONDE 1A, discussed in Section 4.B. The data

corrector routine was repeated 300 times, using subroutine (RANDN) from the UNIVAC 1108 Math Pack as a source of random numbers. Correlation between parameters was small. The comparison is considered quite good indicating that the system equations accommodate the magnitude of the given variation is such that the magnitude of the given variation in parameters does not exceed limits of validity.

TABLE A.1
Comparison of Approximated and Simulated $\sigma_{T_{\text{air}}}$

Altitude	Approximation (°K)	Simulation (normal distribution) (°K)	Simulation (uniform distribution) (°K)
70	11.99	11.71	11.65
65	7.03	7.00	6.98
60	4.18	4.16	4.14
55	2.49	2.48	2.47
50	1.60	1.60	1.59

APPENDIX B

EXPRESSIONS FOR SENSITIVITY COEFFICIENTS

A. The $\frac{\partial f^i}{\partial p^i}$ are computed as follows. Superscript i is omitted in the right-hand members of the following statements since it is obvious.

$$\frac{\partial f^i}{\partial h_b} = \frac{1}{(h_b + H_K K_1)^2} \left[(h_b + H_K K_1) \left(T_b - r_b \frac{v^2}{2c_p} \right) - E1 \right]$$

where

$$E1 = \frac{(\rho c D)_b}{6} \dot{T}_b + \left(h_b + 4\sigma \epsilon_b T_b^3 + H_K \right) T_b$$

$$- \left(h_b r_b \frac{v^2}{2c_p} + 3\sigma \epsilon_b T_b^4 + q_b + H_K P \right) - H_K Q T_f$$

$$\frac{\partial f^i}{\partial r_b} = - \frac{h_b \frac{v^2}{2c_p}}{h_b + H_K K_1}$$

$$\frac{\partial f^i}{\partial h_w} = -E^2 \frac{H_K \frac{\partial K_1}{\partial h_w} + K_1 \frac{\partial H_K}{\partial h_w}}{(h_b + H_K K_1)^2} + \frac{\frac{\partial H_K}{\partial h_w} (h_b + H_K K_1) - H_K \left(H_K \frac{\partial K_1}{\partial h_w} + K_1 \frac{\partial H_K}{\partial h_w} \right)}{(h_b + H_K K_1)^2} T_b$$

$$- \frac{\left(\frac{\partial H_K}{\partial h_w} P + \frac{\partial P}{\partial h_w} H_K \right) (h_b + H_K K_1) - H_K P \left(H_K \frac{\partial K_1}{\partial h_w} + K_1 \frac{\partial H_K}{\partial h_w} \right)}{(h_b + H_K K_1)^2}$$

$$- \frac{\left(\frac{\partial H_K}{\partial h_w} Q + \frac{\partial Q}{\partial h_w} H_K \right) (h_b + H_K K_1) - H_K Q \left(H_K \frac{\partial K_1}{\partial h_w} + K_1 \frac{\partial H_K}{\partial h_w} \right)}{(h_b + H_K K_1)^2} T_f$$

where

$$\frac{\partial \lambda_w}{\partial h_w} = \frac{2}{(kd)_w \lambda_w}$$

$$\frac{\partial H_K}{\partial h_w} = \left(\frac{\partial \lambda_w}{\partial h_w} \right) \left(-C_2 \lambda_w \ell \cosech^2 \lambda_w \ell + C_2 \coth \lambda_w \ell \right)$$

$$\frac{\partial K_1}{\partial h_w} = \frac{\left(h_w + 4\sigma \varepsilon_w T_{aw}^3 \right) h_w \ell_w \operatorname{sech} \lambda_w \ell_w \tanh \lambda_w \ell_w \left(\frac{\partial \lambda}{\partial h_w} \right)}{\left(h_w + 4\sigma \varepsilon_w T_{aw}^3 \right)^2}$$

$$+ \frac{4\sigma \varepsilon_w T_{aw}^3 \left(1 - \operatorname{sech} \lambda_w \ell_w \right)}{\left(h_w + 4\sigma \varepsilon_w T_{aw}^3 \right)^2}$$

$$A(h_w) = 1 - \operatorname{sech} \frac{\lambda_w}{w} \ell$$

$$B(h_w) = h_w r_w \frac{v^2}{2c_p} + \frac{q_w}{A_w} + 3\sigma \epsilon_w T_{aw}^4$$

$$\frac{\partial P}{\partial h_w} = \frac{1}{\left(h_w + 4\sigma \epsilon_w T_{aw}^2 \right)^2} \left[\left[A(h_w) r_w \frac{v^2}{2c_p} + B(h_w) \ell \operatorname{sech} \frac{\lambda_w}{w} \ell \right. \right.$$

$$\left. \tanh \frac{\lambda_w}{w} \ell \left(\frac{\partial \lambda_w}{\partial h_w} \right) \right] \left(h_w + 4\sigma \epsilon_w T_{aw}^3 \right) - A(h_w) B(h_w)$$

$$\frac{\partial Q}{\partial h_w} = - \ell \operatorname{sech} \frac{\lambda_w}{w} \ell \tanh \frac{\lambda_w}{w} \ell \left(\frac{\partial \lambda_w}{\partial h_w} \right)$$

$$E_2 = \frac{(\rho c D)_b}{6} \dot{T}_b + \left(h_b + 4\sigma \epsilon_b T_{ab}^3 \right) T_b - \left(h_b r_b \frac{v^2}{2c_p} + 3\sigma \epsilon_b T_{ab}^4 \frac{W}{A_b} + q_b \right)$$

$$\frac{\partial f^i}{\partial r_w} = - \frac{h_K}{h_b + h_K k_1} \frac{h_w \frac{v^2}{2c_p} \left(1 - \operatorname{sech} \frac{\lambda_w}{w} \ell \right)}{h_w + 4\sigma \epsilon_w T_{aw}^3}$$

$$\frac{\partial f^i}{\partial h_f^i} = 0$$

$$\frac{\partial f^i}{\partial r_f^i} = 0$$

$$\frac{\partial f^i}{\partial V^i} = - \frac{1}{h_b + H_K K_1} \left(h_b r_b \frac{V}{c_p} + H_K \frac{\partial P}{\partial V} \right)$$

where

$$\frac{\partial P}{\partial V} = \frac{h_w r_w V}{c_p} \left(\frac{1 - \operatorname{sech} \lambda_w \ell}{h_w + 4\sigma \epsilon_w T_{aw}^3} \right)$$

$$\begin{aligned} \frac{\partial f^i}{\partial T_b^i} &= \frac{1}{(h_b + H_K K_1)^2} \left\{ \left[h_b + 4\sigma \epsilon_b T_{ab}^3 + \frac{\partial H_K}{\partial T_b} T_b + H_K - \frac{\partial H_K}{\partial T_b} P \right. \right. \\ &\quad \left. \left. - \frac{\partial P}{\partial T_b} H_K - T_f \left(H_K \frac{\partial Q}{\partial T_b} + Q \frac{\partial H_K}{\partial T_b} \right) \right] (h_b + H_K K_1) - E1 \left(\frac{\partial H_K}{\partial T_b} K_1 + \frac{\partial K_1}{\partial T_b} H_K \right) \right\} \end{aligned}$$

where

$$\frac{\partial T_{aw}}{\partial T_b} = \frac{1}{2}$$

$$\frac{\partial \lambda_w}{\partial T_b} = \frac{12\sigma\epsilon_w T_{aw}^2}{\lambda_w (kd)_w}$$

$$\frac{\partial H_K}{\partial T_b} = C_2 \left\{ \frac{\partial \lambda_w}{\partial T_b} \coth \lambda_w \ell - \lambda_w \left(\operatorname{cosech}^2 \lambda_w \ell \right) \ell \frac{\partial \lambda_w}{\partial T_b} \right\}$$

$$\frac{\partial T_{aw}^3}{\partial T_b} = \frac{3}{2} T_{aw}^2$$

$$\frac{\partial K_1}{\partial T_b} = \frac{1}{\left(h_w + 4\sigma\epsilon_w T_{aw}^3 \right)^2} \left[\left(h_w + 4\sigma\epsilon_w T_{aw}^3 \right) \left(h_w \operatorname{sech} \lambda_w \ell \right. \right.$$

$$\left. \tanh \lambda_w \ell \right) \ell \frac{\partial \lambda_w}{\partial T_b} - h_w \left(1 - \operatorname{sech} \lambda_w \ell \right) 4\sigma\epsilon_w \frac{\partial T_{aw}^3}{\partial T_b} \left. \right]$$

$$\frac{\partial T_{aw}^4}{\partial T_b} = 2 T_{aw}^3$$

$$\frac{\partial P}{\partial T_b} = \frac{1}{\left(h_w + 4\sigma\varepsilon_w T_{aw}^3\right)^2} \left\{ \left[\left(\operatorname{sech} \lambda_w \ell \operatorname{tanh} \lambda_w \ell \right) \ell \frac{\partial \lambda_w}{\partial T_b} \right. \right.$$

$$\left. \left(h_w r_w \frac{v^2}{2c_p} + q_w + 3\sigma\varepsilon_w T_{aw}^4 \right) + 6 \left(1 - \operatorname{sech} \lambda_w \ell \right) \sigma\varepsilon_w T_{aw}^3 \right] \left(h_w + 4\sigma\varepsilon_w T_{aw}^3 \right)$$

$$\left. - \left(1 - \operatorname{sech} \lambda_w \ell \right) \left(h_w r_w \frac{v^2}{2c_p} + q_w + 3\sigma\varepsilon_w T_{aw}^4 \right) 6\sigma\varepsilon_w T_{aw}^2 \right\}$$

$$\frac{\partial Q}{\partial T_b} = \left(\operatorname{sech} \lambda_w \ell \operatorname{tanh} \lambda_w \ell \right) \ell \frac{\partial \lambda_w}{\partial T_b}$$

$$\frac{\partial f^i}{\partial T_b^i} = \frac{\rho c D_b}{6 \left(h_b + H_K K_1 \right)}$$

$$\frac{\partial f^i}{\partial f_{11}^i} = \frac{\partial f^i}{\partial q_b} I_1 \alpha_{11}$$

where

$$\frac{\partial f^i}{\partial q_b} = - \frac{1}{h_b + H_K K_1}$$

$$\frac{\partial f^i}{\partial f_{12}^i} = \frac{\partial f^i}{\partial q_b^i} I_2 \alpha_{12}$$

$$\frac{\partial f^i}{\partial f_{13}^i} = \frac{\partial f^i}{\partial q_b^i} I_3 \alpha_{13}$$

$$\frac{\partial f^i}{\partial f_{21}^i} = \frac{\partial f^i}{\partial q_w^i} I_1 \alpha_{21}$$

where

$$\frac{\partial f^i}{\partial q_w^i} = - \frac{H_K}{h_b + H_K K_1} \frac{1 - \operatorname{sech} \frac{\lambda_w k}{w}}{h_w + 4\sigma \epsilon_w T_{aw}^3}$$

$$\frac{\partial f^i}{\partial f_{22}^i} = \frac{\partial f^i}{\partial q_w^i} I_2 \alpha_{22}$$

$$\frac{\partial f^i}{\partial f_{23}^i} = \frac{\partial f^i}{\partial q_w^i} I_3 \alpha_{23}$$

$$\frac{\partial f^i}{\partial f_{31}^i} = 0$$

$$\frac{\partial f^i}{\partial f_{32}^i} = 0$$

$$\frac{\partial f^i}{\partial f_{33}^i} = 0$$

$$\frac{\partial f^i}{\partial w_b^i} = - \frac{1}{h_b + H_K K_1} + \left(\frac{\partial f^i}{\partial T_b} \right) \left(\frac{\partial T_b}{\partial w_b^i} \right)$$

$$\frac{\partial f^i}{\partial \varepsilon_b^i} = \frac{\partial f^i}{\partial q_b^i} \left(f_{13} I_3 + f_{14} I_4 \right) + \frac{\sigma T_b^4}{h_b + H_K K_1}$$

$$\frac{\partial f^i}{\partial \varepsilon_w^i} = \frac{\partial f^i}{\partial H_K} \frac{\partial H_K}{\partial \lambda_w} \frac{\partial \lambda_w}{\partial \varepsilon_w}$$

$$+ \frac{\partial f^i}{\partial K_1} \left(\frac{\partial K_1}{\partial \varepsilon_w} + \frac{\partial K_1}{\partial \lambda_w} \frac{\partial \lambda_w}{\partial \varepsilon_w} \right)$$

$$+ \frac{\partial f^i}{\partial P} \left(\frac{\partial P}{\partial \varepsilon_w} + \frac{\partial P}{\partial \lambda_w} \frac{\partial \lambda_w}{\partial \varepsilon_w} \right) + \frac{\partial f^i}{\partial Q} \frac{\partial Q}{\partial \lambda_w} \frac{\partial \lambda_w}{\partial \varepsilon_w}$$

where

$$\frac{\partial f^i}{\partial H_K} = \frac{1}{(h_b + H_K K_1)^2} \left[(T_b - P - Q T_f) (h_b + H_K K_1) - E_1 K_1 \right]$$

$$\frac{\partial f^i}{\partial K_1} = \frac{1}{(h_b + H_K K_1)^2} - \left[E_1 H_K \right]$$

$$\frac{\partial f^i}{\partial P} = \frac{-H_K}{h_b + H_K K_1}$$

$$\frac{\partial f^i}{\partial Q} = \frac{-H_K T_f}{h_b + H_K K_1}$$

$$\frac{\partial H_K}{\partial \lambda_w} = C_2 \left(\coth \lambda_w \ell - \lambda_w \ell \operatorname{cosech}^2 \lambda_w \ell \right)$$

$$\frac{\partial K_1}{\partial \lambda_w} = \frac{h_w \ell \operatorname{sech} \lambda_w \ell \tanh \lambda_w \ell}{h_w + 4\sigma \epsilon_w T_{aw}^3}$$

$$\frac{\partial Q}{\partial \lambda_w} = - \ell \operatorname{sech} \lambda_w \ell \tanh \lambda_w \ell$$

$$\frac{\partial \lambda_w}{\partial \varepsilon_w} = \frac{8\sigma T_{aw}^3}{\lambda_w (kd)_w}$$

$$\frac{\partial K_1}{\partial \varepsilon_w} = \frac{-h_w (1 - \operatorname{sech} \lambda_w \ell) 4\sigma T_{aw}^3}{(h_w + 4\sigma \varepsilon_w T_{aw}^3)^2}$$

$$\frac{\partial P}{\partial \varepsilon_w} = \frac{1 - \operatorname{sech} \lambda_w \ell}{(h_w + 4\sigma \varepsilon_w T_{aw}^3)^2} \left[3\sigma T_{aw}^4 (h_w + 4\sigma \varepsilon_w T_{aw}^3) \right.$$

$$\left. - \left(h_w r_w \frac{v^2}{2c_p} + q_w + 3\sigma \varepsilon_w T_{aw}^4 \right) 4\sigma T_{aw}^3 \right]$$

$$\frac{\partial f^i}{\partial \dot{\varepsilon}_f} = 0$$

$$\frac{\partial f^i}{\partial D_b} = \frac{1}{(h_b + H_K K_1)^2} \left[\left(\frac{\rho c}{6} \dot{T}_b + T_b \frac{\partial H_K}{\partial D_b} - P \frac{\partial H_K}{\partial D_b} - Q T_f \frac{\partial H_K}{\partial D_b} \right) \right.$$

$$\left. \left(h_b + H_K K_1 \right) - K_1 \frac{\partial H_K}{\partial D_b} E1 \right]$$

where

$$\frac{\partial C_2}{\partial D_b} = \frac{-(kD_w) D_w}{D_b^3}$$

$$\frac{\partial H_K}{\partial D_b} = \lambda_w \coth \lambda_w \ell \left(\frac{\partial C_2}{\partial D_b} \right)$$

$$\frac{\partial f^i}{(\rho c)_b} = \frac{D_b \dot{T}_b}{6 (h_b + H_K K_1)}$$

$$\frac{\partial f^i}{\partial D_w} = \frac{1}{(h_b + H_K K_1)^2} \left[\left\{ T_b \frac{\partial H_K}{\partial D_w} - H_K \frac{\partial P}{\partial D_w} - P \frac{\partial H_K}{\partial E_w} - T_f \left(\frac{\partial H_K}{\partial D_w} Q + \frac{\partial Q}{\partial h_w} H_K \right) \right\} \right.$$

$$\left. (h_b + H_K K_1) - EI \left(\frac{\partial H_K}{\partial D_w} K_1 + \frac{\partial K_1}{\partial D_w} H_K \right) \right]$$

where

$$\frac{\partial C_2}{\partial D_w} = \frac{k_w D_w}{D_b^2}$$

$$\frac{\partial \lambda_w}{\partial D_w} = - \frac{\lambda_w}{2D_w}$$

$$\frac{\partial H_K}{\partial D_w} = \left(\frac{\partial C_2}{\partial D_w} \lambda_w + C_2 \frac{\partial \lambda_w}{\partial D_w} \right) \coth \lambda_w \ell - C_2 \lambda_w \ell \frac{\partial \lambda_w}{\partial D_w} \operatorname{cosech}^2 \lambda_w \ell$$

$$\frac{\partial K_1}{\partial D_w} = \frac{h_w}{h_w + 4\sigma \varepsilon_w T_{aw}^3} \left(\operatorname{sech} \lambda_w \ell \operatorname{tanh} \lambda_w \ell \right) \ell \frac{\partial \lambda_w}{\partial D_w}$$

$$\frac{\partial P}{\partial D_w} = \frac{\left(h_w r_w \frac{v^2}{2c_p} + q_w + 3\sigma \varepsilon_w T_{aw}^4 \right)}{h_w + 4\sigma \varepsilon_w T_{aw}^3} \left(\operatorname{sech} \lambda_w \ell \operatorname{tanh} \lambda_w \ell \right) \ell \frac{\partial \lambda_w}{\partial D_w}$$

$$\frac{\partial Q}{\partial D_w} = - \left(\operatorname{sech} \lambda_w \ell \operatorname{tanh} \lambda_w \ell \right) \ell \frac{\partial \lambda_w}{\partial D_w}$$

$$\frac{\partial f^1}{\partial k_w} = \frac{1}{(h_b + H_K K_1)^2} \left[T_b \frac{\partial H_K}{\partial k_w} - H_K \frac{\partial P}{\partial k_w} - P \frac{\partial H_K}{\partial k_w} - T_f \left(\frac{\partial H_K}{\partial k_w} Q + \frac{\partial Q}{\partial k_w} H_K \right) \right]$$

$$(h_b + H_K K_1) - E1 \left(\frac{\partial H_K}{\partial k_w} K_1 + \frac{\partial K_1}{\partial k_w} H_K \right)$$

where

$$\frac{\partial C_2}{\partial k_w} = \frac{d_w^2}{2d_b^2}$$

$$\frac{\partial \lambda_w}{\partial k_w} = - \frac{\lambda_w}{2k_w}$$

$$\frac{\partial H_K}{\partial k_w} = \left(\frac{\partial C_2}{\partial k_w} \lambda_w + C_2 \frac{\partial \lambda_w}{\partial k_w} \right) \coth \lambda_w \ell - C_2 \lambda_w \ell \frac{\partial \lambda_w}{\partial k_w} \operatorname{cosech}^2 \lambda_w \ell$$

$$\frac{\partial K_1}{\partial k_w} = \frac{h_w}{h_w + 4\sigma \varepsilon_w T_{aw}^3} \left(\operatorname{sech} \lambda_w \ell \operatorname{tanh} \lambda_w \ell \right) \ell \frac{\partial \lambda_w}{\partial k_w}$$

$$\frac{\partial P}{\partial k_w} = \frac{\left(b_w r_w \frac{V^2}{2c_p} + q_w + 3\sigma \varepsilon_w T_{aw}^4 \right)}{h_w + 4\sigma \varepsilon_w T_{aw}^3} \left(\operatorname{sech} \lambda_w \ell \operatorname{tanh} \lambda_w \ell \right) \ell \frac{\partial \lambda_w}{\partial k_w}$$

$$\frac{\partial Q}{\partial k_w} = - \left(\operatorname{sech} \lambda_w \ell \operatorname{tanh} \lambda_w \ell \right) \ell \frac{\partial \lambda_w}{\partial k_w}$$

$$\frac{\partial f^i}{\partial \ell} = \frac{1}{(h_b + H_K K_1)^2} \left[\left((T_b - P) \frac{\partial H_K}{\partial \ell} - H_K \frac{\partial P}{\partial \ell} - T_f \left(\frac{\partial H_K}{\partial \ell} Q + \frac{\partial Q}{\partial \ell} H_K \right) \right) (h_b + H_K K_1) \right. \\ \left. - E_1 \left(\frac{\partial H_K}{\partial \ell} K_1 + H_K \frac{\partial K_1}{\partial \ell} \right) \right]$$

where

$$\frac{\partial H_K}{\partial \ell} = - C_2 \lambda_w^2 \operatorname{cosech}^2 \lambda_w \ell$$

$$\frac{\partial K_1}{\partial \ell} = \frac{h_w r_w}{h_w + 4\sigma \varepsilon_w T_{aw}^3} \operatorname{sech} \lambda_w \ell \operatorname{tanh} \lambda_w \ell$$

$$\frac{\partial P}{\partial \ell} = \frac{\left(h_w r_w \frac{v^2}{2c_p} + q_w + 3\sigma \varepsilon_w T_{aw}^4 \right) \lambda_w \operatorname{sech} \lambda_w \ell \operatorname{tanh} \lambda_w \ell}{h_w + 4\sigma \varepsilon_w T_{aw}^3}$$

$$\frac{\partial Q}{\partial \ell} = - \lambda_w \operatorname{sech} \lambda_w \ell \operatorname{tanh} \lambda_w \ell$$

$$\frac{\partial f^i}{\partial (\rho c)_f} = 0$$

$$\frac{\partial f^i}{\partial D_f} = 0$$

$$\frac{\partial f^i}{\partial f_{14}} = \frac{\partial f^i}{\partial q_b} \alpha_{14} I_4$$

$$\frac{\partial f^i}{\partial f_{24}} = \frac{\partial f^i}{\partial q_w} \alpha_{24} I_4 = \left(\frac{h_K}{h_b + h_K K_L} \right) \left(\frac{1 - \operatorname{sech} \lambda_w \ell}{h_w + 4\sigma \varepsilon_w T_{aw}^3} \right) \alpha_{24} I_4$$

$$\frac{\partial f^i}{\partial f_{34}} = 0$$

$$\frac{\partial f^i}{\partial \alpha_{11}} = \frac{\partial f^i}{\partial q_b} (f_{11} I_1 + f_{12} I_2)$$

$$\frac{\partial f^i}{\partial \alpha_{21}} = \frac{\partial f^i}{\partial q_w} (f_{21} I_1 + f_{22} I_2)$$

$$\frac{\partial f^i}{\partial \alpha_{31}} = 0$$

$$\frac{\partial f^i}{\partial I_1} = \frac{\partial f^i}{\partial q_b} f_{11} \alpha_{11} + \frac{\partial f^i}{\partial q_w} f_{21} \alpha_{21}$$

$$\frac{\partial f^i}{\partial I_2} = \frac{\partial f^i}{\partial q_b} f_{12} \alpha_{12} + \frac{\partial f^i}{\partial q_w} f_{22} \alpha_{22}$$

$$\frac{\partial f^i}{\partial I_3} = \frac{\partial f^i}{\partial q_b} f_{13} \alpha_{13} + \frac{\partial f^i}{\partial q_w} f_{23} \alpha_{23}$$

$$\frac{\partial f^i}{\partial I_4} = \frac{\partial f^i}{\partial q_b} f_{14} \alpha_{14} + \frac{\partial f^i}{\partial q_w} f_{24} \alpha_{24}$$

B. Computation of $\frac{\partial f^i}{\partial T_f^i}$. Grouping the set of quantities H_K^i , K_1^i , $P^i Q^i$ as elements of a vector \tilde{G}

$$G^i (T_f, \tilde{P}) = \begin{bmatrix} H_K^i (T_f^i, \tilde{P}^i) \\ K_1^i (T_f^i, \tilde{P}^i) \\ P^i (T_f^i, \tilde{P}^i) \\ Q^i (T_f^i, \tilde{P}^i) \end{bmatrix}$$

$$\frac{\partial f^i}{\partial T_f^i} = \frac{\partial f^i}{\partial G^i} \frac{\partial G^i}{\partial T_f^i}$$

where $\frac{\partial f^i}{\partial G^i}$ and $\frac{\partial G^i}{\partial T_f^i}$ are given as follows:

$$\frac{\partial f^i}{\partial G^i} = \left(\frac{\partial f}{\partial H_K}, \frac{\partial f}{\partial K_1}, \frac{\partial f}{\partial Q}, \frac{\partial f}{\partial P} \right)$$

$$\frac{\partial f}{\partial H_K} = \frac{1}{(h_b + H_K K_1)} \left[(T_b - P - Q T_f) (h_b + H_K K_1) - E1 K_1 \right]$$

$$\frac{\partial f}{\partial K_1} = - \frac{1}{(h_b + H_K K_1)^2} [E1 H_K]$$

$$\frac{\partial f}{\partial P} = - \frac{H_K}{h_b + H_K K_1}$$

$$\frac{\partial f}{\partial Q} = - \frac{H_K T_f}{h_b + H_K K_1}$$

$$\frac{\partial \tilde{G}^i}{\partial T_f^i} = \begin{bmatrix} \frac{\partial H_K}{\partial T_f} \\ \frac{\partial K_1}{\partial T_f} \\ \frac{\partial P}{\partial T_f} \\ \frac{\partial Q}{\partial T_f} \end{bmatrix}$$

$$\frac{\partial H_K}{\partial T_f} = C_2 \left(\coth \lambda_w \ell - \lambda_w \ell \operatorname{cosech}^2 \lambda_w \ell \right) \left(\frac{\partial \lambda_w^i}{\partial T_f^i} \right)$$

$$\frac{\partial K_1}{\partial T_f} = \frac{1}{\left(h_w + 4\sigma \epsilon_w T_{aw}^3 \right)^2} \left[\left(h_w + 4\sigma \epsilon_w T_{aw}^3 \right) \left(h_w \operatorname{sech} \lambda_w \ell \right. \right.$$

$$\left. \tanh \lambda_w \ell \right) \ell \frac{\partial \lambda_w}{\partial T_f} - h_w \left(1 - \operatorname{sech} \lambda_w \ell \right) 6\sigma \epsilon_w T_{aw}^2 \Big]$$

$$\frac{\partial P}{\partial T_f} = \frac{1}{\left(h_w + 4\sigma\varepsilon_w T_{aw}^3\right)^2} \left\{ \left[\left(\operatorname{sech} \lambda_w \ell \operatorname{tanh} \lambda_w \ell \right) \ell \frac{\partial \lambda_w}{\partial T_f} \right. \right.$$

$$\left. \left(h_w r_w \frac{v^2}{2c_p} + q_w + 3\sigma\varepsilon_w T_{aw}^4 \right) + 6 \left(1 - \operatorname{sech} \lambda_w \ell \right) \sigma\varepsilon_w T_{aw}^3 \right]$$

$$\left(h_w + 4\sigma\varepsilon_w T_{aw}^3 \right) - \left(1 - \operatorname{sech} \lambda_w \ell \right) \left(h_w r_w \frac{v^2}{2c_p} + q_w \right.$$

$$\left. + 3\sigma\varepsilon_w T_{aw}^4 \right) 6\sigma\varepsilon_w T_{aw}^2 \Bigg\}$$

$$\frac{\partial Q}{\partial T_f} = - \ell \operatorname{sech} \lambda_w \ell \operatorname{tanh} \lambda_w \ell \left(\frac{\partial \lambda_w}{\partial T_f} \right)$$

where

$$\frac{\partial \lambda_w}{\partial T_f} = \frac{12\sigma\varepsilon_w T_{aw}^2}{(kd)_w \lambda_w}$$

C. $\frac{\partial g^i}{\partial T_f^{i-1}}$, $\frac{\partial g^i}{\partial T_{air}^{i-1}}$, and $\frac{\partial g^i}{\partial p_\ell^{i-1}}$ are computed as follows, this case omitting superscript $i-1$ in the right-hand members.

$$\frac{\partial g^i}{\partial T_f^i - 1} = 1 - \frac{2\Delta t}{(\rho c D)_f} h_f - \frac{8\Delta t \sigma \epsilon_f}{(\rho c D)_f} T_f^3$$

$$\frac{\partial g^i}{\partial T_{air}^i - 1} = 2h_f \frac{\Delta t}{(\rho c D)_f}$$

$$\frac{\partial g^i}{\partial h_f^i - 1} = \frac{2\Delta t}{(\rho c D)_f} \left(r_f \frac{v^2}{2c_p} - T_f + T_{air} \right)$$

$$\frac{\partial g^i}{\partial r_f^i - 1} = \frac{2\Delta t}{(\rho c D)_f} h \frac{v^2}{2c_p}$$

$$\frac{\partial g^i}{\partial V} = \frac{2\Delta t}{(\rho c D)_f} h_f r_f \frac{v}{c_p}$$

$$\frac{\partial g^i}{\partial (\rho c)_f} = - \frac{E3}{(\rho c)_f^2 D_f}$$

$$\frac{\partial g^i}{\partial D_f} = - \frac{E3}{(\rho c)_f D_f^2}$$

where

$$E_3 = -2\Delta t \left(h_f + \sigma \epsilon_f T_f^3 \right) T_f + 2\Delta t \left(q_f + h_f r_f \frac{V^2}{2c_p} \right) + 2\Delta t h_f T_{air}$$

$$\frac{\partial g^i}{\partial f_{31}} = \left(\frac{\partial g^i}{\partial q_f} \right) (\alpha_{31} I_1)$$

$$\frac{\partial g^i}{\partial f_{32}} = \left(\frac{\partial g^i}{\partial q_f} \right) (\alpha_{32} I_2)$$

$$\frac{\partial g^i}{\partial f_{33}} = \left(\frac{\partial g^i}{\partial q_f} \right) (\alpha_{33} I_3)$$

$$\frac{\partial g^i}{\partial f_{34}} = \left(\frac{\partial g^i}{\partial q_f} \right) (\alpha_{34} I_f)$$

where

$$\frac{\partial g^i}{\partial q_f} = \frac{2\Delta t}{(\rho c D)_f}$$

$$\frac{\partial g^i}{\partial \varepsilon_f} = - \frac{2\Delta t}{\rho c D_f} \sigma T_f^4 + \frac{\partial g^i}{\partial q_f} (f_{33} I_3 + f_{34} I_4)$$

$$\frac{\partial g^i}{\partial I_1} = \frac{\partial g^i}{\partial q_f} f_{31} \alpha_{31}$$

$$\frac{\partial g^i}{\partial I_2} = \frac{\partial g^i}{\partial q_f} f_{32} \alpha_{32}$$

$$\frac{\partial g^i}{\partial I_3} = \frac{\partial g^i}{\partial q_f} f_{33} \alpha_{33}$$

$$\frac{\partial g^i}{\partial I_4} = \frac{\partial g^i}{\partial q_f} f_{34} \alpha_{34}$$

$$\frac{\partial g^i}{\partial \alpha_{31}} = \frac{\partial g^i}{\partial q_f} (f_{31} I_1 + f_{32} I_2)$$

APPENDIX C

SENSITIVITY OF TIME INVARIANT PARAMETERS

The computation of the sensitivity coefficient for constant parameters is a special case of the computation for time variant parameters.

Suppose the system is described as

$$x^{i+1} = f^i(x^i, p^i)$$

and if $p^i \neq p^j$ when $i \neq j$, then

$$\frac{\partial x^{i+1}}{\partial p^i} = \frac{\partial f^i}{\partial p^i}$$

$$\frac{\partial x^{i+1}}{\partial p^{i-1}} = \frac{\partial f^i}{\partial x^i} \frac{\partial x^i}{\partial p^{i-1}}$$

$$\frac{\partial x^{i+1}}{\partial p^{i-2}} = \frac{\partial f^i}{\partial x^i} \frac{\partial x^i}{\partial x^{i-1}} \frac{\partial x^{i-1}}{\partial p^{i-2}}$$

$$\begin{array}{ll} \cdot & \cdot \\ \cdot & \cdot \\ \cdot & \cdot \end{array}$$

$$\frac{\partial x^{i+1}}{\partial p^0} = \frac{\partial f^i}{\partial x^i} \frac{\partial x^i}{\partial x^{i-1}} \frac{\partial x^{i-1}}{\partial x^{i-2}} \dots \frac{\partial x^1}{\partial p^0}$$

Now if $p^i = p^j$ for $i \neq j$, then p^i and p^j are completely correlated, then

$$\sigma_{T_{\text{air}}^{i+1}} = \sum_{j=0}^i \frac{\partial X^{i+1}}{\partial p^j} \sigma_{p^j}$$

$$\text{Assuming } \sigma_{p^j} = \sigma_p$$

$$\sigma_{T_{\text{air}}^{i+1}} = \sum_{j=0}^i \frac{\partial X^{i+1}}{\partial p^j} \sigma_p$$

$$= \left(\frac{\partial f^i}{\partial p^i} + \frac{\partial f^i}{\partial X^i} \frac{\partial X^i}{\partial p^{i-1}} \right.$$

$$+ \frac{\partial f^i}{\partial X^i} \frac{\partial X^i}{\partial X^{i-1}} \frac{\partial X^{i-1}}{\partial p^{i-2}} + \frac{\partial f^i}{\partial X^i} \frac{\partial X^i}{\partial X^{i-1}} \frac{\partial X^{i-1}}{\partial X^{i-2}} \frac{\partial X^{i-2}}{\partial p^{i-3}}$$

$$\left. + \frac{\partial f^i}{\partial X^i} \frac{\partial X^i}{\partial X^{i-1}} \frac{\partial X^{i-1}}{\partial X^{i-2}} \dots \frac{\partial X^2}{\partial X^1} \frac{\partial X^1}{\partial p} \right) \sigma_p$$

$$= \left(\frac{\partial f^i}{\partial p^i} + \frac{\partial f^i}{\partial X^i} \left\{ \frac{\partial f^{i-1}}{\partial p^{i-1}} + \frac{\partial f^{i-1}}{\partial X^{i-1}} \left[\frac{\partial X^{i-1}}{\partial p^{i-2}} + \frac{\partial X^{i-1}}{\partial X^{i-2}} \frac{\partial X^{i-2}}{\partial p^{i-3}} \right. \right. \right. \right.$$

$$\left. \left. \left. \left. + \dots + \frac{\partial X^{i-1}}{\partial X^{i-2}} \dots \frac{\partial X^2}{\partial X^1} \frac{\partial X^1}{\partial p} \right] \right] \right\} \right) \sigma_p$$

$$\begin{aligned}
&= \left(\frac{\partial f^i}{\partial p} + \frac{\partial f^i}{\partial x^i} \left\{ \frac{\partial f^{i-1}}{\partial p} + \frac{\partial f^{i-1}}{\partial x^{i-1}} \left[\frac{\partial x^{i-1}}{\partial p} + \frac{\partial x^{i-1}}{\partial x^{i-2}} \frac{\partial x^{i-2}}{\partial p} \right. \right. \right. \\
&\quad \left. \left. \left. + \cdots + \frac{\partial x^{i-1}}{\partial x^{i-2}} \cdots \frac{\partial x^2}{\partial x^1} \frac{\partial x^1}{\partial p} \right] \right\} \right) \sigma_p
\end{aligned}$$

The coefficient of σ_p is the solution of the following difference equation:

$$\frac{\partial x^i + 1}{\partial p} = \frac{\partial f^i}{\partial p} + \frac{\partial f^i}{\partial x^i} \frac{\partial x^i}{\partial p}$$

Therefore

$$\sigma_{T_{air}^{i+1}} = \frac{\partial x^{i+1}}{\partial p} \sigma_p = \sum_{j=0}^i \frac{\partial x^{i+1}}{\partial p^j} \sigma_p$$

APPENDIX D

RADIATION HEAT TRANSFER

The radiative heat input power to the sensor is given by the general expression,

$$Aq_R = \int_A \int_{\Omega} \int_{\lambda} \frac{\cos \theta}{\pi} \alpha_{\lambda} \varepsilon_{\lambda} E_{b\lambda}(T) d\lambda d\Omega dA \quad (D.1)$$

where

α_{λ} = spectral absorptivity of the body

ε_{λ} = spectral emissivity of the source in $d\Omega$

$E_{b\lambda}(T)$ = plank radiant energy spectral distribution function for the source in $d\Omega$ at temperature T

λ = solid angle subtended by the environment

A = total sensor surface area

θ = angle between sensor surface element dA and the direction toward $d\Omega$

λ = radiation wavelength

Consider the four principal environmental radiation sources seen by the sensor:

j = 1 sun

j = 2 earth and atmosphere as a source of reflected solar radiation

j = 3 earth and atmosphere as a long wave source

j = 4 sonde parts (including shield) in view of the sensor

Assuming the radiant emittance

$$I_j = \int_0^{\infty} \varepsilon_{\lambda j} E_{b\lambda}(T_j) d\lambda \quad (D.2)$$

and the mean absorptivity

$$\bar{\alpha}_j = \frac{\int_0^{\infty} \alpha_{\lambda j} \varepsilon_{\lambda j} E_{b\lambda}(T_j) d\lambda}{I_j}$$

are independent of the angle (taken as an appropriate mean value, if necessary and practical, for this assumption), then the geometric factor, f_j

$$f_j = \frac{1}{A} \int_A \int_{\Omega_j} \cos \theta dA \frac{d\Omega_j}{\pi} \quad (D.3)$$

may be calculated separately and treated as a multiplicative factor, and the radiation input term takes the form

$$q_R = \sum_j \bar{\alpha}_j f_j I_j \quad (D.4)$$

Geometric Factor f_j

- A. $f_{1,1}, f_{2,1}, f_{3,1}$ (geometric factor with respect to the sun). The solid angle subtended by the sun is $\pi R_s^2 / D_{es}$, where R_s is the radius of the sun and D_{es} is the distance between the earth and the sun. Then, referring to Eq.

D.3

$$f_{11} = \frac{R_s^2}{D_{es}} \int_A \cos \theta dA$$

The computed value of $f_{1,1}$ is listed in Table 3.

- B. $f_{1,4}, f_{2,4}, f_{3,4}$ (geometric factor with respect to the sonde). Figure D.1 shows $f_4(\theta_0)$ for the three shapes when the sonde surfaces occupy a "polar cap" with half-angle θ_0 as shown in the figure [14, Staffanson 1969]. The curves are given by

$$\begin{aligned} f_4 &= 0.5 (1 - \cos \theta_0) \\ &= (\theta_0 - 0.5 \sin 2\theta_0) / \pi \end{aligned}$$

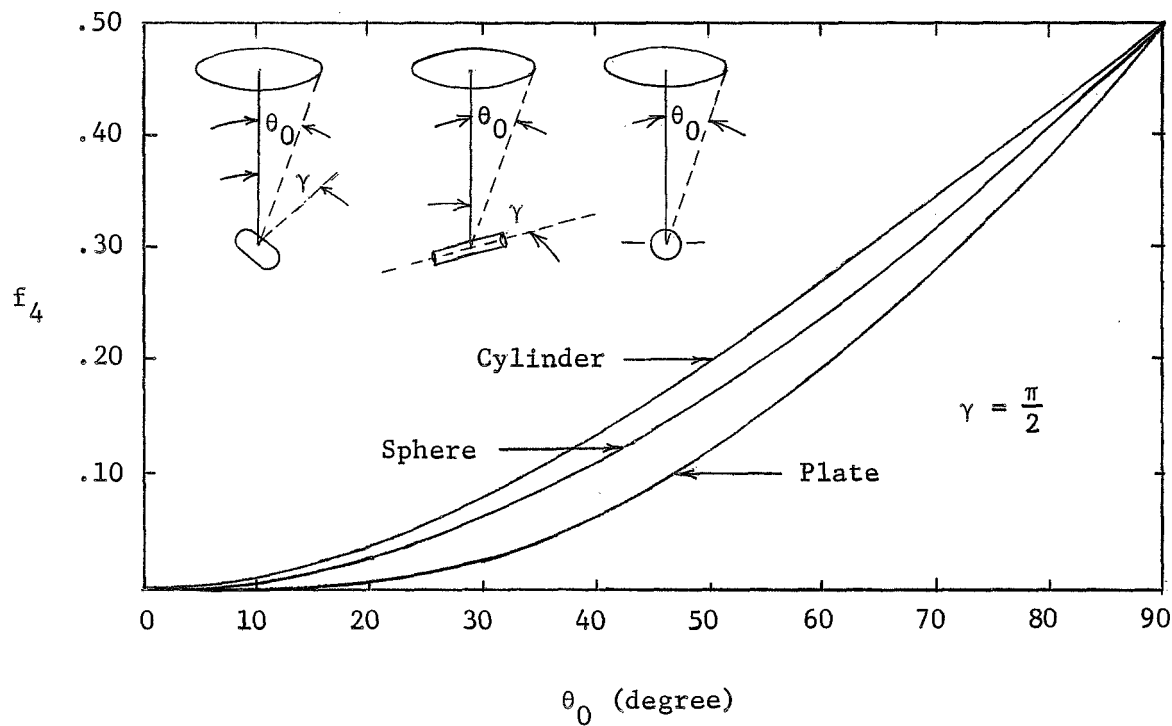


Fig. D.1. Geometric factor for the three sensor shapes of a circular region located 90 degrees from the sensor axis subtending half-angle θ_0 .

for the sphere and plate, respectively, and by numerical tables from Ballinger [1, 1960]. A half angle of 35° approximates that for the ARCAISONDE 1A.

- C. $f_{1,3}, f_{2,3}, f_{3,3}$ (geometric factor for thermal radiation from the earth). The geometric factors associated with the earth long-wave radiation are computed by the

method used for $f_{i,4}$. Nominal value of $f_{i,4}$ is computed, based on $\gamma = \frac{\pi}{2}$ and the uncertainty is due to the fact that the parachute might have a coning motion which varies γ .

D. $f_{1,2}, f_{2,2}, f_{3,2}$ (geometric factor with respect to earth albedo). Unlike the thermal geometric factor, the albedo geometric factor is dependent on the position of the sun. The values presented in Table 3 are based on the assumption that the sun is high enough to illuminate essentially all of the earth under the sensor.

Radiant Emittance I_j

Values for the radiant emittance, I_j , together with an estimated uncertainty for each source, j , are as follows:

$$A. I_1 = \left(\frac{r_{es}}{r_s} \right)^2 S = 6.456 \times 10^7 \text{ watts/m}^2 \pm 1\%$$

In the calculation of I_1 , r_{es} is the mean earth-to-sun distance 9.29×10^7 mi, r_s is the radius of the sun 4.32×10^5 mi, and S is the solar constant,

$$S = \int_0^{\infty} \epsilon_{\lambda} E_{b\lambda} d\lambda = 1396 \text{ watts/m}^2 \pm 1\% \quad [8, \text{Johnson 1954}]$$

$$B. I_2 = aS = 460.7 \text{ watts/m}^2 \pm 36\%$$

Here, a is the albedo of the earth. It has been estimated

that clouds can reflect back to space 50 percent or more of the solar flux and absorb another 20 percent. The portions of the earth covered with water reflect about 5 percent of the total radiation reaching them, and the land masses, on the average, reflect slightly more [12, Snoddy 1965].

Therefore, cloud cover becomes a very important factor in determining the earth's albedo. P. F. Clapp [3, 1962] presents cloud cover data using Tiro's nephanalysis, showing cloud cover for various seasons at different latitudes on the earth. By averaging cloudiness for the four seasons, assuming values of reflectance of clouds and the surface of the earth, curves of albedo versus latitude were obtained. From this information it was possible to make some estimation of the effect of cloud cover on albedo. Assuming that clouds reflect 50 percent and the surface of the earth reflects 5 percent, the average albedo is about 0.33, with a variability of ± 0.12 or 36 percent.

C. $I_3 = 233.8 \text{ watts/m}^2 \pm 20\%$

The earth's long-wave emittance depends on the surface temperature and its emission characteristics. Neglecting details of the planet surface, it is possible to compute the average energy radiated by a planet using a thermal balance based on the solar radiation absorbed by the planet.

As the temperature of most planets do not vary appreciably over extended periods, it can be concluded that the thermally radiated energy is equivalent to the absorbed solar energy.

Using S as the solar heat flux per unit projected area of the planet (as seen from the sun), a as the planetary albedo, R as the planet radius, and I as the thermal energy radiated per average unit planet area and time, the energy balance is

$$(1 - a) S\pi R^2 = f\pi R^2 I$$

or

$$I = \frac{1 - a}{4} S$$

I_3 for the earth computed by this method equals 233.8 watts/m² \pm 20%, using 36 percent variability in a . Actual measurements of earth long-wave radiation have been made by Tiros II (1960) and Tiros IV (1966). Bandeen [2, 1961] analyzed the Tiros II data, and the results fall within this 20 percent uncertainty.

D. $I_4 = 458 \text{ watts/m}^2 \pm 15, \pm 3\% \text{ (shield)}$

The radiant emittance of the sonde can be found by using the relation $I_4 = \sigma\varepsilon T_4^4$. T_4 is assumed to be 300°K and

$\epsilon_4 = 1.0$. Small f_4 renders this magnitude essentially insignificant. In the case of the shield, however, f_4 is much larger, but T_4 is assumed measured to within 2°K , and the shield interior is assumed black, both by its coating and by the effect of reflections within its concave interior surfaces.

APPENDIX E
SIMULATION PROGRAM

Fortran V was used to program the simulation study discussed in Chapter IV. The organization of the programming is summarized in the flow diagram, Fig. E.1.

In the main program the environmental conditions are established, and thermal properties of the sensors are assigned. Initial conditions and uncertainties of each parameter are also stated in the main program.

Subroutine TRAJ generates the motion of the parachute with given initial conditions and parachute dimensions. Subroutine ATMO is called from TRAJ to find the necessary atmosphere conditions at a given altitude. Computation will be terminated when the parachute reaches to a lower limit in altitude.

Subroutine SIMULA is called and the temperature of the sensor is computed. Subroutine HANDR is called from SIMULA to calculate necessary values of h and r .

HANDR subprogram calls ATMO for necessary atmosphere conditions. INTRE and INTKN are called from HANDR to calculate uncertainties in h and r .

After SIMULA computes T_b , subroutine REDUCT is called and \tilde{T}_{air} is computed. The uncertainty boundary of \tilde{T}_{air} is also computed in REDUCT.

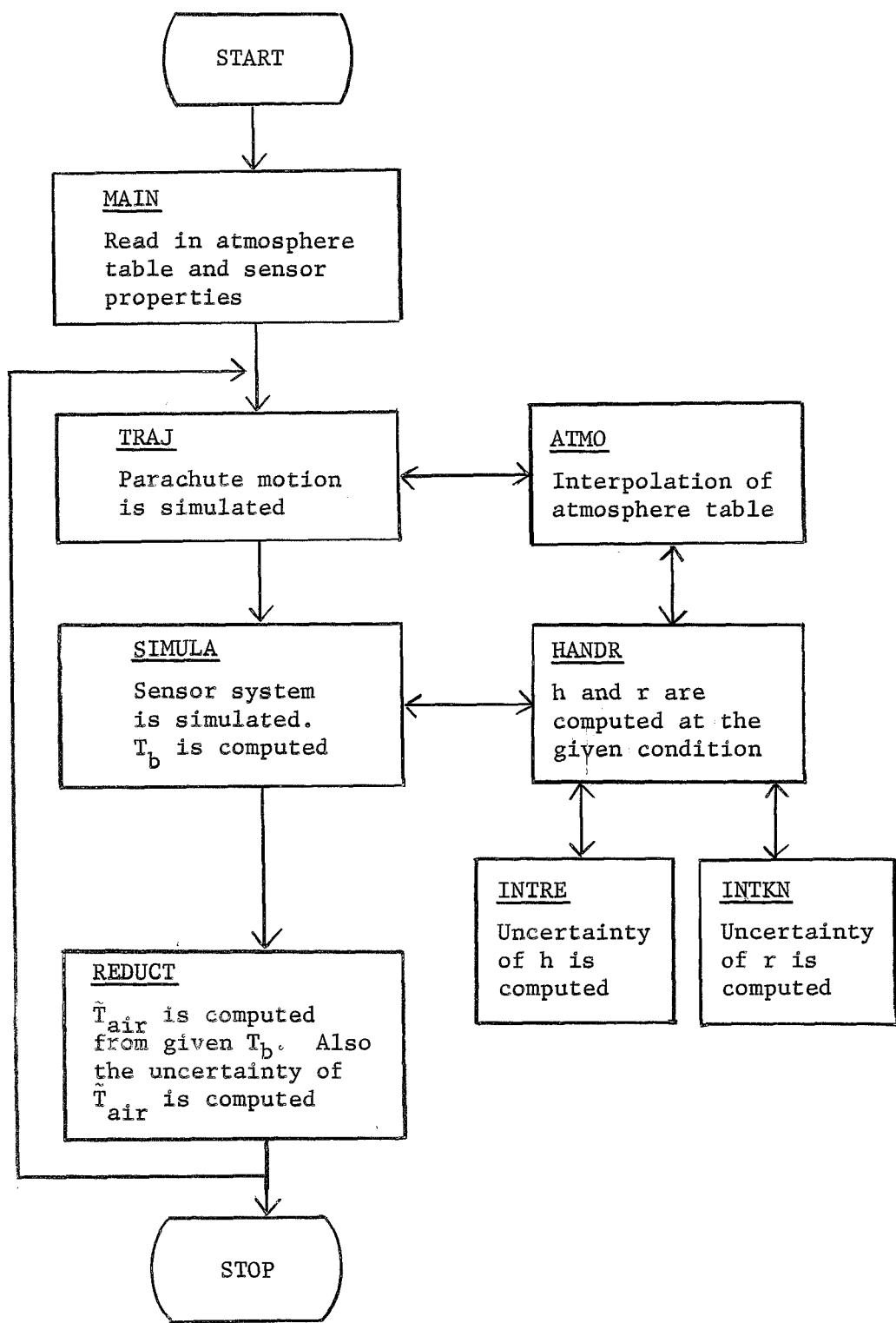


Fig. E.1. Block diagram.

MAIN PROGRAM

```

1000 INPUT QUANTITIES ARE READ IN
1010 C.....LIST OF SYMBOLS
1020 BESS, ZSR, ZB9, ZRV
1030 TC, IS, IT, IF
1040 BE, BES, BESS, ZSR, ZB9, ZRV
1050 ABSORBTIVITY, GEOMETRIC FACTOR
1060 DIAMETER, DENSITY-SPECIFIC HEAT, EMISSIVITY
1070 SELF HEATING CONDUCTIVITY-DIAMETER
1080 WIRE LENGTH, PERTURBATION FACTOR
1090 CHARACTERISTIC LENGTH OF BED, WIRE, FILM
1100 INITIAL ALTITUDE, VERTICAL AND HORIZONTAL SPEED
1110 AREA AND MASS OF PARACHUTE
1120 AREA, MASS
1130 TB, TBR, TE
1140 JACK, JAZZ, JOEY
1150 COMMON /ATHOS/, AL(1250), TEN(250), R(1250), CS(1250)
1160 COMMON /ATHOS/, ZK(1250), ZNFP(250)
1170 COMMON /WIND/, WK(250), R2(1250)
1180 COMMON /FAB/, ZSR(15), ZB9(15)
1190 COMMON /CLEN/, CLB, CLW, CLF
1200 COMMON /AREAS/, IC(15), IT(15)
1210 COMMON /PP/, 20, VNG, VNG, AREA, WMASS
1220 COMMON /DACA/, ALPHA(3,4), BEON(3,4), FLUX(4), BETT(4)
1230 COMMON /DOC/, EPS(3), RHOC(3), D(3), W(3), ZK(3)
1240 COMMON /WIND/, DOCA, R0, ZL, BESS(50)
1250 COMMON /WIND/, AMP
1260 COMMON /JAU/, UN(39), TP
1270 1 FORMAT (1A11)
1280 2 FORMAT (1F10.3)
1290 3 FORMAT (1E10.4)
1300 4 FORMAT (2E15.5)
1310 5 FORMAT (2E15.5)
1320 6 FORMAT (1E15.5)
1330 7 FORMAT (1E15.5)
1340 C.....WIND STRUCTURE IS GIVEN
1350 35*
1360 DO 10 I=1,131
1370 W(11)=0.
1380 37*
1390 38*
1400 39*
1410 40*
1420 41*
1430 42*
1440 43*
1450 44*
1460 45*
1470 46*
1480 47*
1490 48*
1500 49*
1510 50*
1520 51*
1530 52*
1540 53*
1550 54*
1560 55*
1570 56*
1580 57*
1590 58*
1600 59*
1610 60*
1620 61*
1630 62*
1640 63*
1650 64*
1660 65*
1670 66*
1680 67*
1690 68*
1700 69*
1710 70*
1720 71*
1730 72*
1740 73*
1750 74*
1760 75*
1770 76*
1780 77*
1790 78*
1800 79*
1810 80*
1820 81*
1830 82*
1840 83*
1850 84*
1860 85*
1870 86*
1880 87*
1890 88*
1900 89*
1910 90*
1920 91*
1930 92*
1940 93*
1950 94*
1960 95*
1970 96*
1980 97*
1990 98*
2000 99*
2010 100*
2020 101*
2030 102*
2040 103*
2050 104*
2060 105*
2070 106*
2080 107*
2090 108*
2100 109*
2110 110*
2120 111*
2130 112*
2140 113*
2150 114*
2160 115*
2170 116*
2180 117*
2190 118*
2200 119*
2210 120*
2220 121*
2230 122*
2240 123*
2250 124*
2260 125*
2270 126*
2280 127*
2290 128*
2300 129*
2310 130*
2320 131*
2330 132*
2340 133*
2350 134*
2360 135*
2370 136*
2380 137*
2390 138*
2400 139*
2410 140*
2420 141*
2430 142*
2440 143*
2450 144*
2460 145*
2470 146*
2480 147*
2490 148*
2500 149*
2510 150*
2520 151*
2530 152*
2540 153*
2550 154*
2560 155*
2570 156*
2580 157*
2590 158*
2600 159*
2610 160*
2620 161*
2630 162*
2640 163*
2650 164*
2660 165*
2670 166*
2680 167*
2690 168*
2700 169*
2710 170*
2720 171*
2730 172*
2740 173*
2750 174*
2760 175*
2770 176*
2780 177*
2790 178*
2800 179*
2810 180*
2820 181*
2830 182*
2840 183*
2850 184*
2860 185*
2870 186*
2880 187*
2890 188*
2900 189*
2910 190*
2920 191*
2930 192*
2940 193*
2950 194*
2960 195*
2970 196*
2980 197*
2990 198*
2000 199*
2010 200*
2020 201*
2030 202*
2040 203*
2050 204*
2060 205*
2070 206*
2080 207*
2090 208*
2100 209*
2110 210*
2120 211*
2130 212*
2140 213*
2150 214*
2160 215*
2170 216*
2180 217*
2190 218*
2200 219*
2210 220*
2220 221*
2230 222*
2240 223*
2250 224*
2260 225*
2270 226*
2280 227*
2290 228*
2300 229*
2310 230*
2320 231*
2330 232*
2340 233*
2350 234*
2360 235*
2370 236*
2380 237*
2390 238*
2400 239*
2410 240*
2420 241*
2430 242*
2440 243*
2450 244*
2460 245*
2470 246*
2480 247*
2490 248*
2500 249*
2510 250*
2520 251*
2530 252*
2540 253*
2550 254*
2560 255*
2570 256*
2580 257*
2590 258*
2600 259*
2610 260*
2620 261*
2630 262*
2640 263*
2650 264*
2660 265*
2670 266*
2680 267*
2690 268*
2700 269*
2710 270*
2720 271*
2730 272*
2740 273*
2750 274*
2760 275*
2770 276*
2780 277*
2790 278*
2800 279*
2810 280*
2820 281*
2830 282*
2840 283*
2850 284*
2860 285*
2870 286*
2880 287*
2890 288*
2900 289*
2910 290*
2920 291*
2930 292*
2940 293*
2950 294*
2960 295*
2970 296*
2980 297*
2990 298*
2000 299*
2010 300*
2020 301*
2030 302*
2040 303*
2050 304*
2060 305*
2070 306*
2080 307*
2090 308*
2100 309*
2110 310*
2120 311*
2130 312*
2140 313*
2150 314*
2160 315*
2170 316*
2180 317*
2190 318*
2200 319*
2210 320*
2220 321*
2230 322*
2240 323*
2250 324*
2260 325*
2270 326*
2280 327*
2290 328*
2300 329*
2310 330*
2320 331*
2330 332*
2340 333*
2350 334*
2360 335*
2370 336*
2380 337*
2390 338*
2400 339*
2410 340*
2420 341*
2430 342*
2440 343*
2450 344*
2460 345*
2470 346*
2480 347*
2490 348*
2500 349*
2510 350*
2520 351*
2530 352*
2540 353*
2550 354*
2560 355*
2570 356*
2580 357*
2590 358*
2600 359*
2610 360*
2620 361*
2630 362*
2640 363*
2650 364*
2660 365*
2670 366*
2680 367*
2690 368*
2700 369*
2710 370*
2720 371*
2730 372*
2740 373*
2750 374*
2760 375*
2770 376*
2780 377*
2790 378*
2800 379*
2810 380*
2820 381*
2830 382*
2840 383*
2850 384*
2860 385*
2870 386*
2880 387*
2890 388*
2900 389*
2910 390*
2920 391*
2930 392*
2940 393*
2950 394*
2960 395*
2970 396*
2980 397*
2990 398*
2000 399*
2010 400*
2020 401*
2030 402*
2040 403*
2050 404*
2060 405*
2070 406*
2080 407*
2090 408*
2100 409*
2110 410*
2120 411*
2130 412*
2140 413*
2150 414*
2160 415*
2170 416*
2180 417*
2190 418*
2200 419*
2210 420*
2220 421*
2230 422*
2240 423*
2250 424*
2260 425*
2270 426*
2280 427*
2290 428*
2300 429*
2310 430*
2320 431*
2330 432*
2340 433*
2350 434*
2360 435*
2370 436*
2380 437*
2390 438*
2400 439*
2410 440*
2420 441*
2430 442*
2440 443*
2450 444*
2460 445*
2470 446*
2480 447*
2490 448*
2500 449*
2510 450*
2520 451*
2530 452*
2540 453*
2550 454*
2560 455*
2570 456*
2580 457*
2590 458*
2600 459*
2610 460*
2620 461*
2630 462*
2640 463*
2650 464*
2660 465*
2670 466*
2680 467*
2690 468*
2700 469*
2710 470*
2720 471*
2730 472*
2740 473*
2750 474*
2760 475*
2770 476*
2780 477*
2790 478*
2800 479*
2810 480*
2820 481*
2830 482*
2840 483*
2850 484*
2860 485*
2870 486*
2880 487*
2890 488*
2900 489*
2910 490*
2920 491*
2930 492*
2940 493*
2950 494*
2960 495*
2970 496*
2980 497*
2990 498*
2000 499*
2010 500*
2020 501*
2030 502*
2040 503*
2050 504*
2060 505*
2070 506*
2080 507*
2090 508*
2100 509*
2110 510*
2120 511*
2130 512*
2140 513*
2150 514*
2160 515*
2170 516*
2180 517*
2190 518*
2200 519*
2210 520*
2220 521*
2230 522*
2240 523*
2250 524*
2260 525*
2270 526*
2280 527*
2290 528*
2300 529*
2310 530*
2320 531*
2330 532*
2340 533*
2350 534*
2360 535*
2370 536*
2380 537*
2390 538*
2400 539*
2410 540*
2420 541*
2430 542*
2440 543*
2450 544*
2460 545*
2470 546*
2480 547*
2490 548*
2500 549*
2510 550*
2520 551*
2530 552*
2540 553*
2550 554*
2560 555*
2570 556*
2580 557*
2590 558*
2600 559*
2610 560*
2620 561*
2630 562*
2640 563*
2650 564*
2660 565*
2670 566*
2680 567*
2690 568*
2700 569*
2710 570*
2720 571*
2730 572*
2740 573*
2750 574*
2760 575*
2770 576*
2780 577*
2790 578*
2800 579*
2810 580*
2820 581*
2830 582*
2840 583*
2850 584*
2860 585*
2870 586*
2880 587*
2890 588*
2900 589*
2910 590*
2920 591*
2930 592*
2940 593*
2950 594*
2960 595*
2970 596*
2980 597*
2990 598*
2000 599*
2010 600*
2020 601*
2030 602*
2040 603*
2050 604*
2060 605*
2070 606*
2080 607*
2090 608*
2100 609*
2110 610*
2120 611*
2130 612*
2140 613*
2150 614*
2160 615*
2170 616*
2180 617*
2190 618*
2200 619*
2210 620*
2220 621*
2230 622*
2240 623*
2250 624*
2260 625*
2270 626*
2280 627*
2290 628*
2300 629*
2310 630*
2320 631*
2330 632*
2340 633*
2350 634*
2360 635*
2370 636*
2380 637*
2390 638*
2400 639*
2410 640*
2420 641*
2430 642*
2440 643*
2450 644*
2460 645*
2470 646*
2480 647*
2490 648*
2500 649*
2510 650*
2520 651*
2530 652*
2540 653*
2550 654*
2560 655*
2570 656*
2580 657*
2590 658*
2600 659*
2610 660*
2620 661*
2630 662*
2640 663*
2650 664*
2660 665*
2670 666*
2680 667*
2690 668*
2700 669*
2710 670*
2720 671*
2730 672*
2740 673*
2750 674*
2760 675*
2770 676*
2780 677*
2790 678*
2800 679*
2810 680*
2820 681*
2830 682*
2840 683*
2850 684*
2860 685*
2870 686*
2880 687*
2890 688*
2900 689*
2910 690*
2920 691*
2930 692*
2940 693*
2950 694*
2960 695*
2970 696*
2980 697*
2990 698*
2000 699*
2010 700*
2020 701*
2030 702*
2040 703*
2050 704*
2060 705*
2070 706*
2080 707*
2090 708*
2100 709*
2110 710*
2120 711*
2130 712*
2140 713*
2150 714*
2160 715*
2170 716*
2180 717*
2190 718*
2200 719*
2210 720*
2220 721*
2230 722*
2240 723*
2250 724*
2260 725*
2270 726*
2280 727*
2290 728*
2300 729*
2310 730*
2320 731*
2330 732*
2340 733*
2350 734*
2360 735*
2370 736*
2380 737*
2390 738*
2400 739*
2410 740*
2420 741*
2430 742*
2440 743*
2450 744*
2460 745*
2470 746*
2480 747*
2490 748*
2500 749*
2510 750*
2520 751*
2530 752*
2540 753*
2550 754*
2560 755*
2570 756*
2580 757*
2590 758*
2600 759*
2610 760*
2620 761*
2630 762*
2640 763*
2650 764*
2660 765*
2670 766*
2680 767*
2690 768*
2700 769*
2710 770*
2720 771*
2730 772*
2740 773*
2750 774*
2760 775*
2770 776*
2780 777*
2790 778*
2800 779*
2810 780*
2820 781*
2830 782*
2840 783*
2850 784*
2860 785*
2870 786*
2880 787*
2890 788*
2900 789*
2910 790*
2920 791*
2930 792*
2940 793*
2950 794*
2960 795*
2970 796*
2980 797*
2990 798*
2000 799*
2010 800*
2020 801*
2030 802*
2040 803*
2050 804*
2060 805*
2070 806*
2080 807*
2090 808*
2100 809*
2110 810*
2120 811*
2130 812*
2140 813*
2150 814*
2160 815*
2170 816*
2180 817*
2190 818*
2200 819*
2210 820*
2220 821*
2230 822*
2240 823*
2250 824*
2260 825*
2270 826*
2280 827*
2290 828*
2300 829*
2310 830*
2320 831*
2330 832*
2340 833*
2350 834*
2360 835*
2370 836*
2380 837*
2390 838*
2400 839*
2410 840*
2420 841*
2430 842*
2440 843*
2450 844*
2460 845*
2470 846*
2480 847*
2490 848*
2500 849*
2510 850*
2520 851*
2530 852*
2540 853*
2550 854*
2560 855*
2570 856*
2580 857*
2590 858*
2600 859*
2610 860*
2620 861*
2630 862*
2640 863*
2650 864*
2660 865*
2670 866*
2680 867*
2690 868*
2700 869*
2710 870*
2720 871*
2730 872*
2740 873*
2750 874*
2760 875*
2770 876*
2780 877*
2790 878*
2800 879*
2810 880*
2820 881*
2830 882*
2840 883*
2850 884*
2860 885*
2870 886*
2880 887*
2890 888*
2900 889*
2910 890*
2920 891*
2930 892*
2940 893*
2950 894*
2960 895*
2970 896*
2980 897*
2990 898*
2000 899*
2010 900*
2020 901*
2030 902*
2040 903*
2050 904*
2060 905*
2070 906*
2080 907*
2090 908*
2100 909*
2110 910*
2120 911*
2130 912*
2140 913*
2150 914*
2160 915*
2170 916*
2180 917*
2190 918*
2200 919*
2210 920*
2220 921*
2230 922*
2240 923*
2250 924*
2260 925*
2270 926*
2280 927*
2290 928*
2300 929*
2310 930*
2320 931*
2330 932*
2340 933*
2350 934*
2360 935*
2370 936*
2380 937*
2390 938*
2400 939*
2410 940*
2420 941*
2430 942*
2440 943*
2450 944*
2460 945*
2470 946*
2480 947*
2490 948*
2500 949*
2510 950*
2520 951*
2530 952*
2540 953*
2550 954*
2560 955*
2570 956*
2580 957*
2590 958*
2600 959*
2610 960*
2620 961*
2630 962*
2640 963*
2650 964*
2660 965*
2670 966*
2680 967*
2690 968*
2700 969*
2710 970*
2720 971*
2730 972*
2740 973*
2750 974*
2760 975*
2770 976*
2780 977*
2790 978*
2800 979*
2810 980*
2820 981*
2830 982*
2840 983*
2850 984*
2860 985*
2870 986*
2880 987*
2890 988*
2900 989*
2910 990*
2920 991*
2930 992*
2940 993*
2950 994*
2960 995*
2970 996*
2980 997*
2990 998*
2000 999*
2010 1000*
2020 1001*
2030 1002*
2040 1003*
2050 1004*
2060 1005*
2070 1006*
2080 1007*
2090 1008*
2100 1009*
2110 1010*
2120 1011*
2130 1012*
2140 1013*
2150 1014*
2160 1015*
2170 1016*
2180 1017*
2190 1018*
2200 1019*
2210 1020*
2220 1021*
2230 1022*
2240 1023*
2250 1024*
2260 1025*
2270 1026*
2280 1027*
2290 1028*
2300 1029*
2310 1030*
2320 1031*
2330 1032*
2340 1033*
2350 1034*
2360 1035*
2370 1036*
2380 1037*
2390 1038*
2400 1039*
2410 1040*
2420 1041*
2430 1042*
2440 1043*
2450 1044*
2460 1045*
2470 1046*
2480 1047*
2490 1048*
2500 1049*
2510 1050*
2520 1051*
2530 1052*
2540 1053*
2550 1054*
2560 1055*
2570 1056*
2580 1057*
2590 1058*
2600 1059*
2610 1060*
2620 1061*
2630 1062*
2640 1063*
2650 1064*
2660 1065*
2670 1066*
2680 1067*
2690 1068*
2700 1069*
2710 1070*
2720 1071*
2730 1072*
2740 1073*
2750 1074*
2760 1075*
2770 1076*
2780 1077*
2790 1078*
2800 1079*
2810 1080*
2820 1081*
2830 1082*
2840 1083*
2850 1084*
2860 1085*
2870 1086*
2880 1087*
2890 1088*
2900 1089*
2910 1090*
2920 1091*
2930 1092*
2940 1093*
2950 1094*
2960 1095*
2970 1096*
2980 1097*
2990 1098*
2000 1099*
2010 1100*
2020 1101*
2030 1102*
2040 1103*
2050 1104*
2060 1105*
2070 1106*
2080 1107*
2090 1108*
2100 1109*
2110 1110*
2120 1111*
2130 1112*
2140 1113*
2150 1114*
2160 1115*
2170 1116*
2180 1117*
2190 1118*
2200 1119*
2210 11110*
2220 11111*
2230 11112*
2240 11113*
2250 11114*
2260 11115*
2270 11116*
2280 11117*
2290 11118*
2300 11119*
2310 111110*
2320 111111*
2330 111112*
2340 111113*
2350 111114*
2360 111115*
2370 111116*
2380 111117*
2390 111118*
2400 111119*
2410 1111110*
2420 1111111*
2430 1111112*
2440 1111113*
2450 1111114*
2460 1111115*
2470 1111116*
2480 1111117*
2490 1111118*
2500 1111119*
2510 11111110*
2520 11111111*
2530 11111112*
2540 11111113*
2550 11111114*
2560 11111115*
2570 11111116*
2580 11111117*
2590 11111118*
2600 11111119*
2610 111111110*
2620 111111111*
2630 111111112*
2640 111111113*
2650 111111114*
2660 111111115*
2670 111111116*
2680 111111117*
2690 111111118*
2700 111111119*
2710 1111111110*

```

SUBROUTINE TRAJ

```

1# SUBROUTINE TRAJ
2# C*** THE PARACHUTE MOTION IS SIMULATED
3# C*** LIST OF SYMBOLS
4# C      TH      TIME, TIME INCREMENT
5# C      VEL,ZOT  VELOCITY, ALTITUDE
6# C      DIMENSION 2K(1),VVK(12),VK(12),VRK(12),XMK(12),YMK(12)
7# C      COMMON /PP/ 20, VIO, VHO, AREA, YMASS
8# C      COMMON /AP/ 20, TINF, RAD, VS, ARD, AK, ANFP, VEL
9# C      COMMON /W/ 20, VWP, HMV
10# C      COMMON /AR/ 20, ARP
11# C      COMMON /ETK/ TB, TBD, JACK, JOEY, TP, JAZZ
12# C      PRINT 1, AREA, BRASS
13# C      1 FORMAT (1H15DHFOR A PARACHUTE SYSTEM WITH CROSS SECTIONAL AREA =,
14# C      1F6.2*7H METERS SQUARED, AND MASS =F5.2,10H KILOGRAMS)
15# C      PRINT 2, ZD
16# C      2 FORMAT (1H ,5X,35H AND INITIAL CONDITIONS: ALTITUDE =,F9.2,
17# C      17H METERS)
18# C      PRINT 3, VHO, VHO
19# C      3 FORMAT (1H15DX 20HORIZONTAL VELOCITY = ,F7.2,14H METERS/SECOND,
20# C      12H, HORIZONTAL VELOCITY = ,F7.2,14H METERS/SECOND)
21# C      PRINT 4
22# C      4 FORMAT (1H ,5X,26H AND A STANDARD ATMOSPHERE:)
23# C      PRINT 5
24# C      5 FORMAT (1H ,5X,24H AND A ZERO WIND PROFILE:)
25# C      NEM
26# C      A=20.
27# C      T=0.
28# C      X0=0.
29# C      V=0.0T(VW0**2+VHO**2)
30# C      HEL=0
31# C      IN,A=0
32# C      C*** ALITUDE
33# C      10 20*ZD
34# C      YZOT=1.20
35# C      INKA=11MK(1)+VW0
36# C      VWT=VW0
37# C      X0T=X0
38# C      D=20  J=1*4
39# C      IATE=0
40# C      C*** ATMOSPHERIC CONDITION IS FOUND AT THIS ALTITUDE
41# C      CALL ATRO (IATE)
42# C      IF (IATE .EQ. 1) GO TO 21
43# C      C*** RELATIVE WIND SPEED
44# C      VZ=VW01-VW0
45# C      VZ=VW01-VW0
46# C      D=20
47# C      IATE=0
48# C      C*** TOTAL VELOCITY IS FOUND
49# C      VEL=SQRT(VZ**2+VX**2)
50# C      C*** AREA/MASS
51# C      G=*.80663-201*(3.01E-6)
52# C      IF (J .NE. 1) GO TO 17
53# C      G=*.5*RHOM*VEL**2
54# C      XX=(1/INKA)*VEL
55# C      ZD=ZDT/1000.
56# C      YY=(1/INKA)*ZD
57# C      17 ZK(J)=H*YYUT
58# C      CALL SIMULA
59# C      VRK(J)=H=(-0.5*c*c*RHO*VEL*VZ-G)
60# C      XK(J)=H*HUT
61# C      VRK(J)=H=(0.5*c*c*RHO*VEL*VX)
62# C      IF (J .NE. 1) GO TO 18
63# C      G=*.01*ZD*0.5*ZK(1)
64# C      VV=TE*VW0+.5*VK(1)

```

SUBROUTINE ATMO

SUNDAY TIME HANDBOOK

```

C..... SUBROUTINE ATMO (IATE)
C..... LINEAR INTERPOLATION OF THE ATMOSPHERE TABLE IS DONE
COMMON ATMOS / ALT(250), TNP(250), R(250), CS(250), ZNP(250),
COMMON ATROS / ALT(250), TNP(250), R(250), CS(250),
COMMON AWDY / ZNK(250), ZNP(250),
COMMON AWDY / X(250), VZ(250),
COMMON AWP / ZNP, RHO, VS, ANU, AR, APP, VEL,
COMMON /VNP, HNP/
COMMON NMW / NMW/
COMMON NMW / NMW/
IF (T >0.7 .LT. ALT(1) .OR. 20T .GT. AL(133)) GO TO 2
DO 1 1-1,31
 1 D2=ALT(1)-20
 1 IF (D2 .LT. 0.) GO TO 1
 1 ERRODZ=(ALT(1)-ALT(1-1))
 1 DIFFER=(TENV(1)-TENV(1-1))
 1 DIFFCS=(S(1)-S(1-1))
 1 DIFFAU=(M(1)-2AU(1-1))
 1 DIFFPK=(2K(1)-2K(1-1))
 1 DIFFMP=(MFP(1)-2MFP(1-1))
 1 DIFFRZ=(RZ(1)-RZ(1-1))
 1 DIFFNA=(N(1)-N(1-1))
 1 CORRIE=ERRDIFFTE
 1 CORRES=ERRRADIFCS
 1 CORRMU=ERRRADIFNU
 1 CORKE=ERRRADIFKE
 1 CORNP=ERRRADIFNP
 1 CORRA=ERRRADIFRA
 1 CORNW=ERRRADIFWX
 1 TINF=TENV(1)-CORRIE
 1 RHOR(1)=CORR
 1 V5=S(1)-CORRES
 1 AMFP=2MFP(1)-CORRMU
 1 AMFP=2MFP(1)-CORRMU *#4185.
 1 AMFP=2MFP(1)-CORRMU
 1 VNP=VZ(1)-CORRMU
 1 HNP=X(1)-CORRMU
 1 HNP=X(1)-CORRMU
 1 GO TO 3
 1 CONTINUE
 2 IATE=1
 2 CONTINUE
 3 CONTINUE
END

```

```

SUBROUTINE HANDB AND RECOVERY FACTORS ARE FOUND
C.....LIST OF SYMBOLS NACH NUMBER, SPEED RATIO, PRANDTL NUMBER
C.....AM,SPR REYNOLDS NUMBER OF BEAD, WIRE FILM
C.....REB,AKIN,AKAF KNODLES NUMBER OF BEAD, WIRE FILM
C.....HB,HBF,REF RECOVERY FACTOR OF BEAD,WIRE FILM
C.....RBC,RFC,REC CONNECTIVE COEFFICIENT OF BEAD,WIRE FILM
C.....RBF,REF,RPF RECOVERY FACTOR IN CONTINUUM FLOW
C.....HSC,HCF,HPC CONNECTIVE COEFFICIENT IN FREE MOLECULAR FLOW
C.....HFS,HFF,HPP CONNECTIVE COEFFICIENT IN FREE MOLECULAR FLOW
C.....UHS,UHL,UHK,UHS UNCERTAINTIES OF MB,MN,MF
C.....URB,URF UNEARTHED LIMITS OF RB,RN,RF
C.....CONHN,ABP,ZDT,THT,THT,RHO,NS,AMU,AK,AMFP,VEL
C.....CONHN,AVAC,ZEP(13),ZEP(15),ZEP(15)
C.....CONHN,CLB,CLB,CLB,CLB,CLF
C.....CONHN,REG,IC,IS,IT,TF
C.....CONHN,DIC,EPS(13),RHOC(31),D(3),N(3),ZK(3)
C.....CONHN,UBU/UNC(39)/TF
C.....CONHN,H13/REEF(3)
C.....CONHN,MNP
C.....CONDONE18,TB,D,B,JACK,JOEY,TJ,JAZZ
DATA ACB,ACW,ACF/0.9,0.9,0.9/
DATA AGB,ACV,ACF/0.9,0.9,0.9/
C.....COMPUTATION FOR SPHERE
C.....FREE MOLECULAR FLOW RECOVERY FACTOR
C.....AHE,TEL/AS
SRE=.837*AR
PRP=.1AU/AK
AR351=167
AR351=167
IF (SR < 1.0) GO TO 2
DO 1 L=1,13
DSR=2*SR(L)*SR
IF (DSR .LT. 0.) GO TO 1
ERRSDSR=2*SR(L)-2*SR(L-1)
DIFFRSR=2*SR(L)-2*SR(L-1)
DIFFRSR=2*SR(L)-2*SR(L-1)
CORRBSERR=0.0*FRB
ARBSR(L)=CORRBS
ARBSR(L)=CORRBS
60 70 2
1 CONTINUE
2 REBERM01*CLB/AHU
AHBRM01*CLB/AHU
ANSBRM01*CLB/AHU
ANSBRM01*CLB/AHU
1
TRBIC
IF (TRB .LE. 1.0) AND. AMRB .GT. 0.01) TRB=15
IF (TRB .LE. 1.0) AND. AMRB .GT. 0.01) TRB=15
IF (TRB .GT. 1.0) AND. AMRB .GT. 0.01) TRB=15
IF (TRB .GT. 1.0) AND. AMBR .GT. 0.01) TRB=15
IF (TRB .GT. 1.0) AND. AMBR .GT. 0.01) TRB=15
IF (TRB .GT. 1.0) AND. AMBR .GT. 0.01) TRB=15
IF (TRB .GT. 1.0) AND. AMBR .GT. 0.01) TRB=15
IF (TRB .GT. 1.0) AND. AMBR .GT. 0.01) TRB=15
IF (TRB .GT. 1.0) AND. AMBR .GT. 0.01) TRB=15
AKBFRM01*CLB
C.....RECOVERY FACTOR
RBS=0.85*(AKMR=(TRB-0.845))/((AKNB+0.3)
C.....FREE MOLECULAR FLOW CONNECTIVE COEFFICIENT
FHBRM01=.9*CBV5*PR0
1
TR (SR .LT. 1.0) AND. AMRB .GT. 0.01) TR=3
Tz/.1/.0377651158
ENFBM01=.433525707*TR*.254495736*TR*.216137417*TR*.3
ENFBM01=.433525707*TR*.254495736*TR*.216137417*TR*.3

```

```

65$ C***UNCERTAINTIES OF RECOVERY FACTOR
FB=4.31*SFH&C*(12.*5*P+1./3)*SF&P+1.*12336*EXP(-SR*P*2)
66$ 5 HBF=HFB
67$ HBF=HFB
68$ C***CONTINUUM FLOW CONVECTIVE COEFFICIENT
69$ 4 ANUB=2.+0.37*RE*0.6*P*0.333
70$ HBC=HBC
71$ HBC=HBC&HBF/CB
72$ UBR=UNCR
73$ C***CONVECTIVE COEFFICIENT
74$ HBC=HBC&HBF /HBC+HBF
75$ DKN=KBN
76$ INU=1

77$ REYN=RE
78$ C***UNCERTAINTIES OF CONVECTIVE COEFFICIENT
79$ CALL INTN(NU,NCH)
80$ C***UNCERTAINTIES OF RECOVERY FACTOR
81$ CALL INTN(NUH,UNCR,INU)
82$ UBR=UNCR
83$ UBR=BINCH
84$ C***COMPUTATION FOR CYLINDER
85$ REYNH=NU*CLN/ANU
86$ ARIE=A/REF
87$ C***FLOW REGIME SEARCH
88$ ITRIC
89$ C***FLOW REGIME SEARCH
90$ IF (IREV .LE. 1. .AND. ARIE .GT. 0.01) ITRIS
91$ IF (IREV .LE. 1. .AND. ARIE .GT. 0.1) ITRIT
92$ IF (IREV .GT. 1. .AND. ARIE .GT. 0.01) ITRIS
93$ IF (IREV .GT. 1. .AND. ARIE .GT. 0.1) ITRIT
94$ IF (ARIW .GT. 3.) ITR=IF
95$ AKN=AMP/CLW
96$ C***RECOVERY FACTOR
97$ RHO=0.815*AKN*(ARW-0.845)/(AKN*0.6)
98$ C***FREE MOLECULAR FLOW CONVECTIVE COEFFICIENT
99$ T=0.5*P*SR*E2
2=7*3./75
01$ IF (2.,GT.1.) PRINT 6
02$ FORMAT1H,5*INCH TOO LARGE FOR BESSEL FUNCTION APPROXIMATOR
03$ BN1=1.+3.*156*228*Z**2*5*P+0.*099*28*Z**5*P+1.*206*749*Z**2*5*P
04$ BN2=0.265*732*Z**2*5*P+0.*056*768*Z**10*P+0.*003*581*3*Z**5*P
05$ BH=BS*PO+BH*OB
06$ BN1=BT*0.879*59*Z**2*4*P+0.549*86*9*Z**4*P+0.150*64*9*Z**4*P
07$ BN1=BT*0.025*587*3*Z**2*5*P+0.*003*15*3*Z**10*P+0.*000*32*4*11*Z**12
08$ Hw4=280.*SINH*7*PI*RO*EXP(-T)
09$ Hwz=1.*Z**2.*T1*SHD*4.*T**2*SBM1T
10$ Fh=SH*AH*B
11$ Hw=Hw*Hw
12$ C***CONTINUUM FLOW CONVECTIVE COEFFICIENT
13$ 6 IF (NEW .GT. 4000.) GO TO 9
14$ CHW=(AK/CLW)*(0.43+0.48*RE*0.5)
15$ 60 TO 11
16$ 9 IF (IREW .GT. 40000.) GO TO 10
17$ CHW=(AK/CLW)*(0.43+0.174*RE*0.618)
18$ 60 TO 11
19$ 10 CHW=(AK/CLW)*(0.43+0.0239*RE*0.805)
20$ 11 Hw=CHW
21$ Hw=CHW
22$ C***CONVECTIVE COEFFICIENT
23$ HB=HBC+HBF /HBC+HBF
24$ INUE2
25$ DKN=KBN
26$ REYN=RE
27$ C***UNCERTAINTIES OF CONVECTIVE COEFFICIENT
28$ CALL INTN(NUH,UNCR)
29$ C***UNCERTAINTIES OF CONVECTIVE COEFFICIENT
30$ CALL INTN(NUH,UNCR,INU)
31$ C***CHARACTERISTIC LENGTH COMPUTATION
32$ SIZ=5.67E-6
33$ IF (JACH .GT. 0.) GO TO 33
34$ CLF=CLF*(ZKD(13)/12.*S(H13)+0.*S1*S(CPS(5)*TF*5*3))
35$ CLF=CLF*3.
36$ CONTINUE
37$ NEX20
38$ CONTINUE
39$ IF (REF .NE. 1. .AND. ARIE .GT. 0.01) ITRIS
40$ IF (REF .NE. 1. .AND. ARIE .GT. 0.1) ITRIT
41$ IF (REF .NE. 1. .AND. ARIE .GT. 0.01) ITRIS
42$ IF (REF .NE. 1. .AND. ARIE .GT. 0.1) ITRIT
43$ IF (ARIW .GT. 3.) ITR=IF
44$ C***FLUX REGIME SEARCH (REF)
45$ ITRIC
46$ C***FREE MOLECULAR FLOW RECOVERY FACTOR
47$ IF (REF .NE. 1. .AND. ARIE .GT. 0.01) ITRIS
48$ IF (REF .NE. 1. .AND. ARIE .GT. 0.1) ITRIT
49$ IF (ARIW .GT. 3.) ITR=IF
50$ RF=1.67
51$ AKP=TA(KNP)*(SRT(REF)/7.2)
52$ RF=1.65
53$ C***FREE MOLECULAR FLOW CONVECTIVE COEFFICIENT
54$ HF=FBP*Z*ACFS*SRHO
55$ ITRIC
56$ C***RECOVERY FACTOR
57$ 13 AKP=TA(KNP)*(SRT(REF)/7.2)
58$ RF=1.65
59$ C***CONTINUUM FLOW CONVECTIVE COEFFICIENT
60$ HF=FBP*Z*ACFS*SRHO
61$ ITRIC
62$ C***CONNECTIVE COEFFICIENT
63$ HF=HFC*CHP*/(HFC+HPF)
64$ AKP=TA(KNP)*CLF
65$ RF=1.65
66$ AKP=TA(KNP)*(SRT(REF)/7.2)
67$ HF=FBP*Z*ACFS*SRHO
68$ ITRIC
69$ C***CONNECTIVE COEFFICIENT
70$ HF=HFC*CHP*/(HFC+HPF)
71$ AKP=TA(KNP)
72$ RF=1.65
73$ C***CONTINUUM FLOW CONVECTIVE COEFFICIENT
74$ HF=FBP*Z*ACFS*SRHO
75$ ITRIC
76$ C***CONNECTIVE COEFFICIENT
77$ HF=HFC*CHP*/(HFC+HPF)
78$ AKP=TA(KNP)
79$ RF=1.65
80$ C***CONTINUUM FLOW CONVECTIVE COEFFICIENT
81$ HF=FBP*Z*ACFS*SRHO
82$ ITRIC
83$ C***CONNECTIVE COEFFICIENT
84$ HF=HFC*CHP*/(HFC+HPF)
85$ AKP=TA(KNP)
86$ RF=1.65
87$ C***CONTINUUM FLOW CONVECTIVE COEFFICIENT
88$ HF=FBP*Z*ACFS*SRHO
89$ ITRIC
90$ C***CONNECTIVE COEFFICIENT
91$ HF=HFC*CHP*/(HFC+HPF)
92$ AKP=TA(KNP)
93$ RF=1.65
94$ C***CONTINUUM FLOW CONVECTIVE COEFFICIENT
95$ HF=FBP*Z*ACFS*SRHO
96$ ITRIC
97$ C***CONNECTIVE COEFFICIENT
98$ HF=HFC*CHP*/(HFC+HPF)
99$ AKP=TA(KNP)
100$ RF=1.65
101$ C***CONTINUUM FLOW CONVECTIVE COEFFICIENT
102$ HF=FBP*Z*ACFS*SRHO
103$ ITRIC
104$ C***CONNECTIVE COEFFICIENT
105$ HF=HFC*CHP*/(HFC+HPF)
106$ AKP=TA(KNP)
107$ RF=1.65
108$ C***CONTINUUM FLOW CONVECTIVE COEFFICIENT
109$ HF=FBP*Z*ACFS*SRHO
110$ ITRIC
111$ C***CONNECTIVE COEFFICIENT
112$ HF=HFC*CHP*/(HFC+HPF)
113$ AKP=TA(KNP)
114$ RF=1.65
115$ C***CONTINUUM FLOW CONVECTIVE COEFFICIENT
116$ HF=FBP*Z*ACFS*SRHO
117$ ITRIC
118$ C***CONNECTIVE COEFFICIENT
119$ HF=HFC*CHP*/(HFC+HPF)
120$ AKP=TA(KNP)
121$ RF=1.65
122$ C***CONTINUUM FLOW CONVECTIVE COEFFICIENT
123$ HF=FBP*Z*ACFS*SRHO
124$ ITRIC
125$ C***CONNECTIVE COEFFICIENT
126$ HF=HFC*CHP*/(HFC+HPF)
127$ AKP=TA(KNP)
128$ RF=1.65
129$ C***CONTINUUM FLOW CONVECTIVE COEFFICIENT
130$ HF=FBP*Z*ACFS*SRHO
131$ ITRIC
132$ C***CONNECTIVE COEFFICIENT
133$ HF=HFC*CHP*/(HFC+HPF)
134$ AKP=TA(KNP)
135$ RF=1.65
136$ C***CONTINUUM FLOW CONVECTIVE COEFFICIENT
137$ HF=FBP*Z*ACFS*SRHO
138$ ITRIC
139$ C***CONNECTIVE COEFFICIENT
140$ HF=HFC*CHP*/(HFC+HPF)
141$ AKP=TA(KNP)
142$ RF=1.65
143$ C***CONTINUUM FLOW CONVECTIVE COEFFICIENT
144$ HF=FBP*Z*ACFS*SRHO
145$ ITRIC
146$ C***CONNECTIVE COEFFICIENT
147$ HF=HFC*CHP*/(HFC+HPF)
148$ AKP=TA(KNP)
149$ RF=1.65
150$ C***CONTINUUM FLOW CONVECTIVE COEFFICIENT
151$ HF=FBP*Z*ACFS*SRHO
152$ ITRIC
153$ C***CONNECTIVE COEFFICIENT
154$ HF=HFC*CHP*/(HFC+HPF)
155$ AKP=TA(KNP)
156$ RF=1.65
157$ C***CONTINUUM FLOW CONVECTIVE COEFFICIENT
158$ HF=FBP*Z*ACFS*SRHO
159$ ITRIC
160$ C***CONNECTIVE COEFFICIENT
161$ HF=HFC*CHP*/(HFC+HPF)
162$ AKP=TA(KNP)
163$ RF=1.65
164$ C***CONTINUUM FLOW CONVECTIVE COEFFICIENT
165$ HF=FBP*Z*ACFS*SRHO
166$ ITRIC
167$ C***CONNECTIVE COEFFICIENT
168$ HF=HFC*CHP*/(HFC+HPF)
169$ AKP=TA(KNP)
170$ RF=1.65
171$ C***CONTINUUM FLOW CONVECTIVE COEFFICIENT
172$ HF=FBP*Z*ACFS*SRHO
173$ ITRIC
174$ C***CONNECTIVE COEFFICIENT
175$ HF=HFC*CHP*/(HFC+HPF)
176$ AKP=TA(KNP)
177$ RF=1.65
178$ C***CONTINUUM FLOW CONVECTIVE COEFFICIENT
179$ HF=FBP*Z*ACFS*SRHO
180$ ITRIC
181$ C***CONNECTIVE COEFFICIENT
182$ HF=HFC*CHP*/(HFC+HPF)
183$ AKP=TA(KNP)
184$ RF=1.65
185$ C***CONTINUUM FLOW CONVECTIVE COEFFICIENT
186$ HF=FBP*Z*ACFS*SRHO
187$ ITRIC
188$ C***CONNECTIVE COEFFICIENT
189$ HF=HFC*CHP*/(HFC+HPF)
190$ AKP=TA(KNP)
191$ RF=1.65
192$ C***CONTINUUM FLOW CONVECTIVE COEFFICIENT
193$ HF=FBP*Z*ACFS*SRHO
194$ ITRIC
195$ C***CONNECTIVE COEFFICIENT
196$ HF=HFC*CHP*/(HFC+HPF)
197$ AKP=TA(KNP)
198$ RF=1.65
199$ C***CONTINUUM FLOW CONVECTIVE COEFFICIENT
200$ HF=FBP*Z*ACFS*SRHO
201$ ITRIC
202$ C***CONNECTIVE COEFFICIENT
203$ HF=HFC*CHP*/(HFC+HPF)
204$ AKP=TA(KNP)
205$ RF=1.65
206$ C***CONTINUUM FLOW CONVECTIVE COEFFICIENT
207$ HF=FBP*Z*ACFS*SRHO
208$ ITRIC
209$ C***CONNECTIVE COEFFICIENT
210$ HF=HFC*CHP*/(HFC+HPF)
211$ AKP=TA(KNP)
212$ RF=1.65
213$ C***CONTINUUM FLOW CONVECTIVE COEFFICIENT
214$ HF=FBP*Z*ACFS*SRHO
215$ ITRIC
216$ C***CONNECTIVE COEFFICIENT
217$ HF=HFC*CHP*/(HFC+HPF)
218$ AKP=TA(KNP)
219$ RF=1.65
220$ C***CONTINUUM FLOW CONVECTIVE COEFFICIENT
221$ HF=FBP*Z*ACFS*SRHO
222$ ITRIC
223$ C***CONNECTIVE COEFFICIENT
224$ HF=HFC*CHP*/(HFC+HPF)
225$ AKP=TA(KNP)
226$ RF=1.65
227$ C***CONTINUUM FLOW CONVECTIVE COEFFICIENT
228$ HF=FBP*Z*ACFS*SRHO
229$ ITRIC

```

```

1958      RECFT1=RS
1968      RECFT2=RS
1978      RECFT3=RS
1988      URC(1)=UR3/2.
1998      URC(2)=UR3/2.
2008      URC(3)=UR3/2.
2018      URC(4)=UR3/2.
2028      URC(5)=UR3/2.
2038      URC(6)=UR3/2.
333  FORMAT(1H ,9E19.3)
2048      RETURN
2058      END
2068

SUBROUTINE SIMULA
1* C.....SECTOR SYSTEM IS SIMULATED
38  C.....LI-T OF SYMBOLS
48  C       GRA
52  C       TW
58  C       DELT
75  C       DIMENSION RAD(3,4),GRA(3)
88  COMMON /P/ 207,TINF,RHO,V,S,AMU,AK,ANFP,VEL
98  COMMON /R/ H(3),RECFT(3),ALPHA(3,4),BEOF(3,4),FLUX(4),BETA(4)
108  COMMON /D/ EPS(3),RHOC(3),D(3),N(3),TKD(3)
118  COMMON /DCC/ RO2,BESS(50)
128  COMMON /UNU/ UNC(39),TF
138  COMMON /NMP/ NMP
148  COMMON /CLB/ CLB,CLF
158  COMMON /ERK/ TB,TB0,JACK,JOET,TJAZZ
168  DATA CP/1.016/1000.,3.1416/5.6587E-9/
178  CALL HANDR
188  IF(JACK.EQ.0) TF=TB
198  IF(JACK.EQ.0) TB=TBS
208  5 CONTINUE
218
238  TM=(TB+TF)/2.
248  C.....RADITION HEAT INPUT
258  DO 2 I=1,3
278  DO 2 J=1,4
288  RAD((J)RAD(I,J)+GRA(I))
298  IF(JACK.NE.JOET) GO TO 15
2  GRA(I)=0,
308  RAD((J)RAD(I,J)+GRA(I))
318  PRINT 209,JACK
328  PRINT 110,T,207,TINF,VEL,TF,TB,TBD
338  PRINT 115,(H(I),I=1,3),RECFT(I,I=1,3),(GRA(I),I=1,3)
348  PRINT 115,(UNC(I),I=1,6),CLF
15  CONTINUE
358  GRA(I)=GRA(I)+N(I)
368  DELT=.0
378  C.....TIME
388  T=T+DELT
398  C.....CALCULATION OF BEAD TEMPERATURE
408  C.....PRELIMINARY COMPUTATION 1
418  C.....SIGEPS(1)*(TB**3)
428

```

SUBROUTINE REJECT

```

18 C...REDUCT TEMPERATURE REDUCTION AND UNCERTAINTY BOUNDARY IS FOUND
28 C...LIST OF SYMBOLS NUMBER OF TOTAL PARAMETER, TIME VARIANT PARAMETER
36 C N&NP
48 C SDVZ S<SS
58 C D6P, S<SS
68 C STOU
78 C T1
98 C DIMENSION RAD(3+1)SRA(3)
118 COMMON /AP/ AP, TIME, RAD, VS, AM, AK, APP, VEL,
128 COMMON /HR/ H(3), REC(3)
138 COMMON /DRC/ ALPHA(3,4), SEDOF(3,4), FLUX(4), BETAL6
148 COMMON /DTC/ EPS(3), RHOC(3), O(3), N(3), ZKD(3)
158 COMMON /DOC/ R6_2L,BESS(5)
168 COMMON /DUN/ URC(39),TF
178 COMMON /PAR/ PARP
188 COMMON /ETR/ TB,TBD,JACK,WEET,YP,JAZZ
198 DIMENSION S(40), SIN(40), SS(40,40), SSV(40,40), ESS(40,40), SRS(40),
199 I40(40), DS(1-NP)
208 DIMENSION PR(40), SDV(40,40), SDVZ(40,40), STM(40,40), STMZ(40,40), S
218 ITW(40)
228 IWT(40)
238 IWTN(40), SAV(40), SAV1(40), SAV1(40), PGR(40)
248 DIMENSION ST(40,40), SVP(40);
258 C...NUMBER OF PARAMETER IS SET
268 JI=9
278 NP=39
288 NG=19
298 NAI=NG-1
308 DATA CP/PI,SIGE/1000.,3,14159,5,6687E-3/
318 TB=TP
328 IF(JACK,NE,0) TF=TA
338 DELT=1.0
348 C...TIME
358 C...TEND,T
368 C...RADATION INPUT
378 DO 2 I=1,5
379 6RA(1)=30.
388 DO 2 J=1,4
398 RAD(J)=ALPHA(I,J)*GEOMF(I,J)*FLUX(J)*BETA(J)
408 2 ORNL1=ORAL1*(M1)
418 C...REDUCTION OF STANDARD DEVIATION
428 C...REDUCTION OF STANDARD DEVIATION
438 PR(1)=SH11
448 PR(2)=REC(1)
458 PR(3)=H12
468 PR(4)=REC(2)
478 PR(5)=H13
488 PR(6)=REC(3)
498 PR(7)=VEL
508 PR(8)=TB
518 PR(9)=TBD
528 PR(10)=SEOF(1,1)
538 PR(11)=SEOF(1,2)
548 PR(12)=SEOF(1,3)
558 PR(13)=SEOF(2,1)
568 PR(14)=SEOF(2,2)
578 PR(15)=SEOF(2,3)
588 PR(16)=SEOF(3,1)
598 PR(17)=SEOF(3,2)
608 PR(18)=SEOF(3,3)
618 PR(19)=E11
628 PR(20)=ALPHA(1,3)
638 PR(21)=ALPHA(2,3)

```

```

658 PR(22)=ALPHA(2,3)
668 PR(23)=D11
678 PR(24)=E2E(1)
688 PR(25)=D13
698 PR(26)=SEOF(2)/D12
708 PR(27)=SEOF(3)
718 PR(28)=D13
728 PR(29)=E2E(1)
738 PR(30)=E2E(2)
748 PR(31)=E2E(3)
758 PR(32)=E2E(3)
768 PR(33)=ALPHA(1,3)
778 PR(34)=ALPHA(2,1)
788 PR(35)=ALPHA(3,1)
798 PR(36)=FLUX(1)
808 PR(37)=FLUX(2)
818 PR(38)=FLUX(3)
828 PR(39)=FLUX(4)
838 DO 9 NP=1,NP
848 SDV2(NP)=PRC(NP1)*PR(NP1)
858 9 CONTINUE
868 SAY2(6)=21.0
878 DO 11 I=1,6
888 SDV1@PUNCT(16)
898 11 CONTINUE
908 10 CONTINUE
918 C...PRELIMINARY COMPUTATION 1
928 TM=(TB+TP)/2.
938 TYSB4=SEISCEPS(1)*(TB-3)
948 TYSB4=SEISCEPS(2)*(TM-3)
958 TT3B3=SEISCEPS(2)*(TM-3)
968 VCPART=LVER/(2.*CP)
978 HRVBH(1)=SECFC(1)*VCO
988 HRVBH(2)=SECFC(2)*VCO
998 HRVBH(3)=SECFC(3)*VCP
1008 C...PRELIMINARY COMPUTATION 2
1018 C2=(ZKD(210)/210)/(2.*D11)*D(1)
1028 C2=(ZKD(210)/210)/(2.*D12)*D(1)
1038 RAM=(SORT(IVAN))
1048 PCHOT=H(12)-TTH(1)/20002
1058 C...PRELIMINARY COMPUTATION 3 HYPERBOLIC FUNCTION
1068 EE=EXP(TRANS*ZL)
1078 PSECH2./((EE+EM))
1088 PTANHSECH2*((EE-EM))/2.
1098 PCOTH2./((EE-EM))
1108 PCOSH2./((EE-EM))
1118 PRELIMINARY COMPUTATION 4
1128 HEC2PTRANS*ZL*TH
1138 O12=-PSECH
1148 O2=HRVH*GRA(2)+TT3W
1158 O3=PSECHHT*ANH
1168 O4=GRAH*((ZL*PCOSH2*2))
1178 O5=H(11)+EM*V2
1188 O6=H(11)+EM*V1
1198 O7=H(11)+EM*V2
1208 T0=ZKH(11)*TBD/6.
1218 T0=ZKH(11)*TBD/6.
1228 T0=ZKH(11)*TBD/6.
1238 T0=ZKH(11)*TBD/6.
1248 T0=ZKH(11)*TBD/6.
1258 T0=ZKH(11)*TBD/6.
1268 T0=ZKH(11)*TBD/6.
1278 T0=ZKH(11)*TBD/6.
1288 T0=ZKH(11)*TBD/6.
1298 T0=ZKH(11)*TBD/6.

```



```

260*    72 CONTINUE
261*    C.....FOR STEP IA=1
262*    IA=IA+1
263*    DFTDF=DFTF4(INDH,INDR,DFDK1*DK1DR4DFD*DBR+DFD*DFD*DPR1*DPR1)
264*    DFTDF=DFTF4(INDH,INDR,DFDK1*DK1DR4DFD*DBR+DFD*DFD*DPR1*DPR1)
265*    CONTINUE
266*    DELT15=CON*V111-V11*V111+V11*V111*(V11*2)/(12.*SCP1)
267*    DELT16=(CON*V111*V111*V111*2)/(8.*SCP1)
268*    DELT17= CON*RT11AV1*HF11/CP
269*    CF=2.*DELT1/IRHC(3)*DI(31)
270*    DDF16FC0N
271*    DFL1(22)=CF*SIG*(TF11*3)+DDGFM*(GEOMF(5,3)*FLUX(3)+EOMF(5,4)*FL
272*    1UX(6))
273*    C....RH0C OF
274*    RSR=(1.*DEL17*(-(HF11+5*G*EP5(3))*TF11*3)+TF11*6RA(3)*HF11*RF11*(V1
275*    1*2*2)+RNR/(IRHC(3)*2*2))
276*    DFL1(28)=RNR/(IRHC(3)*(D(3)*2*2))
277*    C....F2F F3F F4F
278*    DFL1(16)=D8GOF*(FLUX(1)*ALPHA(3,1))
279*    DFL1(17)=D8GOF*(FLUX(2)*ALPHA(3,2))
280*    DFL1(18)=D8GOF*(FLUX(3)*ALPHA(3,3))
281*    DFL1(32)=D8GOF*(FLUX(4)*ALPHA(3,4))
282*    C....ALFS
283*    DFL1(35)=D8GOF*(GEOMF(3,1)*FLUX(1)+EOMF(3,2)*FLUX(2))
284*    C....I1=12,15,I4
285*    DFL1(36)=D8GOF*(EOMF(3,1)*ALPHA(3,1))
286*    DFL1(37)=D8GOF*(EOMF(3,2)*ALPHA(3,2))
287*    DFL1(38)=D8GOF*(EOMF(3,3)*ALPHA(3,3))
288*    DFL1(39)=D8GOF*(EOMF(3,4)*ALPHA(3,4))
289*    DGTINM=IF11*CON
290*    DGTINM=IF11*-CON*HF11*-4.*EP5(3)*SIG*(TF11*3)*CON
291*    DO 85 IHO=1,NG
292*    SSI(IHO,IA)=DGCPL(IHO)*DGTINM*SSI(IHO)
293*    SII(IHO)=SII(IHO)
294*    83 CONTINUE
295*    DO 84 IHO=1,NG
296*    STH(IPI,IA)=DDFTF*SS(IHO,IA)
297*    SSI(IHO,IA)=DDFTF*SS(IHO,IA)
298*    84 CONTINUE
299*    IF(JACK,EQ,1) GO TO 80
300*    C.....STANDARD DEVIATION
301*    JAY=JACK-IA
302*    DO 75 NP1=1,NG
303*    STH(IPI,IA)=SSS(SNP1,IA)*SDV(NP1,IA)
304*    73 CONTINUE
305*    C....FOR STEP IA=2
306*    IA=IA+1
307*    DO 85 IHO=1,NG
308*    SSI(IHO,IA)=DDFTIN*SSS11(IHO,IA)*DGTDF*SS11(IHO,IA)
309*    85 CONTINUE
310*    DO 86 IHO=1,NG
311*    SSI(IHO,IA)=DDFTF*SS(IHO,IA)
312*    86 CONTINUE
313*    IF(JACK,EQ,2) GO TO 80
314*    C.....STANDARD DEVIATION
315*    JAY=JACK-IA
316*    DO 74 NP1=1,NG
317*    SSI(IPI,IA)=SSS(SNP1,IA)*SDV(NP1,IA)
318*    74 CONTINUE
319*    C....FOR STEP IA GREATER OR EQUAL 3
320*    IA=IA+1
321*    DO 88 IHO=1,NG
322*    SSI(IHO,IA)=DDFTIN*SSS11(IHO,IA)*DGTDF*SS11(IHO,IA)
323*    SSS(SNP1,IA)=SS(IHO,IA)*DDFTF
324*    88 CONTINUE
325*    C.....STANDARD DEVIATION
326*    JAY=JACK-IA
327*    IF(JACK,EQ,0) GO TO 80
328*    DO 69 IHO=1,NG
329*    STH(IHO,IA)=SSS(SNP1,IA)*SDV(IHO,IA)
330*    69 CONTINUE
331*    IF(JACK,NE,JIN) GO TO 69
332*    CONTINUE
333*    C....COMPUTATION OF OVER ALL STANDARD DEVIATION
334*    DO 76 NP1=1,NG
335*    STH(NP1,IA)=SSS(SNP1,IA)*SDV(NP1,IA)*SDV(NP1,IA)
336*    76 CONTINUE
337*    C....CONTINUE
338*    DO 81 NP1=1,NG
339*    SAV(NP1)=SDP1(NP1)+DDFTF*SAV(NP1)+DGTIN*SAU(NP1)
340*    SAU(NP1)=SSA(NP1)*SAU(NP1)*SDP2(NP1)
341*    81 CONTINUE
342*    DO 82 NP1=1,NG
343*    SAV(NP1)=SSA(NP1)*SAV(NP1)*SDP2(NP1)
344*    SSA(NP1)=SSA(NP1)*SAU(NP1)
345*    SAU(NP1)=SAU(NP1)
346*    82 CONTINUE
347*    C....COMPUTATION OF SITE
348*    STDV=0.0
349*    DO 77 IA=1,JIN
350*    STE(IA)=0.0
351*    77 CONTINUE
352*    DO 79 IA=1,JIN
353*    DO 80 IA=1,NG
354*    EEE=STH(NP1,IA)*SAE2
355*    STP(NP1,IA)=EEE
356*    STE(IA)=STP(IA)+EEE
357*    78 CONTINUE
358*    SIG1A=SP1*STE(IA)
359*    SOD1=SDV(STE(IA))
360*    79 CONTINUE
361*    DO 84 NP1=1,NG
362*    STDV=STDV*AAA(NP1)*#2
363*    84 CONTINUE
364*    CORN=0.0
365*    DO 91 NP1=1,NG
366*    CORN=CORN*TH2(NP1)*#2
367*    91 CONTINUE
368*    CORNSRT(CORN)
369*    STDV=STDV*CORN
370*    STDV=SOR11(STDV)
371*    DO 96 NP1=1,NG
372*    PER(NP1)=0.0
373*    DO 95 IA=1,JIN
374*    PER(NP1)=STH(NP1,IA)*#2*PER(NP1)
375*    95 CONTINUE
376*    PER(NP1)=PER(NP1)+STH2(NP1)*#2
377*    96 CONTINUE
378*    IF(JACK,NE,-JHEY) GO TO 13
379*    PRINT 527
380*    PRINT 521,0.01,0.02,0.03,0.04,0.05,0.06,0.07,0.08
381*    PRINT 521,P,GHK,XK,DGTDF,B60F,B60FT,B60FTN
382*    PRINT 521,DGFL(1),185,77,(DGL(1),1816,18),DGPL(22),DGPL(28)
383*    PRINT 521,DGFL(29),DGL(32),(DGL(1),1816,18),DGPL(35,39)
384*    PRINT 524
385*    PRINT 524
386*    PRINT 211,(SLIP),IP1,39
387*    PRINT 523
388*    PRINT 211,CORN,(STE11),II=1,JIN
389*

```

```

3500* PRINT 520, (PERMNP1),NP1,KEY1
3510* PRINT 520, (SAVNP1),NP1,KEY1,NP1
13 CONTINUE
3920* IF(JACK,NE.,JAZZ) GO TO 518
DO 515 I=1,N
      SPP1(I)=SPP1(I)+TAPE1(I)
      PRINT 491,SPP1(I),NP1,I
      PRINT 492,STMP1(I),NP1,I
      PRINT 493,STMP1(I),NP1,I
      PRINT 494,STMP1(I),NP1,I
      PRINT 495,STMP1(I),NP1,I
      PRINT 496,STMP1(I),NP1,I
      PRINT 497,STMP1(I),NP1,I
      PRINT 498,STMP1(I),NP1,I
      PRINT 499,STMP1(I),NP1,I
      PRINT 500,STMP1(I),NP1,I
      PRINT 501,CONTINUE
      JAZZ=JAZZ+100
315 CONTINUE
DO 63 I=1,N
      IIZ=I+1
      DO 63 I=1,N
          DO 63 I=1,N
              SS11(I,I0,I1)=SS11(I0,I1)
              SS11(I0,I1)=SS11(I0,I1)
63 CONTINUE
4070* 60 TO 93
4080* 92 STDV=0.0
4100* STDV=STDV+15*(NP1)*SDV2(NP1)*e**2
93 CONTINUE
4110* STDV=STDV/
4130* STDV=STDV/
DO 61 I=1,NP
61 S11(I0)=S11(I0)
95 CONTINUE
IF(JACK,NE.,JOEY) GO TO 14
PRINT 210,STDV
14 CONTINUE
4150* C.....DATA REDUCTION
4200* TREDUC=0/04
4210* T=TRREDUC
4220* T1=TRREDUC
C....CALCULATION OF FILM TEMPERATURE
4230* COL=2,*DELY(RHOC(3))+(3)
4240* PIGEL="GOLs(H(3))+SIGMEPS(3))/AT*sec3"
4250* HOLECOL=(H(3))*SIGMEPS(3))/AT*sec3)
4260* TF=PI*G*TF+40*F
4270* 4280* SAVE PREVIOUS PARAMETER VALUES
4290* 4300* TFI=STF
4310* TII=STI
4320* V1=VEL
4330* RF1=RCF(3)
4340* IF(JACK,NE.,JOEY) GO TO 15
4350* PRINT 110,TINF,TREDUC,TF
JOEY=JOEY+10
15 CONTINUE
4360* JACK-JACK+1
C....COMPUTATION OF PARAMETER SHIFT
4370* JEEP=JIN
4380* IF(JACK,LE.,JIN) JEEP=JACK
4390* IF(JEEP,LE.,1) GO TO 52
DO 50 KEY=2,JEEP
      KKEYKEY=1
4450* DO 50 NP=1,NP
      SAV(NP1,KEY)=SAV(NP1,KEY)
4460* 50 CONTINUE
4470* 52 CONTINUE
DO 53 NP1=1,NP
53 SDV(NP1,1)=SDV2(NP1)
51 CONTINUE
4520* 137 FORMAT(SDH NOT CONVERSE
4530* 210 FORMAT(LH,19HSTANDARD DEVIATIONS,E15.6)
4540*

```

SUBROUTINE INTRE

```

14 SUBROUTINE INTRE(IREYN,UNCH)
26 DIMENSION APE(9),APE(9)
34 P=1,E=3
44 C.....UNCERTAINTY TABLE FOR DIFFERENT REYNOLDS NUMBER
44 DO 2 I=1,9
54 P=P*10.
2 APE(I)=P
54 DPE(1)=.05
64 DPE(2)=.075
74 DPE(3)=.10
84 DPE(4)=.15
94 DPE(5)=.18
104 DPE(6)=.15
114 DPE(7)=.10
124 DPE(8)=.075
134 DPE(9)=.05
144 IF(IREYN.GT.APE(9)) GO TO 50
154 IF(IREYN.LT.APE(1)) GO TO 50
164 C....LINEAR INTERPOLATION
174 DO 10 NANAS=29,
184 NANAH=0
194 IF(IREYN.LT.APE(NANAH)) GO TO 12
204 NANAH=NANAS
214 NONAH=1
224 IF(IREYN.LT.APE(NONAH)) GO TO 12
234 10 CONTINUE
244 12 A2=APE(NON)
244 B2=DPE(NON)
244 A1=APE(NON-1)
244 B1=DPE(NON-1)
254 RCCC=REYN/A1
264 UNCH=B1+(B2-B1)*ALOG10(RCCC)/( ALOG10(A2)-ALOG10(A1))
274 60 TO 51
304 50 UNCH=0.05
51 51 CONTINUE
324 RETURN
END
334

```

SUBROUTINE INTKN

```

14 SUBROUTINE INTKN(DKN,UNCR,ZNU)
24 C.....DIMENSION BMA(5),BMB(5)
34 C.....UNCERTAINTY TABLE FOR DIFFERENT KNUDSEN NUMBER
34 IF (ZNU.EQ.2) GO TO 5
44 C.....FOR BEAD AND PLATE
44 BMA(1)=3, E=2
54 BMA(2)=0.1
64 BMA(3)=.3
74 BMA(4)=.0
84 BMA(5)=.0
94 104 GO TO 7
114 C....FOR WIRE
124 124 5 CONTINUE
134 BMA(1)=26, E=2
144 BMA(2)=0.2
154 BMA(3)=.6
164 BMA(4)=.0
174 BMA(5)=.0
184 7 CONTINUE
194 BMB(1)=.05
204 BMB(2)=0.05
214 BMB(3)=.10
224 BMB(4)=.075
234 BMB(5)=.05
244 244 IF (DKN.GT.BMA(5)) GO TO 50
254 IF (DKN.LT.BMB(1)) GO TO 50
264 C....LINEAR INTERPOLATION
274 DO 10 NANAS=2,5
284 NANAH=1
294 NONAH=1
304 IF(DKN.LT.BMA(NANAH)) GO TO 12
314 10 CONTINUE
324 12 CONTINUE
334 A2=BIA(NON)
344 B2=BIB(NON)
354 A1=BIA(NON-1)
354 B1=BIB(NON-1)
364 DDD=KVA3
374 UNCR=BL1*(B2-B1)*(ALOG10(DDD)/(ALOG10(A2)-ALOG10(A1)))
384 60 TO 51
404 404 50 CONTINUE
414 UNCR=.05
424 51 CONTINUE
434 RETURN
END
444

```

REFERENCES

1. J. C. Ballinger, J. C. Elizalde, R. M. Garcia-Varela, and E. H. Christensen, "Environmental Control Study of Space Vehicles," Technical Report No. ERR-AN-016, Convair Division, General Dynamics, San Diego, California, 1960.
2. W. R. Bandeen, R. H. Hanel, J. Licht, R. A. Stampfli, and W. G. Stroud, "Infrared and Reflected Solar Radiation Measurements from the Tiros II Meteorological Satellite," *Journal of Geophysical Research*, Vol. 66, 1961, pp. 3169-3185.
3. P. F. Clapp, "Global Cloud Cover for Seasons Using Tiros Nephanalysis," *Monthly Weather Review*, Vol. 92, 1962, p. 495.
4. W. A. Drews, "Final Report on Research and Development to Improve Temperature Measurements at High Altitudes," Report TR-PL-8876 under Contract No. NAS1-1611, Atlantic Research Corporation, Alexandria, Virginia, January 1966.
5. Dupont DeNemours & Company, "Mylar Polyester Film," Technical Information Bulletin No. M-2B, n.d.
6. A. Eddy, C. E. Duchon, F. M. Haase, and D. R. Haragan, "Determination of Winds from Meteorological Rocketsondes," Report No. 2, Atmospheric Science Group, College of Engineering, The University of Texas, Contract No. DA-23-072-AMC-1564, November 1965.
7. C. Eisenhart, "Realistic Evaluation of the Precision and Accuracy of Instrument Calibration Systems," *Journal of Research National Bureau of Standards*, Vol. 67C, No. 2, 1963, p. 161.
8. F. S. Johnson, "The Solar Constant," *Journal of Meteorology*, Vol. 11, 1954, p. 431.
9. S. J. Kline and F. A. McClintock, "Describing Uncertainties in Single-Sample Experiments," *Mechanical Engineering*, Vol. 75, 1953, p. 3.
10. A. Papoulis, *Probability, Random Variables, and Stochastic Processes*, McGraw-Hill Book Company, New York, 1965, p. 212.
11. R. W. Powell, C. Y. Ho, and P. E. Liley, "Thermal Conducting of Selected Materials," National Standard Reference Data Series, National Bureau of Standards-8, NSRDS-NBS-8, November 25, 1966.

12. W. C. Snoddy, "Irradiation Above the Atmosphere Due to Rayleigh Scattering and Diffuse Terrestrial Reflections," AIAA Paper, No. 65-666, 1965, p. 17-21.
13. F. L. Staffanson and S. J. Alsaji, "Thermometric Convection Coefficients for Parachutesondes in the Mesosphere," *Rarefied Gas Dynamics*, Vol. 2, Academic Press, New York, 1968, p. 1559.
14. F. L. Staffanson, "Theoretical Comparison of Beads, Wires, and Films as Rocketsonde Temperature Sensors in the Mesosphere," NASA Contractor Report CR-1286, 1969.
15. D. C. Thompson, "The Accuracy of Miniature Bead Thermistors in the Measurement of Upper Air Temperatures," AF CRL-66-773, Scientific Report No. 1, Contract No. AF 19(628)-4165, Project No. 6670, Task No. 667001, October 1966.
16. R. Tomovic, *Sensitivity Analysis of Dynamic Systems*, McGraw-Hill Book Company, New York, 1963.
17. UNIVAC 1108 Math-Pack, "Random Number Generation," UP-7542, Section 14, p. 8.
18. R. C. Weast and S. M. Selby, *Handbook of Chemistry and Physics*, 47th Edition, Chemical Rubber Publishing Company, Cleveland, Ohio, 1966.
19. F. W. Right, "A Survey for Naval Ordnance Laboratory of High Altitude Atmospheric Temperature Sensors and Associated Problems," Final Report performed under Navy Contract N-60921-6136 for the NAVAL Ordnance Laboratory, 1961, p. 92.